

## THE EVOLUTION OF LARGE PLANETARY NEBULAE AND THEIR CENTRAL STARS

JAMES B. KALER

Astronomy Department, University of Illinois  
 Received 1982 June 28; accepted 1983 January 21

### ABSTRACT

New absolute and relative line fluxes are presented for 57 large planetary nebulae, defined here as having maximum radii greater than 0.175 pc. H and He II Zanstra temperatures and luminosities, with a full evaluation of the errors, are calculated for the central stars of these nebulae and for the 25 additional objects for which the appropriate data are available. The ratios of the H and He II temperatures are used to establish whether or not the nebulae are optically thick in the H and He<sup>+</sup> Lyman continua, and consequently to determine in which cases the derived values of  $T$  and  $L$  may only be limits. The full set of central stars is plotted on the  $\log L$ - $\log T$  plane for comparison with theoretical evolutionary tracks.

If in the ensemble of planetaries, we properly take account of the stars with only limiting values of  $L$  and  $T$ , we see that the planetary nuclei are distributed along the evolutionary tracks as theoretically expected consistent with a range of final core masses from  $\approx 0.55 M_{\odot}$  up to about  $1 M_{\odot}$ . The core mass distribution is broader than that derived by Schönberner, with between 35% and 48% of the stars above  $0.6 M_{\odot}$ , over double his number. Given the various uncertainties and selection effects, the true mass distribution of planetary cores probably lies about midway between that found by Schönberner and the one determined in this paper.

N/O ratios derived from the relative emission line fluxes correlate qualitatively with position on the  $\log L$ - $\log T$  plane in the manner predicted by Renzini and by Iben and Renzini: through processes of convective dredge-up, high nebular N/O tends to associate with low luminosity stars of higher remnant core mass, which result from stars of higher initial mass. The N/O ratios also correlate with nebular morphology in the sense that ellipsoidal bi-nebulous objects tend to have distinctly higher nitrogen abundances than do nebulae with smoother more symmetrical structure; the morphology independently correlates with position on the  $\log L$ - $\log T$  plane the same way as N/O. Thus, the variety of nebular structures may at least in part be traced to stars with different initial masses.

The correlations are not strict, however, in that there is a significant mixture of nebulae with lower N/O within the sets of objects that appear to have higher mass cores, indicating either improper placement on the  $\log L$ - $\log T$  plane, or that higher mass stars do not necessarily convectively dredge-up fresh nitrogen and helium. The core masses found here are smaller than expected for the initial masses implied by the N/O ratios, suggesting either that significant dredge-up may take place at masses lower than now expected, or that the cores do not grow as large as currently anticipated. This result is in the same direction as indicated in Schönberner's work, but not as extreme, consistent with the wider mass distribution found here. In spite of the remaining difficulties, this study demonstrates at least the qualitative consistency of theories of stellar evolution, mass loss, and convective dredge-up.

*Subject headings:* nebulae: abundances — nebulae: planetary — stars: evolution — stars: interiors

### I. INTRODUCTION

The first large-scale studies of the evolution of planetary nebulae and their central stars go back nearly 20 years. The empirical work of O'Dell (1963*a*, 1968), Abell (1966), and Seaton (1966) founded the field, and provided the background for later research. A landmark paper by Abell and Goldreich (1966), following the lead of several earlier discussions, argued convincingly that stars pass naturally through the planetary stage during their transition between the red giant and white dwarf states. Somewhat later, Paczyński (1971) produced the

first comprehensive theoretical analysis, with calculation of evolutionary tracks through the  $\log L$ - $\log T$  plane.

The studies were successful in that the theoretical tracks passed through the general area defined by the observed stellar temperatures and luminosities, but the detailed comparison was disappointing. The Harman-Seaton track (Seaton, 1966), the widely accepted path for many years, exhibits a sharp initial rise absent from the Paczyński tracks, and the stars with the highest predicted temperatures could not be found. We have seen a new burst of activity in this subject over the past

few years, particularly in recent attempts at theoretical interpretations of the observations. Renzini (1979) suggested that the distribution of planetary nuclei on the  $\log L$ - $\log T$  plane could be understood by appealing to the time scales of the evolution for stars of different mass. Stars of high initial (and final core) mass would evolve rapidly, and would be detected only when they were of low luminosity, on the cooling portions of the tracks. The more slowly evolving low-mass stars would be seen at higher stellar luminosity ( $L$ ) and lower stellar effective temperature ( $T$ ) on the horizontal portions. In contrast, Schönberner (1981) and Schönberner and Weidemann (1981a), with the aid of new theoretical calculations by Schönberner (1979), interpret the data to show that nearly all planetary nuclei have about the same final masses, around  $0.6 M_{\odot}$ . Renzini (1979) and Iben and Renzini (1982), further suggest that if the initial stellar mass controls both the observed position of the star on the  $\log L$ - $\log T$  plane and the abundance of helium and nitrogen in the planetary through convective dredge-up, a correlation between abundance and position ought to be observed. Schönberner (1981), however, found no relation between the state of nebular and stellar evolution and the helium abundance and concluded that dredge-up must also occur for low-mass stars.

The spectrophotometry of the planetaries is strongly affected by observational selection. Observers have concentrated mostly on the smaller objects of high surface brightness, and there is a serious lack of data on the larger ones. A few prominent nebulae such as the Ring and the Dumbbell have been observed in detail, but there have been few systematic studies, the most extensive being those of Kondratyeva (1979) and Kaler (1981a). The well-observed small nebulae, however, are just those for which the stellar data are the most difficult to obtain. In some instances, a nebula is so bright that the star is lost. These problems have prompted the present effort to increase greatly the amount of data available, and to re-examine the entire problem of planetary evolution. Because of differences in the types of data required, the work is being divided into two broad areas dependent on nebular radius: the large nebulae, for which new absolute and relative nebular fluxes are being observed, and the small, compact objects, for which both nebular spectroscopy and improved central star magnitudes are needed.

This paper presents full results on wide aperture spectrophotometry of large planetary nebulae, and the interpretation of the data in terms of location on the  $\log L$ - $\log T$  plane, abundances, and morphology. Some results in this area have already been published: Kaler and Hartkopf (1981) observed two large Abell nebulae and found great dissimilarity between the states of the stars' evolution; Kaler (1981a) examined a set of large high-excitation nebulae and found that the central stars and nebular morphology were all quite similar; Iben *et al.* (1983) discuss the nature of these latter stars and explain their high luminosities in terms of a late thermal pulse that causes the star to move back to the horizontal

portion of the evolutionary track. Future papers will treat more detailed spectrophotometry and abundance analyses of large nebulae, the ultraviolet spectra of a large selection of central stars, and analogous examinations of compact nebulae wherein these two broad sets will be joined.

## II. THE OBSERVATIONS

The criterion for inclusion in this paper is that the nebular radius be larger than 0.175 pc, where the distance and radius are based upon the distance scale used by Cahn and Kaler (1971), the measured  $H\beta$  flux and extinction, and the largest angular radius given in Perek and Kohoutek (1967). As we shall see later, this criterion divides the central stars quite well at  $\log L/L_{\odot} = 3$ . Consequently, two additional objects for which  $r < 0.175$  pc, but which have  $\log L/L_{\odot} < 3$  were included, in order to obtain as physically complete a sample as possible. Over two-thirds of the data used in subsequent analyses are new. The remainder come from the literature.

### a) *Prairie Photometry*

Most of the new observational data presented here were taken with the University of Illinois 1 m reflector at Prairie Observatory, a single channel photometer, and a set of interference filters. The nebulae were generally selected for observation on the basis of observability and the existence of a measured central star magnitude. The observation and reduction techniques are explained by Kaler (1976a, 1980a). The absolute fluxes are based on Shaw and Kaler's (1982) recalibration of NGC 7027, which in turn is tied to the absolute flux of Vega measured by Oke and Schild (1970). Errors are calculated as before from the statistics of the raw counts. Radial velocity shifts, when known, were incorporated into the reductions for all line filters. Temperature shifts were explicitly considered for the blue filters, but the effects were only added into the errors for the red filters. Additional sources of error, which are not accounted for, are the inclusion of field stars in the wide 4' aperture, and the unknown radial velocities of most of the nebulae, where the latter affect the simultaneous solutions for  $H\alpha$  and  $[N II]$ : see Kaler (1981a) for further discussion, and § IIc below. When needed, some unpublished data from Kitt Peak Intensified Reticon Scanner (IRS) observations (Kaler 1983a) were incorporated into the Illinois 1 m data.

The new data are presented in Table 1. Columns (1) and (2) give the common names of the objects (ordered by NGC, IC, and then alphabetically), and the Perek-Kohoutek (1967) number. Column (3) gives the aperture sizes (A), and the positions (P) at which the nebulae were observed in the cases where they were larger than the aperture. Where needed, the exact positions are given by the remarks referred to in column (14). Several nebulae were observed with different apertures and/or at different positions, and thus have multiple entries. In some instances, a large aperture was used to obtain a total absolute  $H\beta$  or  $H\alpha$  flux, and a small aperture to find relative fluxes for other lines.

TABLE 1  
PHOTOMETRY OF LARGE PLANETARY NEBULAE

| Nebula<br>(1) | PK<br>(2) | A&P <sup>a</sup><br>(3) | observed <sup>b</sup><br>-log F(H $\beta$ )<br>(4) | observed <sup>b</sup><br>-log F(H $\alpha$ )<br>(5) | Total <sup>c</sup><br>-log F(H $\beta$ )<br>(6) | 3727<br>[OII]<br>(7) | I(H $\beta$ ) = 100 |                       |                            | N/ $\alpha$<br>(12) | c<br>(13) | Rmks<br>(14) |
|---------------|-----------|-------------------------|--|---|---|----------------------|---------------------|-----------------------|----------------------------|---------------------|-----------|--------------|
|               |           |                         |  |   |   |                      | 4686<br>HeII<br>(8) | 4959<br>[OIII]<br>(9) | 6563<br>H $\alpha$<br>(10) |                     |           |              |
| NGC 1360      | 220-53°1  | 4'                      | 10.2 ±0.1  |   | 11.26±0.2                                       | 258±25               | 99±2                | 244±9                 | 279                        | 2.1 ±.3             | 0.0       | 1,2          |
| NGC 2474-5    | 164+31°1  | 4'N<br>4'S              | 11.52±0.03<br>11.61±0.06                           |   |   | 28±3                 | 252±30              |                       |                            | 0.0                 | 0.0       | 3,4          |
| NGC 6058      | 64+48°1   | 40''                    | 11.32±0.05   | 11.32±0.05  | 11.77±0.03 <sup>d</sup>                         | 128±8                | 110±6               | 328±51                | 328±51                     | <0.055              | 0.18±0.19 | 5            |
| NGC 6765      | 62+ 9°1   | 26''C                   | 12.23±0.02   | 11.62±0.04  | 11.90±0.10                                      | 64±20                | 8±4                 | 405±46                | 405±46                     | 0.54±0.06           | 0.46±0.15 | 6            |
| NGC 6894      | 69- 2°1   | 40''                    | 11.34±0.02   | 10.58±0.04  | 11.41±0.05 <sup>d</sup>                         |                      |                     | 581±70                | 457±50                     | 0.78±0.10           | 0.92±0.16 | 7,8          |
| NGC 7094      | 66-28°1   | 4'                      | (11.77±0.06) <sup>e</sup>                          | 11.25±0.06  |   |                      |                     | 324                   |                            | 0.16                | 0.16      | 1,2          |
| IC 972        | 326+42°1  | 40''C                   | 12.19±0.09   | 11.71±0.08  | 12.05±0.10                                      | 260±46               | 20±8                | 304±56                | 163±29                     | 0.54±0.07           | 0.08±0.08 |              |
| A 2           | 122- 4°1  | 40''                    | 12.37±0.03   | 11.83±0.05  |   |                      | 61±21               | 487±5                 | 380±50                     | 0.27±0.03           | 0.37±0.17 |              |
| A 3           | 13+ 2°1   | 40''C                   | 13.17±0.06   | 12.28±0.04  |   | 101±88               | 66±33               | 409±93                | 779±143                    | 0.61±0.07           | 1.30±0.24 |              |
| A 4           | 144-15°1  | 40''                    | (12.61±0.10)                                       | 11.72±0.07  |   | 88±14                | 23±10               | 408±51                | 334                        | 0.26±0.11           | 0.21      | 2            |
| A 5           | 141- 7°1  | 4'                      | 12.9 ±0.2  | 12.14±0.11  |   |                      |                     |                       |                            | 3.0 ±0.9            | 0.9 ±0.5  | 9            |
| A 6           | 136+ 4°1  | 4'                      | 12.43±0.06   | 11.48±0.04  |   | neg. <sup>f</sup>    | <7                  | 519±113               | 884±167                    | 0.13±0.04           | 1.46±0.25 |              |
| A 8           | 167- 0°1  | 40''                    | 12.6 ±0.3  | 12.6 ±0.3   | (13.0 ±0.3)                                     | 180±110              | <45                 | 1580±950              | 3980±1940                  | 1.3 ±1.2            | 0.8       | 2            |
| A 13          | 204- 8°1  | 4'                      | 12.62±0.14   | 11.42±0.16  |   |                      | 128±17              | 127±29                | 294±46                     | 2.5 ±1.2            | 2.2 ±0.9  |              |
| A 15          | 233-16°1  | 40''                    | 12.47±0.04   | 12.01±0.05  |   |                      |                     |                       |                            | 0.12±0.06           | 0.04±0.15 | 1,10         |
| A 16          | 153+22°1  | 4'                      | 12.31±0.06   | 11.70±0.05  |   | <58                  | 33±14               | 306±75                | 411±89                     | 0.15±0.09           | 0.47±0.29 |              |
| A 20          | 214+ 7°1  | 40''S                   | 12.71±0.02   | 12.39±0.06  |   | neg.                 | 149±13              | 150±50                | 210±31                     | 0.34±0.10           | 0.0       | 1,10         |
| A 24          | 214+14°1  | 4'W                     | (12.04±0.05)                                       | 11.59±0.05  |   |                      |                     |                       |                            | 0.09±0.05           |           |              |
| A 28          | 158+37°1  | 4'E                     | 11.68±0.04   | 10.90±0.05  | 11.35±0.05                                      | <51                  | <33                 | 56±46                 | 414±87                     | 4.2 ±0.8            | 0.48±0.28 | 3            |
| A 30          | 208+33°1  | 4'                      | 11.82±0.07   | 11.61±0.18  |   | <33                  | 30±13               | 163±91                | 72±45                      | 2.0 ±0.4            | 0.0       |              |
| A 31          | 219+31°1  | 4'E                     | 12.19±0.04   | 11.84±0.09  |   | neg.                 | 152±7               | 138±27                | 230±40                     | 0.44±0.35           | 0.0       | 1            |
| A 33          | 238+34°1  | 40''SW                  | 11.45±0.06   | 11.01±0.14  | 10.54±0.3                                       | 225±40               | 32±20               | <125                  | 280±112                    | <66                 | 0.60±0.36 | 11           |
| A 34          | 248+29°1  | 4'                      | 12.94±0.08   | 12.50±0.11  | 11.3 ±0.3                                       | neg.                 | 58±18               | 160±30                | 279±85                     | 0.13±0.12           | 0.0 ±0.28 | 12           |
| A 35          | 303+40°1  | 4'W                     | 11.84±0.05   | 11.38±0.05  |   | neg.                 | 40±8                | 269±30                | 258±44                     | 0.48±0.12           | 0.0 ±0.08 |              |
| A 39          | 47+42°1   | 4'E                     | 11.66±0.08   | 11.29±0.10  | 11.3 ±0.2                                       | 420±80               | neg.                | 120±10                | 299±45                     | 0.75±0.08           | 0.0       | 3,13         |
| A 46          | 55+16°1   | 40''C                   | 11.57±0.05   | 11.19±0.05  |   | 85±10                | <15                 | 120±40                | 229±40                     | 0.74±0.08           | 0.0       |              |
| A 51          | 17-10°1   | 40''N                   | 11.79±0.02   | 11.42±0.05  |   | <17                  | 69±11               | 356±33                | 243±34                     | <.05                | 0.0       |              |
| A 53          | 40- 0°1   | 40''                    | 12.42±0.08   | 11.97±0.06  |   | 63±23                | <5                  | 93±35                 | 276±71                     | <.08                | 0.0 ±0.23 |              |
| A 62          | 47- 4°1   | 4'                      | (11.85±0.11)                                       | 11.40±0.06  |   | <15                  | 90±23               | 200±68                | 268±64                     | <.04                | 0.0 ±0.19 | 1            |
| A 65          | 17-21°1   | 4'                      | 12.66±0.06   | 12.23±0.08  |   |                      |                     |                       |                            | <.21                | 0.0 ±0.19 |              |
| A 70          | 38-25°1   | 40''C                   | (11.80±0.10)                                       | 11.35±0.08  |   |                      |                     |                       |                            | neg.                | 1.74±0.25 | 7            |
| A 71          | 85+ 4°1   | 4'                      | 12.61±0.05   | 11.58±0.06  |   | 825±125              | 35±28               | 240±49                | 1093±210                   | 0.76±0.15           | 2.18±0.53 |              |
| A 72          | 59-18°1   | 40''E                   | 12.01±0.06   | 10.82±0.13  |   |                      | <20                 | 615±110               | 1535±590                   | 0.18±0.13           |           |              |
| A 73          | 95+ 7°1   | 40''C                   | 11.63±0.05   | 11.11±0.05  | 12.34±0.10                                      | 64±20                | 38±17               | 204±28                | 331±60                     | 0.15±0.06           | 0.19±0.24 |              |
|               |           | 4'                      | 12.41±0.09   | 11.88±0.06  |   | 42±23                | 46±13               | 326±113               | 342±91                     | 0.80±0.11           | 0.23±0.31 |              |
|               |           | 4'                      | 11.75±0.02   | 10.92±0.04  |   | neg.                 | 29±5                | 112±16                | 681±79                     | 1.50±0.17           | 1.12±0.15 |              |
|               |           | 4'                      | 12.89±0.02   | 11.56±0.12  |   |                      | 106±11              |                       |                            | 0.0 ±0.06           |           | 1,14         |
|               |           | 4'                      | 11.88±0.07   | 12.63±0.11  | (12.82±0.08)                                    | neg.                 | 111±18              | 183±30                | 266±33                     | 1.02±0.30           | 1.14±0.95 |              |
|               |           | 4'                      | 13.45±0.24   | 11.90±0.15  |   |                      | 686±547             | 702±540               | 686±547                    | 0.94±0.48           |           | 15           |

TABLE 1—Continued

| Nebula<br>(1) | PK<br>(2) | A&P <sup>a</sup><br>(3) | observed <sup>b</sup><br>-log F(H $\beta$ )<br>(4) | observed <sup>b</sup><br>-log F(H $\alpha$ )<br>(5) | Total <sup>c</sup><br>-log F(H $\beta$ )<br>(6) | 3727<br>[OII]<br>(7) | 4686<br>HeII<br>(8) | I(H $\beta$ ) = 100   |                            |                       | N/ $\alpha$<br>(12) | c<br>(13) | Rmks<br>(14) |
|---------------|-----------|-------------------------|--|---|---|----------------------|---------------------|-----------------------|----------------------------|-----------------------|---------------------|-----------|--------------|
|               |           |                         |  |   |   |                      |                     | 4959<br>[OIII]<br>(9) | 5563<br>H $\alpha$<br>(10) | 6584<br>[NII]<br>(11) |                     |           |              |
| A 75          | 101+ 8°1  | 40°N                    | 12.60±0.07   | 11.85±0.01  | 12.00±0.10                                      | 56±44                | 81±12               | 473±120               | 580±120                    | <24                   | <0.04               | 0.92±0.27 | 1            |
| A 78          | 81-14°1   | 40°SW                   | 13.00±0.06   | 12.53±0.12  |   | <69                  | 135±36              |                       | 294±100                    | <28                   | <0.10               | 0.04±0.42 | 1            |
| A 79          | 102- 2°1  | 40°N                    | 12.04±0.04   | 11.94±0.04  | (12.6 ±0.3)                                     |                      | 187±54              | 440±150               | <1800                      |                       | 1.43±0.16           | 1.4 ±1.2  |              |
| A 80          | 102- 5°1  | 4°S                     | 12.87±0.33   | 11.05±0.05  |   |                      | <56 :               | 2240 :                | 565±185                    | 812±265               | 1.45±0.16           | 0.88±0.44 |              |
| A 82          | 114- 4°1  | 40°N                    | 11.80±0.12   | 11.30±0.15  | 11.72±0.12                                      | 209±24               | 15±5                | 309±19                | 366±167                    | 340±96                | 0.93±0.49           | 0.32±0.49 | 16           |
|               |           | 4°S                     | 11.87±0.15   |   |   |                      |                     |                       |                            |                       |                     |           |              |
|               |           | 4°S                     | 11.62±0.07   |   |   |                      |                     |                       |                            |                       |                     |           |              |
| A 84          | 112-10°1  | 4°S                     | 11.74±0.05   | 11.18±0.05  |   | 306±84               | 17±13               | 306±49                | 395±60                     | 327±48                | 0.83±0.10           | 0.42±0.20 |              |
| BV 3          | 131- 5°1  | 40°N                    | 12.40±0.07   | 11.67±0.06  |   |                      | 25±19               | 376±61                | 393±70                     | 296±57                | 0.75±0.14           | 0.42±0.23 |              |
| Jn 1          | 104-29°1  | 4°N                     | 11.79±0.03   | 11.49±0.04  | 11.48±0.03                                      | 94±17                | 62±21               | 385±45                | 205±74                     | 85±31                 | 0.42±0.15           | 0.0       | 3            |
| K1 7          | 197-14°1  | 4°S                     | 11.77±0.06   | 11.58±0.05  |   |                      | 37±10               | 353±57                |                            |                       |                     |           |              |
| K1 14         | 45+24°1   | 4°S                     | (12.13±0.05)                                       | 11.95±0.10  |   |                      | 13                  |                       | 640                        |                       | 0.93±0.07           | 0.27      | 2,17         |
|               |           | 4°S                     | (12.40±0.10)                                       |   |   |                      | 160 :               | 145 :                 | 260 :                      |                       | 0.0 ±0.1            |           | 1,2          |
| K1 16         | 94+27°1   | 4°S                     | 12.00±0.04   | 11.55±0.14  |   | <83                  | 126±20              | 134±60                | 250±100                    | <75                   | <0.3                | 0.0 ±0.26 | 1            |
| K1 20         | 110-12°1  | 40°N                    | (12.93±0.09)                                       | 12.33±0.09  |   |                      | <10                 |                       | 400                        |                       | 0.45±0.16           | 0.44      | 2            |
| K1 22         | 283+25°1  | 4°S                     | 11.42±0.10   | 10.86±0.04  |   |                      | <50                 | 333±175               | 359±103                    | 59±17                 | 0.16±0.02           | 0.29±0.34 | 18           |
| K2 1          | 173- 5°1  | 4°S                     | 11.81±0.02   | 11.18±0.04  |   | 85±23                | 114±36              | 892±64                | 447±54                     | 42±14                 | 0.09±0.03           | 0.58±0.16 |              |
| K2 2          | 204+ 4°1  | 4°C                     | 11.22±0.01   | 10.89±0.04  | 11.12±0.10                                      | 108±27               | 7±5                 | 196±55                | 214±25                     | 53±9                  | 0.25±0.04           | 0.0       | 19           |
| K3 27         | 61+ 8°1   | 40°N                    | 12.11±0.03   | 11.69±0.05  |   | neg.                 | 92±10               | 198±26                | 267±26                     | <10                   | <0.04               | 0.0 ±0.07 | 1            |
| LT 5          | 339+88°1  | 4°S                     | 12.1 ±0.2  | 12.1 ±0.2   | (11.8 ±.3)                                      |                      |                     |                       |                            |                       | <0.34               | 0.0       | 20           |
| M2 51         | 103+ 0°1  | 40°N                    | 12.23±0.01   | 11.30±0.01  |   | 153±6                | 13±5                | 343±14                | 838±123                    | 820±126               | 0.98±0.18           | 1.39±0.19 | 7            |
|               |           | 4°S                     | (11.97±0.04)                                       | 11.04±0.04  |   |                      |                     |                       |                            |                       | 1.49±0.16           |           |              |
| M2 55         | 116+ 8°1  | 40°N                    | 12.20±0.01   | 11.27±0.08  | 12.16±0.01                                      | 46±24                | 4±2                 |                       | 776±146                    | 376±125               | 0.49±0.17           | 1.29±0.25 |              |
| M3 3          | 221+ 5°1  | 40°N                    | 12.29±0.02   | 11.71±0.05  |   | 124±9                |                     |                       | 397±44                     | 985±138               | 2.48±0.35           | 0.43±0.14 |              |
| PW 1          | 158+17°1  | 4°N                     | 11.89±0.08   | 11.89±0.08  | 10.85±0.10                                      |                      |                     |                       |                            |                       |                     | 0.72±0.17 | 21           |
|               |           | 4°C                     | 11.67±0.05   | 11.67±0.05  |   |                      |                     |                       |                            |                       |                     | 0.36±0.07 |              |
|               |           | 4°S                     | 12.26±0.07   | 11.80±0.13  |   | 73±31                | 37±18               | 303±93                | 294±113                    | 222±56                | 0.76±0.28           |           |              |
| Sh2 71        | 36- 1°1   | 4°S                     | 11.60±0.05   | 10.66±0.04  |   | 20±17                | 67±11               | 171±43                | 874±143                    | 2065±335              | 2.50±0.32           | 1.45±0.21 |              |
| Ym 29         | 205+14°1  | 4°NE                    | 10.91±0.03   | 10.56±0.14  | 10.4 ±0.2                                       | 180±41               | 26±8                |                       | 224±89                     | 284±47                | 1.27±0.52           | 0.0 ±0.12 | 22           |

<sup>a</sup> Aperture and position. C refers to center of nebula, N, S to north, south etc. of central star.

<sup>b</sup> Unless there is an entry in col. (6), the total flux is that appropriate to the larger of the two apertures where both are given.

<sup>c</sup> Entry if nebula observed with aperture smaller than nebular diameter, and value in col. (4) is not a total flux but is a surface flux appropriate to the aperture given in col. (3). See remarks for exceptions.

<sup>d</sup> Adopted H $\beta$  flux average of new and previous data: see remarks.

<sup>e</sup> H $\beta$  fluxes in parentheses are deduced from H $\alpha$  fluxes and the measured extinction.

<sup>f</sup> "neg." indicates that the formal upper limit is <0, that is, no detection.

Remarks to Table 1 are on next page.

## REMARKS TO TABLE 1

1. Kaler 1981a.
2. Data without errors: preliminary IRS.
3. Total flux is sum of observed regions. True flux may be higher because of faint envelope surrounding bright observed zones.
4.  $N/\alpha$  from Chopinet and Lortet-Zuckerman 1976, and Doroshenko and Kolotilov 1973.
5. Adopted  $H\beta$  flux in col. (6) from new data and Collins, Daub, and O'Dell 1961.
6. Faint outer envelope not included.
7. Included because of low stellar luminosity or large outer radius.
8. Adopted  $H\beta$  flux in col. (6) from new data and Collins, Daub, and O'Dell 1961.
9. Extinction from J. C. Cahn's (1982, private communication) dust model.
10. [N II] detection probably spurious.
11. Brightest area 9'E, 1'18"S of central star.
12. 35"E, 1'45"N of bright field star at SW edge of nebula.  $I(\lambda 4686)$  is mean of new value ( $13 \pm 11$ ), and those given by Chopinet

and Lortet-Zuckerman 1976, Kaler 1976, and Kondratyeva 1979. Stratification must be severe.

13. Lower bright bar. W: 3'S of central star (Jacoby 1981); E: 2'S, 3'E of central star.
14. Center of east arc.
15. Total  $H\beta$  flux mean of that derived from aperture-corrected 40" flux and that inferred from 4'  $H\alpha$  observation and the 40" extinction.
16. 4' data poor. Total  $H\beta$  flux mean of 4' observation and aperture-corrected 40"  $H\beta$ .
17. Abell 10.
18. Discovery by Kohoutek 1971.
19. Center of visible arc. Total flux refers only to arc.
20. Discovery by Longmore and Tritton 1980. Total  $H\beta$  flux calculated from  $H\alpha$  assuming  $c = 0$ .  $\phi$  in Table 5 is from this reference.
21. Discovery by Purgathofer and Weinberger 1980. N: 6'N of central star; C: 1'5"N of central star; S: 6'S of central star. Total  $H\beta$  flux calculated from diameter and mean surface brightness.
22. Abell 21. Observed 2'N, 2'E of central star. Total flux refers to visible arc; see Abell 1966.

The absolute  $H\beta$  and  $H\alpha$  fluxes appropriate to the apertures in column (3) are given in columns (4) and (5). If there are two entries for a nebula, that for the larger aperture gives the total flux (unless there is an entry in column 6; see below). If  $H\beta$  was not explicitly observed, this flux was computed from the  $H\alpha$  flux in column (5) and the  $H\alpha/H\beta$  ratio measured with either a smaller aperture or with the IRS. These converted  $H\beta$  fluxes are set into parentheses. If the nebula is larger than the largest aperture used, an estimate of the total absolute  $H\beta$  flux based on the surface flux and nebular diameter and structure is shown in column (6). Parentheses again show converted  $H\alpha$  fluxes. Column (6) always takes precedence over column (4) for total flux. In the cases of bi-lobed nebulae (NGC 2474-5, A24 and Jn-1, also A35) the total flux in column (6) is the sum of those measured for each lobe, converted again to  $H\beta$  where necessary. See the remarks for specific information and exceptions.

Relative fluxes on the scale  $I(H\beta) = 100$  are given in columns (7)-(11) for  $\lambda 3727$  [O II],  $\lambda 4686$  He II,  $\lambda 4959$  [O III],  $\lambda 6563$   $H\alpha$ , and  $\lambda 6584$  [N II]. The  $H\alpha/H\beta$  ratio given by column (10) will not always be the same as that derived from columns (4) and (5) because of weighting effects applied to different nights of observation. Column (12) explicitly presents the  $\lambda 6584$  [N II]/ $H\alpha$  ratios, here called  $N/\alpha$ . These values will be the same as ratios of column (11) to column (10), but the errors will be smaller since the errors in columns (7)-(11) must include the errors in the  $H\beta$  fluxes.

The logarithmic extinctions,  $c$ , derived from the  $H\alpha/H\beta$  ratios, the theoretical ratio of 2.85 (Brocklehurst 1971) and the Whitford (1958) reddening curve, are given in column (13). The remarks coded in column (14) are listed at the end of the table. The IRS data are not assigned errors at this time.

Table 1 represents a portion of all the nebulae actually observed at Prairie Observatory. Data on the smaller nebulae are being published separately (Kaler 1983b).

## b) Published Photometry

It is important to this study that the sample size be as large as possible, and consequently the observations of Table 1 are supplemented by data taken from the literature, including earlier results from Prairie Observatory. These are presented in Table 2, where again columns (1) and (2) give the common name and the Perek-Kohoutek (1967) designation. Columns (3) and (4) give the absolute  $H\beta$  fluxes and the references. All the old fluxes are converted to the modern photometry of Vega given by Oke and Schild (1970) and Hayes (1970). This requires that all the Wisconsin fluxes, or those based on them (OS, COAL, OD62, OD63, AF, P71, WB; see references to Table 2) be lowered by 0.02 in the log (see Shaw and Kaler 1982). All the KA2 fluxes measured at Prairie were raised by 0.07 in the log to conform to the new calibration of NGC 7027 by Shaw and Kaler (1982). Some of the published Prairie fluxes were also adjusted for known temperature effects. When possible, individual measurements are averaged. Errors are derived either from authors' remarks or from the comparison between sources.

The fluxes for  $\lambda 3727$  [O II] and  $\lambda 4686$  He II relative to  $F(H\beta) = 100$ , the  $\lambda 6584$  [N II]/ $H\alpha$  ratio ( $N/\alpha$ ), and the extinction constants are presented in columns (5)-(8), with the references supplied in column (9). An attempt is made to list relative fluxes representative of the whole nebula, although this can be rendered difficult because of stratification. Values are taken preferably from earlier wide aperture Prairie photometry, or they are averaged from the other references. The extinctions are generally found as before from the  $H\alpha/H\beta$  ratio, but when that is not available, or is not reliable, from  $H\gamma/H\beta$ , ratio data, or central star color. Errors assigned to both the absolute and relative fluxes, and to  $c$ , are taken either from the authors' statements, or are the mean error of the average. Errors are not assigned for single observational values.

TABLE 2  
COMPILED DATA FOR OTHER LARGE PLANETARIES

| Nebula<br>(1)         | PK<br>(2)           | Total<br>-log F(H $\beta$ )<br>(3) | I(H $\beta$ ) = 100  |                     | References<br>(4) | N/ $\alpha$<br>(7) | c<br>(8)                    | References<br>(9)                       |
|-----------------------|---------------------|------------------------------------|----------------------|---------------------|-------------------|--------------------|-----------------------------|---|
|                       |                     |                                    | 3727<br>[OII]<br>(5) | 4686<br>HeII<br>(6) |                   |                    |                             |   |
| NGC 246               | 118-74 <sup>1</sup> | 10.53 $\pm$ 0.05                   | <12                  | 121 $\pm$ 14        | KAZ               | <0.03              | 0.00                        | K, KAZ                                  |
| NGC 650               | 130-10 <sup>1</sup> | 10.68 $\pm$ 0.01                   | 500 $\pm$ 150        | 54 $\pm$ 7          | KAZ               | 1.91 $\pm$ 0.78    | 0.20 $\pm$ .15              | ACP, AC, C, M, MI73                     |
| NGC 1514              | 165-15 <sup>1</sup> | 10.98 $\pm$ 0.03                   |                      | 17 $\pm$ 9          | KAZ               |                    | 0.92 $\pm$ .10              | ACPG, C                                 |
| NGC 2371              | 189+19 <sup>1</sup> | 10.99 $\pm$ 0.01                   | 64 $\pm$ 16          | 93 $\pm$ 7          | KAZ, OD62         | 0.31 $\pm$ 0.08    | 0.11 $\pm$ .01              | ACPG, C, M, MI73, O, ORF, TPP           |
| NGC 2438              | 231+ 4 <sup>2</sup> | 11.04 $\pm$ 0.07                   | 320 $\pm$ 68         | 41 $\pm$ 3          | KAZ, OD63, P71    | 0.66               | 0.20                        | KAZ, TPP                                |
| NGC 2610              | 239+13 <sup>1</sup> | 11.38 $\pm$ 0.02                   | 13 $\pm$ 8           | 95 $\pm$ 10         | KAZ, OD63, P71    | <.01:              | 0.12 $\pm$ .03              | KAZ, TPP                                |
| NGC 3587              | 148+57 <sup>1</sup> | 10.42 $\pm$ 0.02                   | 342 $\pm$ 56         | 11 $\pm$ 1          | KAZ               |                    | 0.01                        | KAZ, M, TPP                             |
| NGC 4361              | 294+43 <sup>1</sup> | 10.53 $\pm$ 0.03                   | 6 $\pm$ 1            | 115 $\pm$ 5         | KAZ, OD62         | 0.006 $\pm$ 0.002  | 0.04                        | BAR, HAC, KAZ, TPP                      |
| <sup>a</sup> NGC 6445 | 8+ 3 <sup>1</sup>   | 11.23 $\pm$ 0.01                   | 353 $\pm$ 38         | 51 $\pm$ 12         | OD63, P71         | 1.12:              | 0.50 $\pm$ .10 <sup>b</sup> | A, ACCG, C, MA                          |
| NGC 6563              | 358- 7 <sup>1</sup> | 10.95 $\pm$ 0.03                   | 15 $\pm$ 15          | 15 $\pm$ 15         | OD63, P71         | 2.3                | 0.03 $\pm$ .10              | KGH                                     |
| <sup>a</sup> NGC 6720 | 63+13 <sup>1</sup>  | 10.08 $\pm$ 0.03                   | 500 $\pm$ 150        | 30 $\pm$ 5          | COAL              | 1.30 $\pm$ 0.24    | 0.27 $\pm$ .05              | AW, ACP, BAR, C, CAM, HM, LA, P, TP, W  |
| NGC 6772              | 33- 6 <sup>1</sup>  | 11.67 $\pm$ 0.02                   | 140                  | 31 $\pm$ 10         | OD63              |                    | 1.06 $\pm$ .10              | M                                       |
| NGC 6781              | 41- 2 <sup>1</sup>  | 11.27 $\pm$ 0.04                   | 360 $\pm$ 70         | 22 $\pm$ 5          | COAL              | 0.08               | 0.94 $\pm$ .20              | AKI, K, M                               |
| NGC 6842              | 65+ 0 <sup>1</sup>  | 11.73 $\pm$ 0.03                   | <30                  | 44 $\pm$ 10         | OD63              | 1.78 $\pm$ 0.46    | 0.97 $\pm$ .10              | K                                       |
| NGC 6853              | 60- 3 <sup>1</sup>  | 9.46 $\pm$ 0.06                    | 600 $\pm$ 150        | 33 $\pm$ 6          | OS                |                    | 0.02 $\pm$ .10              | AKI, C, HM <sup>a</sup> , M, MI73, SAB3 |
| NGC 7048              | 88- 1 <sup>1</sup>  | 11.41 $\pm$ 0.01                   |                      | 46 $\pm$ 10         | OD63              | 1.26               | 0.88 $\pm$ .14              | ORF                                     |
| NGC 7139              | 104+ 7 <sup>1</sup> | 11.80 $\pm$ 0.02                   | 280                  | 18 $\pm$ 9          | OD63              |                    | 0.54 $\pm$ .20              | M                                       |
| NGC 7293              | 36-57 <sup>1</sup>  | 9.37 $\pm$ 0.02                    | 385 $\pm$ 38         | 10 $\pm$ 5          | OD62              | 1.38 $\pm$ 0.21    | 0.04                        | HAW2, LO, M, WR, Y                      |
| IC 1454               | 117+18 <sup>1</sup> | 12.17 $\pm$ 0.03                   | 79                   | 24 $\pm$ 4          | KAZ               |                    | 0.20 $\pm$ .10              | KAZ, KGH                                |
| <sup>a</sup> IC 4406  | 319+15 <sup>1</sup> | 10.76 $\pm$ 0.02                   | 510 $\pm$ 140        | 7 $\pm$ 2           | AF, P71           | 1.42               | 0.25 $\pm$ .15              | AF, TPP                                 |
| A 36                  | 318+41 <sup>1</sup> | 10.86 $\pm$ 0.03                   | <10                  | 118 $\pm$ 10        | KAZ               |                    | 0.0                         | KAZ                                     |
| A 43                  | 36+17 <sup>1</sup>  | 12.40 $\pm$ 0.07                   |                      | 93 $\pm$ 8          | KH                | 0.14 $\pm$ .04     | 0.38 $\pm$ .22              | KH                                      |
| A 50                  | 78+18 <sup>1</sup>  | 12.02 $\pm$ 0.02                   | 105 $\pm$ 16         | 34 $\pm$ 2          | KH                | 0.28 $\pm$ .05     | 0.0 $\pm$ 0.04              | KH                                      |
| Ba 1                  | 171-25 <sup>1</sup> | 12.44 $\pm$ 0.02                   |                      | 90 $\pm$ 10         | KAZ               | <.02:              | 0.76 $\pm$ .20              | ORF                                     |
| Sp 1                  | 329+ 2 <sup>1</sup> | 11.50 $\pm$ 0.02                   |                      |                     | WB                |                    | 0.21 $\pm$ .02              | WB                                      |

<sup>a</sup> Included because of low stellar luminosity or large outer radius.

<sup>b</sup> Error increased to (+0.5, -0.1) for later analysis; see text.

## REFERENCES

- A: Aller 1951.  
 AC: Aller and Czyzak 1979.  
 ACCG: Aller *et al.* 1973.  
 ACP: Aller and Czyzak (unpublished).  
 ACPG: Aller and Czyzak (unpublished).  
 AF: Aller and Faulkner 1964.  
 AKI: Kaler, Aller, and Czyzak 1976.  
 AW: Aller and Walker 1965.  
 BAR: Barker 1978.  
 C: Chopinet 1963.  
 CAM: Campbell 1968.  
 COAL: Collins, Daub, and O'Dell 1961.  
 HAC: Heap, Aller and Czyzak 1969.
- HAW2: Hawley 1978.  
 HM: Hawley and Miller 1977.  
 HM4: Hawley and Miller 1978.  
 K: Kaler 1983a.  
 KAZ: Kaler 1976a.  
 KGH: Kaler, Gallagher, and Hunter 1983.  
 KH: Kaler and Hartkopf 1981.  
 LA: Liller and Aller 1963.  
 LO: Louise 1969.  
 M: Minkowski 1942.  
 MA: Minkowski and Aller 1956.  
 MI73: Miller 1973.
- O: O'Dell 1963b.  
 OD62: O'Dell 1962.  
 OD63: O'Dell 1963c.  
 ORF: D'Odorico, Rubin, and Ford 1973.  
 OS: Osterbrock and Stockhausen 1961.  
 P71: Perik 1971.  
 PTP: Peimbert and Torres-Peimbert 1971.  
 SAB3: Sabbadin 1977.  
 TPP: Torres-Peimbert and Peimbert 1978.  
 W: White 1952.  
 WB: Webster 1969.  
 WR: Warner and Rubin 1975.  
 Y: Young 1982.

### c) Systematic Errors

Note in Table 1 that there are some measured values of  $H\alpha/H\beta$  that are significantly less than the minimum possible 2.85, which indicates the presence of a source of systematic error. As pointed out above, radial velocities are not known for most of the nebulae. Since the  $[N II]$  line is on the wing of the  $H\alpha$  filter, and vice versa, a true velocity other than the assumed value of zero will result in oppositely directed errors in  $H\alpha$  and  $[N II]$ . For example, the low  $H\alpha$  flux (relative to that for  $H\beta$ ) for Abell 20 is consistent with the high  $[N II]$  flux and such a systematic error. Recent IIDS photometry of Abell 20 at Kitt Peak indicates virtually no  $[N II]$  line, certainly none as strong as shown in Table 1. But in order to bring the  $[N II]$  line to zero, we would have to adopt a radial velocity of  $+200 \text{ km s}^{-1}$ , which seems unlikely. The IIDS spectrophotometry shows that the  $[N II]$  detection for A15 is also probably spurious. Field stars that may have  $H\alpha$  and  $H\beta$  absorption lines could be part of the problem. Thus the reader might wish to allow an additional error for observations made with the 4' aperture of  $\pm 0.03$  in  $\log F(H\alpha)$  and  $\pm 0.02$  in  $\log F(H\beta)$ , to be added quadratically to the errors in Table 1.

Generally, however, any systematic errors that may be present are not deleterious to the goals of this program. The  $H\alpha/H\beta$  intensity ratios agree with those derived from unpublished reticon spectrophotometry of nine nebulae to within  $\pm 10\%$ , where the error is added into the formal errors of the  $H\alpha$  and  $[N II]$  fluxes. The  $[N II]/H\alpha$  ratios,  $(N/\alpha)$ , cannot be similarly evaluated because of severe stratification effects, but there is broad agreement with the reticon data to within a factor of 2. The most serious problem will occur for weak  $[N II]$  lines, which must be checked by improved spectrophotometry.

### d) Calibration of Photographic Fluxes

Until this paper, few photoelectrically derived absolute fluxes have been measured for large nebulae. Most of the analyses of these planetaries have rested on photographic surface brightnesses, estimated usually from the Palomar Sky Survey, and converted to  $H\beta$  or  $H\alpha + [N II]$  fluxes; see for example Abell (1966). Cahn and Kaler (1971) present an extensive list of these estimated converted photographic fluxes.

The new photoelectric fluxes presented here can be used to recalibrate the photographic work. Although they are only employed in this paper as a check on the fluxes of two nebulae, the corrected photographic fluxes may be of general use to others. Figure 1 shows  $\log F_{\text{red}}$  from Cahn and Kaler (1971), as derived from Abell (1966), plotted as circles against  $\log F(H\alpha + [N II])$  from Table 1. The nebulae whose total fluxes required an aperture correction, or which are the sums of the fluxes of two lobes (entries in col. [6] of Table 1), are represented by filled circles. We see that the Abell-derived fluxes are too bright by, on the average, 0.23 in the log, and that there seems to be little difference between the filled and open circles. A least squares fit

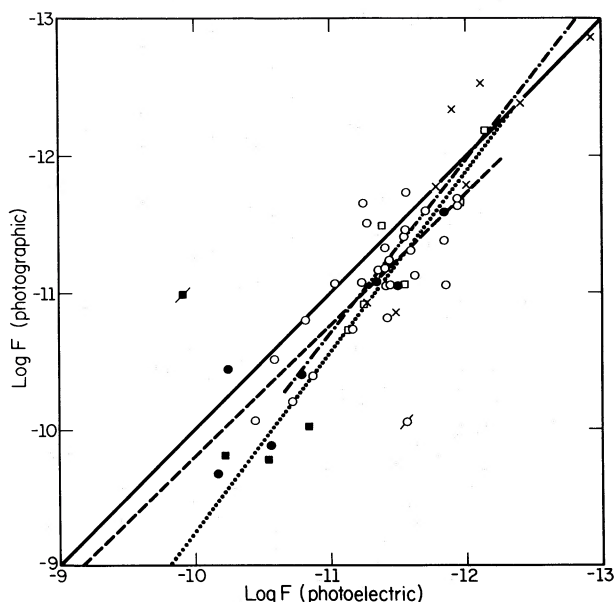


FIG. 1.—Photographic fluxes from Cahn and Kaler 1971 plotted against the analogous new photoelectric fluxes. Circles:  $\{F(H\alpha) + F[N II]\}$  from Abell 1966; boxes:  $\{F(H\alpha) + F[N II]\}$  from Kohoutek (Perek and Kohoutek 1967); Xs:  $F(H\beta)$  from Kohoutek (Perek and Kohoutek 1967). Filled symbols indicate nebulae for which an aperture correction was required. Solid line: 45° line; dashed line: least squares fit to the Abell 1966 data; dotted line: fit to the red Kohoutek data; dot-dash line: fit to the blue Kohoutek data. Symbols with a diagonal slash were excluded from the least squares fit.

through all the Abell points (excluding the anomalous point for A72) yields the calibration relation:

$$\text{Abell: } \log F(H\alpha + [N II]) = 1.036 \log F(\text{red}) + 0.157. \quad (1)$$

The mean error for any given value of converted Abell flux is  $\pm 0.19$  in the log, or  $\pm 54\%$ .

Similar Kohoutek (see Perek and Kohoutek 1967) red fluxes are plotted in Figure 1 as boxes, and average 0.36 in the log brighter than the photoelectric. The least-squares calibration relation, excluding the one anomalous nebula (Sh 2-71), is:

$$\begin{aligned} \text{Kohoutek: } \log F(H\alpha + [N II]) \\ = 0.766 \log F(\text{red}) - 2.90. \quad (2) \end{aligned}$$

The mean error for a given value is  $\pm 0.24$  in the log, or  $\pm 72\%$ .

Finally, the estimated Kohoutek  $\log F(H\beta)$  are plotted in Figure 1 as Xs (the lower two are aperture-corrected points), and average only 0.04 brighter than the photoelectric, with a larger individual mean error of  $\pm 0.33$  in the log, or about a factor of 2. The least squares calibration is

$$\begin{aligned} \text{Kohoutek: } \log F(H\beta) \\ = 0.79 \log F(\text{photographic } H\beta) - 2.52. \quad (3) \end{aligned}$$

A least squares fit to all points (less the two with anomalous positions) yields

$$\log F(\text{photoelectric}) = 0.89 \log F(\text{photographic}) - 1.42. \quad (4)$$

These relations applied to the photographic fluxes of two of the bi-lobed nebulae, A24 and Jn-1, give average fluxes a factor of 2 higher than the photoelectric, possibly a significant difference, implying that some outlying nebulosity not included in the photometry may be important.

The major problem with using the red photographic fluxes is not the conversion, but the presence of the [N II] lines. Abell (1966) assumed from an early study by White (1952) that  $F(\lambda 6584 \text{ [N II]})/F(\text{H}\alpha) = \text{N}/\alpha = 0.43$ , as did Cahn and Kaler (1971), so that  $F(\text{H}\alpha) = 0.65 F(\text{red})$ . Examination of column (12) of Table 1 shows that  $\text{N}/\alpha$  varies widely, from zero to a maximum observed value of 4.2 for Abell 24. Thus  $\log F(\text{H}\alpha)$  can be over- or underestimated by up to factors of 4.3 and 1.5, respectively. The principal result is a gross overestimate of Zanstra temperature (see § IIIe) for some stars. All the stars in Abell's (1966) Table 6 with  $\log T_{\min} > 5.3$ , whose nebulae have been observed here, A13, A21 = Ym 29, A24, A71, and A80, have very high  $\text{N}/\alpha$ . It is quite possible to pick out other nebulae, such as A29, that should exhibit strong [N II] lines.

#### e) Comparison with Radio Fluxes

The photometry in Tables 1 and 2 can be further checked by comparing the listed extinction constants, generally derived from the Balmer line ratios, with those found from the ratios of radio flux densities and the  $\text{H}\beta$  fluxes. The results are presented in Table 3, where columns (1) and (2) give the common names and the nebular optical extinctions simply repeated from Tables 1 and 2. The radio/ $\text{H}\beta$  extinctions are presented in column (3) and are derived from radio data given by the references in column (4), the  $\text{H}\beta$  fluxes of Tables 1 and 2, the formulation given by Cahn and Kaler (1971), an assumed electron temperature of 10,000 K, and  $\text{He}/\text{H} = 0.10$ , where  $\text{He}^{++}/\text{H}^+$  is calculated from Tables 1 and 2 and Brocklehurst (1971). The radio data are preferably the 5 mHz data of Milne and Aller (1975) and Milne (1979); otherwise, they are the same as used by Cahn (1976). Reference notes are in column (4), where the key and the radio frequencies used are listed at the end of the table. Column (5) gives a third value of extinction derived from the color excess of the central star, assuming an unreddened color of  $(B-V)_0 = -0.38$  for the Rayleigh-Jeans tail of the blackbody curve (see Cahn 1983). These are derived from the data of Table 5, are needed here for comparison, and will be considered again in § IIIa.

For the majority of the nebulae, the agreement between columns (2) and (3) is satisfactory: the error bars overlap, or they can be made to do so with a not unreasonable increase in the errors. The others generally divide into two interesting groups. For a set of five high-excitation

planetaries near the top of the table, the radio  $c$  is considerably in excess of the optical. Because  $I(\lambda 4686)$  is comparable to  $I(\text{H}\beta)$  for all these, the difference is logically consigned to electron temperature: column (6) gives the value of  $T_e$  needed to bring the radio and optical extinctions to within one another's error bars (a method first used by Ko 1967). The [O III] electron temperatures are given in parentheses for comparison. There is general qualitative agreement between the "radio" and the "[O III]" temperatures in that all are quite high. But with one exception the former are over 20,000 K and are above the latter. Because of the high excitation of this set of nebulae, the [O III] temperature is appropriate only to the outer zones, near the periphery, whereas the radio temperature, derived from hydrogen emission, is more typical of the nebula as a whole. Although the values given here are subject to considerable error, the difference between the two types of temperatures is clearly consistent with a gradient and high central nebular electron temperature. Aller *et al.* (1979) in fact predict just such a situation for nebulae such as NGC 4361.

For the other group, the radio fluxes are clearly in error (see col. [6]). For A15, A20, and A36 the stellar extinction (col. [5]) confirms the nebular optical. A35 is at high latitude, and the extinction is certainly low: see also Jacoby (1981). Part of the difference for A36 might also be ascribed to a high electron temperature for this very high excitation object. For Sh 2-71, the preliminary IRS measurements confirm the optical value in column (2).

This discussion leaves one outstanding anomaly, NGC 6445, for which the radio  $c$  is much in excess of the optical. This is a particularly important object since it often provides extreme values of parameters. Some of the difference can be accounted for by the high  $\text{He}/\text{H}$  ratio ( $\approx 0.22$ ) and electron temperature (15,000 K) found by Aller *et al.* (1973). But even at 20,000 K, the radio  $c$  can be reduced only to 1.0. The two available measurements of the  $\text{H}\beta$  flux agree; and other radio measurements are quite consistent with the one presented here (see Higgs 1971). The  $\text{H}\alpha/\text{H}\beta$  ratio has never been measured, and the optical extinction is derived from the  $\text{H}\delta:\text{H}\gamma:\text{H}\beta$  ratios, which are less precise. However, they have been measured by three independent studies (see Kaler 1976b), and all agree that  $c$  is  $\leq 0.50$ , the value adopted here. The less precise  $\lambda 5876/\lambda 4471 \text{ He I}$  ratio yields 0.8, the value adopted as most likely by Aller *et al.* (1973). Resolution of the problem requires the badly needed  $\text{H}\alpha/\text{H}\beta$  ratio. In the analysis of the data,  $c = 0.5(+0.5, -0.1)$  will be used for this object. Further discussion and analysis of the nebulae is carried out with the extinctions in Tables 1 and 2.

#### f) Coordinates of the Nebulae

Most of the nebulae could not be seen at the telescope and had to be located by blind offset from a nearby star. The 1950 coordinates of the central stars (or of the optical centers of the nebular images) measured on the Palomar Sky Survey from SAO stars are given in

TABLE 3  
COMPARISON OF EXTINCTION CONSTANTS,  $C$ , COMPUTED FROM THREE METHODS

| NEBULA<br>(1) | NEBULAR<br>OPTICAL<br>(2) | RADIO                   |             | STELLAR<br>( $B-V$ ) <sub>0</sub> = -0.38<br>(5) | $T_e$ (K) <sup>a</sup><br>and Remarks<br>(6) |
|---------------|---------------------------|-------------------------|-------------|--|--|
|               |                           | $T_e = 10,000$ K<br>(3) | REF.<br>(4) |  |  |
| NGC 246       | 0.00 <sup>b</sup>         | 0.31 ± 0.06             | MA, M       | 0.01   | 25000 ( $T_e$ [O III] = 16,000) <sup>d</sup> |
| NGC 650       | 0.20 ± 0.15 <sup>b</sup>  | 0.13 ± 0.13             | KK          | ...  | ...  |
| NGC 1360      | 0.00 <sup>c</sup>         | 0.33 ± 0.11             | MA          | 0.13   | 23000 ( $T_e$ [O III] = 18,000) <sup>d</sup> |
| NGC 1514      | 0.92 ± 0.10 <sup>b</sup>  | 0.95 ± 0.09             | KK          | ...  | ...  |
| NGC 2371      | 0.11 ± 0.01 <sup>b</sup>  | 0.38 ± 0.08             | HI          | ...  | 21000 ( $T_e$ [O III] = 15,000) <sup>e</sup> |
| NGC 2438      | 0.20 <sup>b</sup>         | 0.48 ± 0.10             | MA          | ...  | ...  |
| NGC 2610      | 0.12 ± 0.03 <sup>b</sup>  | 0.35 ± 0.10             | MA          | 0.25   | 16000 ( $T_e$ [O III] = 17,000) <sup>e</sup> |
| NGC 3587      | 0.01 <sup>b</sup>         | 0.10 ± 0.18             | HI          | 0.00   | ...  |
| NGC 4361      | 0.04 <sup>b</sup>         | 0.27 ± 0.06             | MA          | 0.11   | 20000 ( $T_e$ [O III] = 19,000) <sup>e</sup> |
| NGC 6058      | 0.18 ± 0.19               | ...                     | ...         | 0.10   | ...  |
| NGC 6445      | 0.50 ± 0.10 <sup>b</sup>  | 1.26 ± 0.05             | MA          | ...  | Unexplained difference; see text             |
| NGC 6563      | 0.03 ± 0.10 <sup>b</sup>  | 0.34 ± 0.08             | MA          | ...  | ...  |
| NGC 6720      | 0.27 ± 0.05 <sup>b</sup>  | 0.13 ± 0.08             | HI          | 0.10   | ...  |
| NGC 6772      | 1.06 ± 0.10 <sup>b</sup>  | 1.07 ± 0.07             | MA          | ...  | ...  |
| NGC 6781      | 0.94 ± 0.20 <sup>b</sup>  | 1.29 ± 0.06             | MA          | 1.89   | Stellar magnitudes questionable              |
| NGC 6842      | 0.97 ± 0.10 <sup>c</sup>  | 1.32 ± 0.19             | HI          | 0.07   | Stellar magnitudes questionable              |
| NGC 6853      | 0.02 ± 0.10 <sup>b</sup>  | 0.06 ± 0.06             | MA          | 0.13   | ...  |
| NGC 6894      | 0.92 ± 0.16               | 0.61 ± 0.22             | HI          | ...  | ...  |
| NGC 7048      | 0.88 ± 0.14 <sup>b</sup>  | 1.03 ± 0.11             | KK          | ...  | ...  |
| NGC 7094      | 0.16 <sup>c</sup>         | <0.19                   | M           | 0.18   | ...  |
| NGC 7293      | 0.04 <sup>b</sup>         | 0.04                    | MA          | 0.05   | ...  |
| IC 972        | 0.08 ± 0.08               | <0.68                   | M           | ...  | ...  |
| IC 4406       | 0.25 ± 0.15 <sup>b</sup>  | 0.30 ± 0.15             | MA          | ...  | ...  |
| A13           | 2.21 ± 0.90               | ...                     | ...         | 0.80   | ...  |
| A15           | 0.04 ± 0.15               | 1.22 ± 0.17             | M           | 0.10   | Radio weak and incorrect                     |
| A20           | 0.00                      | 1.25 ± 0.18             | M           | 0.15   | Radio weak and incorrect                     |
| A24           | 0.48 ± 0.28               | 0.56 ± 0.22             | MA, M       | 0.24   | ...  |
| A30           | 0.00                      | ...                     | ...         | 0.44   | Internal dust; see Greenstein 1981           |
| A31           | 0.00 ± 0.41               | ...                     | ...         | 0.10   | ...  |
| A33           | 0.00 ± 0.28               | 0.00 ± 0.50             | MA, M       | 0.31   | ...  |
| A34           | 0.00 ± 0.08               | <0.77                   | M           | 0.17   | ...  |
| A35           | 0.00                      | 1.22 ± 0.20             | M           | ...  | Radio Incorrect, large radio corr.           |
| A36           | 0.00 <sup>f</sup>         | 0.61 ± 0.11             | M           | 0.07   | High $T_e$ ; large radio corr.               |
| A39           | 0.00                      | ...                     | ...         | 0.07   | ...  |
| A43           | 0.38 ± 0.22               | ...                     | ...         | 0.28   | ...  |
| A51           | 0.00 ± 0.19               | ...                     | ...         | 0.36   | Internal dust?                               |
| A65           | 0.19 ± 0.24               | 0.15 ± 0.47             | MA, M       | 0.41   | ...  |
| A70           | 0.23 ± 0.31               | 0.89 ± 0.53             | M           | ...  | ...  |
| A71           | 1.12 ± 0.15               | ...                     | ...         | 1.06   | ...  |
| A72           | 0.00 ± 0.06               | ...                     | ...         | 0.07   | ...  |
| A78           | 0.04 ± 0.42               | ...                     | ...         | 0.24   | ...  |
| A84           | 0.42 ± 0.20               | ...                     | ...         | 0.79   | Prelim. IRS $c = 0.27$ confirms optical      |
| Ba 1          | 0.76 ± 0.20 <sup>b</sup>  | 0.98 ± 0.22             | MA          | ...  | ...  |
| Jn 1          | 0.00                      | ...                     | ...         | 0.00   | ...  |
| K1 7          | 0.27                      | <0.63                   | M           | ...  | ...  |
| K1 16         | 0.00 ± 0.26               | ...                     | ...         | 0.00   | ...  |
| M3 3          | 0.43 ± 0.14               | <1.1                    | M           | ...  | ...  |
| Sh2 71        | 1.45 ± 0.21               | 0.97 ± 0.09             | MA          | 1.41 <sup>g</sup>                                | Prelim. IRS, $c = 1.7$ confirms optical      |
| Sp 1          | 0.21 ± 0.02 <sup>b</sup>  | 0.45 ± 0.11             | MA          | ...  | ...  |
| Ym 29         | 0.00 ± 0.12               | 0.39 ± 0.21             | MA          | 0.08   | ...  |

<sup>a</sup>  $T_e$  required such that radio  $c$  includes optical within the error bars.

<sup>b</sup>  $c$  taken from other than filter photometry.

<sup>c</sup>  $c$  taken from preliminary Intensified Reticon Scanner (IRS) reductions.

<sup>d</sup>  $T_e$ [O III] from preliminary IRS reductions.

<sup>e</sup> Torres-Peimbert and Peimbert 1977; Aller *et al.* 1979 find 23,000 K.

<sup>f</sup> Assumed to be zero from the high galactic latitude.

<sup>g</sup> Taken from Kohoutek 1979; not true central star.

#### REFERENCES

- HI: Higgs 1971, 6.63 mHz (NGC 2371, NGC 6720); 10.63 mHz (NGC 3587, NGC 6842); 3.24 mHz (NGC 6894).  
 KK: Kaftan-Kassim 1969, 5 mHz.  
 M: Milne 1979, 5 mHz.  
 MA: Milne and Aller 1975, 5 mHz.

Table 4. Where possible, two nearby SAO stars were used, and an error is assigned to the mean coordinates of the nebula. The average error is  $\pm 3''$ , consistent with the measurement precision of 0.05 mm. These coordinates are frequently a significant improvement over earlier published values, especially for the Abell nebulae. The new values agree quite well with those measured by Kohoutek (see Perek and Kohoutek 1967).

### III. ANALYSIS

The data in Tables 1 and 2 are used here to derive spatial parameters of the nebulae such as distances and radii, properties of the central stars, specifically temperatures and luminosities, and physical properties of the nebulae, notably the N/O ratios and measures of optical depth. Before such analyses can proceed we must compile considerably more pertinent data: central star magnitudes, nebular angular radii, and information on the nebular structures. These input data and the results of the various analyses are presented in detail in Table 5, in which the separate lists of Tables 1 and 2 are now merged.

#### a) Central Star Magnitudes

The blue and visual magnitudes adopted for the central stars are given in columns (2) and (3) of Table 5, with references in column (4). An attempt is made to derive the most self-consistent set, but of necessity, they come from a wide variety of sources, one going back to 1918! The most accurate are the photoelectric values, from AB (those with errors  $\leq 0.20$ ), KA3, K81, and SL, which were usually preferentially selected in that order (see the References to Table 5). But photoelectric photometry is available generally only for the brighter stars, and to avoid serious selection effects the less accurate photographic magnitudes absolutely must be included. Even the photoelectric values can be subject to considerable error because of contamination by the surrounding nebula: the smaller and brighter the object, the poorer they will be. The blue photographic magnitudes, preferably taken from the extensive lists of AB and KO, are considered to be the equivalent of photoelectric  $B$ . The magnitudes for the nuclei of NGC 2438, K1-14, and K1-22 are taken from Kaler and Feibelman (1983), who derived them from the stellar flux at 1500 Å, as determined from *IUE* data. That for the latter refers to a new identification of the central star.

The problem of the mix in magnitudes is in part relieved by placing realistic errors on the values. The brighter AB magnitudes are assigned errors of  $\pm 0.01$  mag, escalating to  $\pm 0.05$  mag for the fainter stars. Errors on the SL magnitudes, which are generally measured for brighter nebulae, again start at  $\pm 0.01$  mag, but rise to  $\pm 0.2$  mag depending on the brightness of the background nebula. Those from KF are set at  $\pm 0.2$  mag, reflecting uncertainty in the assumed energy distribution and extinction needed to convert fluxes from 1500 Å to 5500 Å. Single photographic values from AB and KO are assigned  $\pm 0.4$  mag (Hayman, Hazard, and Sanitt 1979). If AB and KO photographic values are averaged,

TABLE 4  
MEASURED CENTRAL COORDINATES FOR SELECTED NEBULAE

| Nebula   | $\alpha(1950.0)$                    | $\delta(1950.0)$  |
|----------|-------------------------------------|-------------------|
| NGC 246  | 0 <sup>h</sup> 44 <sup>m</sup> 32.9 | -12°08'44"        |
| NGC 1360 | 3 31 07.6                           | -26 02 15         |
| NGC 2438 | 7 39 32.4                           | -14 37 02         |
| NGC 2474 | 7 53 59.9                           | +53 33 24         |
| NGC 2610 | 8 31 04.9                           | -15 58 38         |
| NGC 6058 | 6 02 43.4 $\pm$ 0.2                 | +40 49 04 $\pm$ 1 |
| NGC 6772 | 19 11 51.6 $\pm$ 0.3                | -02 47 41 $\pm$ 5 |
| NGC 6781 | 19 16 01.7 $\pm$ 0.1                | +06 26 52 $\pm$ 1 |
| NGC 6842 | 19 53 01.4 $\pm$ 0.1                | +29 09 23 $\pm$ 1 |
| NGC 7094 | 21 34 28.0                          | +12 33 48         |
| NGC 7139 | 21 44 51.2                          | +63 33 21         |
| NGC 7293 | 22 26 55.0 $\pm$ 0.1                | -21 05 38 $\pm$ 7 |
| A2       | 00 42 40.6 $\pm$ 0.2                | +57 41 10 $\pm$ 1 |
| A3       | 02 08 19.1 $\pm$ 0.3                | +63 55 02 $\pm$ 4 |
| A4       | 02 42 09.6 $\pm$ 0.3                | +42 20 31 $\pm$ 3 |
| A5       | 02 48 44.9 $\pm$ 0.2                | +50 23 35 $\pm$ 2 |
| A6       | 02 54 31.0                          | +64 18 10         |
| A8       | 05 03 11.4 $\pm$ 0.3                | +39 04 09 $\pm$ 1 |
| A13      | 06 02 08.4 $\pm$ 0.2                | +03 56 42 $\pm$ 6 |
| A15      | 06 24 59.9 $\pm$ 0.1                | -25 21 01 $\pm$ 1 |
| A16      | 06 39 18.9                          | +61 50 26         |
| A20      | 07 20 22.1                          | +01 51 27         |
| A28      | 08 37 37.8                          | +58 24 37         |
| A30      | 08 44 04.4                          | +18 03 35         |
| A31      | 08 51 31.7                          | +09 05 25         |
| A33      | 09 36 37.1                          | -02 34 57         |
| A34      | 09 43 10.0 $\pm$ 0.3                | -12 56 22 $\pm$ 3 |
| A36      | 13 37 57.4                          | -19 37 47         |
| A39      | 16 25 32.2                          | +28 01 12         |
| A43      | 17 51 11.1                          | +10 37 53         |
| A46      | 18 29 18.7 $\pm$ 0.2                | +26 54 05 $\pm$ 3 |
| A51      | 18 58 06.0 $\pm$ 0.2                | -18 16 33 $\pm$ 5 |
| A53      | 19 04 19.2 $\pm$ 0.2                | +06 19 13 $\pm$ 2 |
| A62      | 19 30 56.0 $\pm$ 0.3                | +10 30 29 $\pm$ 1 |
| A65      | 19 43 34.3 $\pm$ 0.2                | -23 15 36 $\pm$ 1 |
| A70      | 20 28 52.7                          | -07 15 32         |
| A71      | 20 30 46.5 $\pm$ 0.3                | +47 10 48 $\pm$ 3 |
| A72      | 20 47 40.1                          | +13 22 15         |
| A73      | 20 55 07.5 $\pm$ 0.3                | +57 14 21 $\pm$ 6 |
| A75      | 21 25 11.3 $\pm$ 0.1                | +62 40 23 $\pm$ 3 |
| A78      | 21 33 20.1 $\pm$ 0.2                | +31 28 18 $\pm$ 1 |
| A79      | 22 24 21.5 $\pm$ 0.1                | +54 34 23 $\pm$ 1 |
| A80      | 22 32 43.8                          | +52 10 32         |
| A82      | 23 43 20.6 $\pm$ 0.5                | +56 47 21 $\pm$ 6 |
| A84      | 23 45 16.0 $\pm$ 0.4                | +51 07 17 $\pm$ 6 |
| Ba 1     | 03 50 42.3 $\pm$ 0.4                | +19 20 37 $\pm$ 1 |
| BV 3     | 01 49 41.2                          | +56 09 34         |
| Jn 1     | 23 33 24.1                          | +30 11 26         |
| K1 7     | 05 29 03.8 $\pm$ 0.2                | +06 53 54 $\pm$ 4 |
| K1 14    | 17 40 29.5                          | +21 28 11         |
| K1 16    | 18 21 35.3                          | +64 20 30         |
| K1 20    | 23 36 44.6                          | +47 55 54         |
| K1 22    | 11 24 17.5                          | -34 05 44         |
| K2 1     | 05 03 56.2                          | +30 46 07         |
| K3 27    | 19 12 30.9 $\pm$ 0.2                | +28 35 27 $\pm$ 3 |
| M2 51    | 22 14 15.6                          | +57 13 42         |
| M2 55    | 23 29 41.0                          | +70 05 40         |
| M3 3     | 07 24 06.1 $\pm$ 0.2                | -05 15 49 $\pm$ 3 |
| PW 1     | 06 15 23.2                          | +55 37 59         |
| Sh 2 71  | 18 58 28.7 $\pm$ 0.2                | +02 05 05 $\pm$ 1 |
| Ym 29    | 07 26 14.5                          | +13 20 44         |

TABLE 5  
TEMPERATURES, LUMINOSITIES, AND N/O RATIOS

| Nebula<br>(1) | B<br>(2)   | V<br>(3)   | Ref<br>(4) | $\theta''$<br>(5) | $\xi$<br>(6) | $D_{\text{kpc}}$<br>(7) | $R_{\text{pc}}$<br>(8) | $Z_{\text{kpc}}$<br>(9) | $10^{-3}$                      |                                  | $T(\text{HeII})/\text{K}$<br>(11) | $T(\text{HeI})/\text{K}$<br>(12) | $L(\text{H})/L_{\odot}$<br>(13) | $L(\text{HeII})/L_{\odot}$<br>(14) | N/O<br>$T=10^4\text{K}$<br>(15) | He/H<br>(16) | Class<br>(17) |
|---------------|------------|------------|------------|-------------------|--------------|-------------------------|------------------------|-------------------------|--------------------------------|----------------------------------|-----------------------------------|----------------------------------|---------------------------------|------------------------------------|---------------------------------|--------------|---------------|
|               |            |            |            |                   |              |                         |                        |                         | $T(\text{H})/\text{K}$<br>(10) | $T(\text{HeI})/\text{K}$<br>(11) |                                   |                                  |                                 |                                    |                                 |              |               |
| NGC 246       | 11.58±0.01 | 11.95±0.01 | SL         | 125               | 1.0          | 0.53                    | 0.32                   | -0.51                   | 33±1                           | 85±2                             | 2.60±0.09                         | H                                | 57±1                            | 739±35                             |                                 |              | C             |
| NGC 650       | 15.90±0.5  | 16.30±0.5  | KA3        | 36                | 0.5          | 1.10                    | 0.19                   | -0.20                   | 131±27                         | 157±17                           | 1.19±0.28                         |                                  | 220±47                          | 534±105                            | 0.50                            | 0.131        | B             |
|               |            |            |            | 69                | 0.5          | 0.74                    | 0.25                   | -0.14                   |                                |                                  |                                   |                                  | 147±21                          | 245±48                             |                                 |              |               |
|               |            |            |            | 36                | 1.0          |                         |                        |                         | 98±19                          | 135±13                           | 1.38±0.30                         |                                  | 138±14                          | 348±78                             |                                 |              |               |
|               |            |            |            | 69                | 1.0          |                         |                        |                         |                                |                                  |                                   |                                  | 63±6                            | 159±36                             |                                 |              |               |
| NGC 1360      | 11.06±0.01 | 11.35±0.01 | SL         | 198               | 1.0          | 0.35                    | 0.33                   | -0.28                   | 34±2                           | 85±3                             | 2.48±0.16                         | H                                | 47±2                            | 536±28                             |                                 |              | C             |
| NGC 1514      |            |            |            | 64                |              | 0.64                    | 0.20                   | -0.17                   |                                |                                  |                                   |                                  |                                 |                                    |                                 |              |               |
|               |            |            |            | 88                |              | 0.53                    | 0.23                   | -0.14                   |                                |                                  |                                   |                                  |                                 |                                    |                                 |              |               |
| NGC 2371      | 14.70±0.10 | 14.80±0.10 | KA3        | 27                | 0.5          | 1.57                    | 0.20                   | 0.53                    | 62±3                           | 118±4                            | 1.91±0.11                         | H                                | 217±5                           | 1350±110                           | 0.80±0.25                       | 0.126        | B             |
|               |            |            |            | 49                | 0.5          | 1.10                    | 0.26                   | 0.37                    |                                |                                  |                                   |                                  | 106±2                           | 659±52                             |                                 |              |               |
|               |            |            |            | 27                | 1.0          |                         |                        |                         | 50±2                           | 105±3                            | 2.11±0.10                         |                                  | 122±4                           | 963±81                             |                                 |              |               |
|               |            |            |            | 49                | 1.0          |                         |                        |                         |                                |                                  |                                   |                                  | 60±2                            | 471±39                             |                                 |              |               |
| NGC 2438      |            | 17.74±0.20 | KF         | 35                | 1.0          | 1.32                    | 0.22                   | 0.09                    | 124±13                         | 143±8                            | 1.16±0.14                         |                                  | 97±14                           | 148±14                             | 0.34                            | 0.103        | C             |
|               |            |            |            | 65                | 1.0          | 0.91                    | 0.29                   | 0.07                    |                                |                                  |                                   |                                  | 46±7                            | 71±6                               |                                 |              |               |
| NGC 2474      | 16.5 ±0.2  | 16.0 ±0.2  | KA3        | 194               | 0.35         | 0.58                    | 0.54                   | 0.30                    | 93±24                          | 116±13                           | 1.24±0.35                         |                                  | 17±6                            | 34±8                               | 1.2 ±0.2                        |              | B             |
|               |            |            |            |                   | 1.0          |                         |                        |                         | 63±14                          | 98±10                            | 1.54±0.37                         |                                  | 6±1                             | 21±5                               |                                 |              |               |
| NGC 2610      | 15.3 ±0.1  | 15.5 ±0.1  | SL         | 19                | 1.0          | 2.37                    | 0.21                   | 0.56                    | 46±1                           | 100±2                            | 2.19±0.09                         | H                                | 118±6                           | 1030±90                            | <0.38                           | 0.110        | C             |
|               |            |            |            | 26                |              | 1.91                    | 0.24                   | 0.46                    |                                |                                  |                                   |                                  | 81±4                            | 709±61                             |                                 |              |               |
| NGC 3587      | 15.59±0.1  | 16.04±0.1  | SL         | 100               | 1.0          | 0.58                    | 0.28                   | 0.48                    | 112±5                          | 107±3                            | 0.95±0.05                         |                                  | 148±2                           | 41±3                               | 0.28±0.11                       | 0.097        | C             |
| NGC 4361      | 12.74±0.1  | 13.04±0.1  | SL         | 58                | 1.0          | 0.83                    | 0.23                   | 0.57                    | 42±2                           | 98±2                             | 2.34±0.10                         | H                                | 100±4                           | 1040±60                            | 0.14±0.05                       | 0.135        | C             |
| NGC 6058      | 13.39±0.2  | 13.70±0.2  | SL         | 11                | 0.5          | 3.69                    | 0.20                   | 2.76                    | 29±1                           | 75±2                             | 2.55±0.12                         |                                  | 624±169                         | 7360±2120                          |                                 |              |               |
|               |            |            |            | 16                | 0.5          | 2.99                    | 0.23                   |                         |                                |                                  |                                   |                                  | 410±111                         | 4840±1390                          |                                 |              |               |
|               |            |            |            | 11                | 1.0          |                         |                        |                         | 26±1                           | 69±2                             | 2.68±0.11                         |                                  | 460±125                         | 5910±1700                          |                                 |              |               |
|               |            |            |            | 16                | 1.0          |                         |                        |                         |                                |                                  |                                   |                                  | 302±82                          | 3880±1120                          |                                 |              |               |
| NGC 6445      | 19±1       |            | HB22       | 17                | 0.75         | 1.94                    | 0.16                   | 0.13                    | 211±96                         | 200±54                           | 0.95±0.50                         |                                  | 530±211                         | 459±144                            | 1.2 ±0.5                        | 0.23         | B             |
|               |            |            |            | 75                | 0.75         | 0.79                    | 0.29                   | 0.05                    |                                |                                  |                                   |                                  | 89±35                           | 77±24                              |                                 |              |               |
|               |            |            |            | 17                | 1.0          |                         |                        |                         | 184±82                         | 186±47                           | 1.01±0.52                         |                                  | 356±133                         | 368±124                            |                                 |              |               |
|               |            |            |            | 75                | 1.0          |                         |                        |                         |                                |                                  |                                   |                                  | 60±22                           | 62±21                              |                                 |              |               |
| NGC 6563      | 18±1       |            | CU         | 24                | 0.5          | 1.72                    | 0.20                   | -0.22                   | 240±111                        | 157±99                           | 0.65±0.51                         |                                  | 449±191                         | 129±115                            |                                 |              | B             |
|               |            |            |            |                   | 1.0          |                         |                        |                         | 173±77                         | 135±83                           | 0.78±0.59                         |                                  | 172±63                          | 84±74                              |                                 |              |               |
| NGC 6720      | 14.69±0.10 | 15.00±0.10 | SL         | 36                | 0.5          | 0.81                    | 0.14                   | 0.20                    | 145±8                          | 145±6                            | 1.00±0.07                         |                                  | 863±75                          | 857±113                            | 0.31±0.05                       | 0.114        | B             |
|               |            |            |            | 75                | 0.5          | 0.52                    | 0.19                   | 0.13                    |                                |                                  |                                   |                                  | 358±35                          | 355±47                             |                                 |              |               |
|               |            |            |            | 36                | 1.0          |                         |                        |                         | 107±5                          | 126±5                            | 1.17±0.08                         |                                  | 363±33                          | 574±72                             |                                 |              |               |
|               |            |            |            | 75                | 1.0          |                         |                        |                         |                                |                                  |                                   |                                  | 150±14                          | 238±30                             |                                 |              |               |
| NGC 6765      |            | 16.0 ±0.5  | SH         | 27                | 0.5          | 2.06                    | 0.26                   | 0.34                    | 46±7                           | 103±9                            | 2.25±0.37                         | H                                | 123±30                          | 1160±370                           | 0.45±0.07                       |              |               |
|               |            |            |            | 48                | 0.5          | 1.45                    | 0.33                   | 0.24                    | 38±5                           | 93±7                             | 2.42±0.35                         |                                  | 61±15                           | 578±185                            |                                 |              |               |
|               |            |            |            | 27                | 1.0          |                         |                        |                         |                                |                                  |                                   |                                  | 77±21                           | 865±290                            |                                 |              |               |
|               |            |            |            | 48                | 1.0          |                         |                        |                         |                                |                                  |                                   |                                  | 39±10                           | 429±144                            |                                 |              |               |

TABLE 5—Continued

| Nebula<br>(1) | B<br>(2)                | V<br>(3)                | Ref<br>(4) | $\theta''$<br>(5)        | $\xi$<br>(6)               | $D_{\text{kpc}}$<br>(7)      | $R_{\text{pc}}$<br>(8) | $Z_{\text{kpc}}$<br>(9) | 10 <sup>-3</sup> |                   | TR <sup>a</sup><br>(12) | L(H)/L <sub>⊙</sub><br>(13)             | L(He II)/L <sub>⊙</sub><br>(14)          | N/O<br>T=10 <sup>4</sup> K<br>(15) | He/H<br>(16) | Class<br>(17) |
|---------------|-------------------------|-------------------------|------------|--------------------------|----------------------------|------------------------------|------------------------|-------------------------|------------------|-------------------|-------------------------|---|--|------------------------------------|--------------|---------------|
|               |                         |                         |            |                          |                            |                              |                        |                         | T(H)K<br>(10)    | T(He II)K<br>(11) |                         |   |  |                                    |              |               |
| NGC 6772      | 18.7 ± 0.4              |                         | KO         | 32<br>45<br>32<br>45     | 0.5<br>0.5<br>1.0<br>1.0   | 1.25<br>1.02<br>0.22<br>0.11 | 0.19<br>0.22           | -0.14<br>-0.11          | 130±21<br>97±15  | 140±41<br>123±11  | 1.08±0.21<br>1.27±0.22  | 306±51<br>203±34<br>133±20<br>88±13     | 385±112<br>256±75<br>261±76<br>173±50    |                                    |              | B             |
| NGC 6781      | 15.91±0.10 <sup>b</sup> | 14.95±0.10 <sup>b</sup> | SL         | 55<br>74<br>55<br>74     | 0.5<br>0.5<br>1.0<br>1.0   | 0.77<br>0.65<br>0.23<br>0.03 | 0.20<br>0.23           | -0.03<br>-0.03          | 65±8<br>52±5     | 96±6<br>87±5      | 1.49±0.20<br>1.68±0.20  | 215±60<br>151±42<br>119±34<br>83±24     | 675±240<br>473±168<br>512±185<br>359±129 |                                    |              | B             |
| NGC 6842      | 15.65±0.10 <sup>b</sup> | 15.98±0.10 <sup>b</sup> | SL         | 29                       | 1.0                        | 1.42                         | 0.20                   | 0.02                    | 41±3             | 85±4              | 2.08±0.19               | 164±28                                  | 1220±300                                 |                                    |              | C             |
| NGC 6853      | 13.53±0.10              | 13.82±0.10              | SL         | 208<br>420<br>208<br>420 | 0.5<br>0.5<br>1.0<br>1.0   | 0.24<br>0.16<br>0.32<br>0.01 | 0.24<br>0.32           | -0.02<br>-0.01          | 170±14<br>125±9  | 159±9<br>137±7    | 0.93±0.09<br>1.10±0.10  | 197±40<br>85±17<br>80±15<br>34±6        | 161±33<br>69±14<br>104±20<br>45±9        |                                    | 0.38±0.01    | B             |
| NGC 6894      | 17.6 ± 0.2              |                         | KO         | 21                       | 0.5<br>1.0                 | 1.53<br>1.0                  | 0.15                   | -0.07                   | 110±10<br>84±7   | 103±9<br>92±8     | 0.93±0.12<br>1.10±0.13  | 549±149<br>249±58                       | 443±160<br>330±116                       |                                    | 0.96±0.34    | C             |
| NGC 7048      | 18±1                    |                         | HB21       | 31                       | 0.75<br>1.0                | 1.24<br>1.0                  | 0.18                   | -0.04                   | 109±45<br>97±38  | 140±28<br>139±25  | 1.27±0.58<br>1.36±0.58  | 220±59<br>157±37                        | 447±209<br>378±186                       |                                    |              | B             |
| NGC 7094      | 13.36±0.10              | 13.61±0.10              | SL         | 47                       | 1.0                        | 1.56                         | 0.36                   | -0.74                   | 26±1             | 73±1              | 2.82±0.09               | 84±5                                    | 1240±90                                  |                                    |              | B             |
| NGC 7139      | 17.7 ± 0.4              |                         | KO         | 39                       | 0.5<br>1.0                 | 1.50<br>1.0                  | 0.28                   | 0.20                    | 84±12<br>65±8    | 104±11<br>94±9    | 1.24±0.22<br>1.43±0.23  | 82±22<br>41±12                          | 151±68<br>112±50                         |                                    |              | B             |
| NGC 7293      | 13.09±0.10              | 13.43±0.10              | SL         | 402<br>476<br>402<br>476 | 0.45<br>0.45<br>1.0<br>1.0 | 0.15<br>0.14<br>0.32<br>0.12 | 0.29<br>0.32           | -0.13<br>-0.12          | 165±8<br>116±5   | 123±12<br>107±9   | 0.74±0.08<br>0.92±0.09  | 113±6<br>92±5<br>40±2<br>33±2           | 48±13<br>39±11<br>32±8<br>26±6           | 1.0 ± 0.05                         | 0.19         | B             |
| IC 972        | 17.7 ± 0.4              |                         | KO,AB      | 24                       | 1.0                        | 2.77                         | 0.32                   | 1.86                    | 57±8             | 89±7              | 1.56±0.25               | 29±5                                    | 100±30                                   |                                    | 0.28±0.06    |               |
| IC 1454       | 18.6 ± 0.4              |                         | AB         | 17                       | 1.0                        | 3.42                         | 0.28                   | 1.11                    | 67±9             | 98±6              | 1.47±0.21               | 41±4                                    | 121±33                                   |                                    |              |               |
| IC 4406       | 17±1                    |                         | EV         | 10<br>58<br>10<br>58     | 0.75<br>0.75<br>1.0<br>1.0 | 2.40<br>1.08<br>0.20<br>0.29 | 0.11<br>0.20           | 0.65<br>0.29            | 153±67<br>135±57 | 112±19<br>106±17  | 0.73±0.34<br>0.79±0.36  | 1060±390<br>213±78<br>726±243<br>146±44 | 423±242<br>85±49<br>370±218<br>75±44     | 0.48                               | 0.141        | B             |
| A 2           | 19.8 ± 0.3              |                         | AB,KO      | 15                       | 1.0                        | 3.74                         | 0.27                   | -0.32                   | 83±9             | 128±11            | 1.54±0.22               | 46±11                                   | 158±56                                   |                                    |              |               |
| A 3           | 18.2 ± 0.3              |                         | AB,KO      | 30                       | 1.0                        | 1.80                         | 0.26                   | 0.08                    | 40±4             | 90±8              | 2.23±0.29               | 74±28                                   | 657±313                                  |                                    | 0.37±0.32    |               |
| A 4           | 19.3 ± 0.3              |                         | AB,KO      | 10                       | 1.0                        | 5.43                         | 0.26                   | 1.45                    | 65±6             | 96±8              | 1.48±0.19               | 51±7                                    | 154±46                                   |                                    | 0.67±0.28    |               |
| A 5           | 20.3 ± 0.4 <sup>c</sup> |                         | AB         | 64                       | 0.3<br>1.0                 | 1.57<br>1.0                  | 0.49                   | -0.21                   | 93±23<br>60±12   | 28±22<br>8±7      |                         |   |  |                                    |              |               |
| A 6           | 19.0 ± 0.3              |                         | AB,KO      | 91                       | 1.0                        | 0.79                         | 0.35                   | 0.07                    | 55±5             | <81               | <1.62                   | 23±7                                    | <84                                      |                                    |              |               |

TABLE 5—Continued

| Nebula<br>(1) | B<br>(2)                | V<br>(3)                | Ref<br>(4) | $\theta''$<br>(5)        | $\xi$<br>(6)       | $D_{\text{kpc}}$<br>(7) | $R_{\text{kpc}}$<br>(8) | $Z_{\text{kpc}}$<br>(9) | $T(\text{H})\text{K}$<br>$10^{-3}$<br>(10) | $T(\text{HeII})\text{K}$<br>$10^{-3}$<br>(11) | $\text{TR}^a$<br>(12)  | $L(\text{H})/L_{\odot}$<br>(13) | $L(\text{HeII})/L_{\odot}$<br>(14) | $N/O$<br>$T=10^4\text{K}$<br>(15) | He/H<br>(16) | Class<br>(17) |
|---------------|-------------------------|-------------------------|------------|--------------------------|--------------------|-------------------------|-------------------------|-------------------------|--|---|------------------------|---------------------------------|------------------------------------|-----------------------------------|--------------|---------------|
| A 8           | 19.7 ± 0.3              |                         | AB,KO      | 30                       | 1.0                | 2.66                    | 0.39                    | -0.05                   | 49±11                                      |   |                        | 18±6                            |                                    |                                   |              |               |
| A 13          | 20.06±0.05 <sup>c</sup> | 19.87±0.05 <sup>c</sup> | AB         | 78                       | 0.50<br>1.0        | 0.67                    | 0.25                    | -0.10                   | 92±19<br>71±13                             | <144<br><125                                  | <1.97<br><2.16         | 119±198<br>58±96                | <950<br><660                       | 0.44±0.30<br>+1.20                |              |               |
| A 15          | 15.41±0.01              | 15.72±0.01              | AB         | 17                       | 1.0                | 4.23                    | 0.35                    | -1.19                   | 27±1                                       | 76±1  | 2.80±0.07              | 76±21                           | 1120±330                           |                                   |              |               |
| A 16          | 17.7 ± 0.3              |                         | AB,KO      | 71                       | 1.0                | 1.37                    | 0.47                    | 0.53                    | 46±4                                       | 87±6  | 1.89±0.22              | 11±5                            | 62±33                              |                                   |              |               |
| A 20          | 16.29±0.01              | 16.56±0.01              | AB         | 34                       | 1.0                | 2.33                    | 0.38                    | 0.32                    | 39±1                                       | 98±2  | 2.49±0.10              | 24±1                            | 293±16                             |                                   |              |               |
| A 24          | 16.97±0.01              | 17.18±0.01              | AB         | 120<br>178<br>120<br>178 | 0.25<br>1.0<br>1.0 | 0.64<br>0.50<br>0.44    | 0.37<br>0.44<br>0.13    | 0.16<br>0.13            | 134±14<br>76±7                             | <150<br><114                                  | <1.25<br><1.65         | 89±40<br>56±25<br>18±7<br>11±5  | <150<br><95<br><72<br><45          | >2.7                              |              | B             |
| A 28          | 16.0 ± 0.3              |                         | AB,KO      | 134                      | 1.0                | 0.93                    | 0.60                    | 0.56                    | 42±4                                       | 82±6  | 1.93±0.21              | 6±1                             | 34±8                               | >0.4                              |              |               |
| A 30          | 14.23±0.01              | 14.30±0.01              | AB         | 64                       | 1.0                | 1.71                    | 0.53                    | 0.94                    | 25±1                                       | 72±2  | 2.94±0.11              | 30±3                            | 490±52                             |                                   |              |               |
| A 31          | 15.20±0.01              | 15.51±0.01              | AB         | 486                      | 1.0                | 0.24                    | 0.56                    | 0.12                    | 85±23                                      | 114±19  | 1.35±0.43              | 5±5                             | 12±11                              | 0.40±0.18                         |              |               |
| A 33          | 15.38±0.01              | 15.54±0.01              | AB         | 134                      | 1.0                | 0.73                    | 0.47                    | 0.42                    | 49±10                                      | 95±11   | 1.95±0.46              | 10±5                            | 64±33                              |                                   |              |               |
| A 34          | 16.06±0.01              | 16.32±0.01              | AB         | 137                      | 1.0                | 0.92                    | 0.61                    | 0.46                    | 42±1                                       | 84±3  | 2.01±0.09              | 5±1                             | 37±5                               |                                   |              |               |
| A 35          |                         |                         |            | 530                      |                    | 0.32                    | 0.82                    | 0.21                    |  |   |                        |                                 |                                    | 0.8 ± 0.6                         |              |               |
| A 36          | 11.18±0.01              | 11.51±0.01              | AB         | 196                      | 1.0                | 0.47                    | 0.45                    | 0.31                    | 26±1                                       | 73±1  | 2.79±0.05              | 39±1                            | 57±22                              |                                   |              |               |
| A 39          | 15.43±0.01              | 15.76±0.01              | AB         | 87                       | 1.0                | 1.18                    | 0.50                    | 0.80                    | 38±1                                       | 86±2  | 2.28±0.06              | 12±1                            | 110±7                              |                                   |              | B             |
| A 43          | 14.53±0.01              | 14.71±0.01              | AB         | 40                       | 1.0                | 2.10                    | 0.41                    | 0.63                    | 24±1                                       | 68±1  | 2.82±0.09              | 73±23                           | 1050±330                           |                                   |              | B             |
| A 46          | 14.88±0.01              | 15.07±0.01              | AB         | 32                       | 1.0                | 2.22                    | 0.34                    | 0.61                    | 32±2                                       | <60   | <2.00                  | 50±19                           | <340                               | <0.3                              |              |               |
| A 50          | 19.4 ± 0.3              |                         | AB         | 13.5                     | 1.0                | 4.02                    | 0.26                    | 1.29                    | 104±12                                     | 126±7   | 1.22±0.16              | 55±5                            | 97±14                              | 0.40±0.09                         | 0.089        |               |
| A 51          | 15.30±0.01              | 15.42±0.01              | AB         | 34                       | 1.0                | 2.09                    | 0.34                    | -0.37                   | 36±2                                       | 86±4  | 2.41±0.19              | 40±12                           | 430±142                            |                                   |              | C             |
| A 53          | 20.3 ± 0.4              |                         | AB         | 15.5                     | 1.0                | 2.18                    | 0.16                    | -0.02                   | 69±10                                      | 108±19  | 1.57±0.35              | 210±76                          | 745±458                            |                                   |              |               |
| A 62          | 18.2 ± 0.4              |                         | AB         | 81                       | 1.0                | 0.50                    | 0.20                    | -0.04                   | 55±7                                       | <95   | <2.0                   | 130±109                         | <1000                              | 0.01?                             |              |               |
| A 65          | 15.99±0.01              | 15.90±0.01              | AB         | 54                       | 1.0                | 1.34                    | 0.35                    | -0.50                   | 46±2                                       | 87±6  | 1.94±0.17              | 27±11                           | 170±80                             | 0.31±0.16                         |              |               |
| A 70          | 18.5 ± 0.3              |                         | AB,KO      | 21                       | 1.0                | 3.22                    | 0.33                    | -1.38                   | 57±7                                       | 101±7   | 1.77±0.25              | 28±16                           | 135±90                             |                                   |              | C             |
| A 71          | 19.32±0.05 <sup>c</sup> | 18.95±0.05 <sup>c</sup> | AB         | 79                       | 0.75<br>1.0        | 0.74                    | 0.28                    | 0.06                    | 127±9<br>112±8                             | 137±7<br>130±6                                | 1.08±0.10<br>1.16±0.10 | 66±17<br>47±12                  | 83±20<br>70±17                     | 2.4<br>-1.0                       |              |               |
| A 72          | 15.79±0.01              | 16.12±0.01              | AB         | 64                       | 0.4<br>1.0         | 1.48                    | 0.46                    | -0.48                   | 49±2<br>39±2                               | 107±4<br>93±3                                 | 2.17±0.13<br>2.40±0.12 | 27±3<br>14±1                    | 234±28<br>157±18                   |                                   |              |               |

TABLE 5—Continued

| Nebula<br>(1) | B<br>(2)               | V<br>(3)   | Ref<br>(4) | $\theta''$<br>(5) | $\xi$<br>(6) | $D_{\text{kpc}}$<br>(7) | $R_{\text{pc}}$<br>(8) | $Z_{\text{kpc}}$<br>(9) | 10 <sup>-3</sup> |                  |                          | TR <sup>a</sup><br>(12) | L(H)/L <sub>⊙</sub><br>(13) | L(HeII)/L <sub>⊙</sub><br>(14) | N/O<br>T=10 <sup>4</sup> K<br>(15) | He/H<br>(16) | Class<br>(17) |
|---------------|------------------------|------------|------------|-------------------|--------------|-------------------------|------------------------|-------------------------|------------------|------------------|--------------------------|-------------------------|-----------------------------|--------------------------------|------------------------------------|--------------|---------------|
|               |                        |            |            |                   |              |                         |                        |                         | T(H)K<br>(10)    | T(HeII)K<br>(11) | 10 <sup>-3</sup><br>(12) |                         |                             |                                |                                    |              |               |
| A 73          | 20.5 ±0.4              |            | KO         | 37                | 1.0          | 1.88                    | 0.34                   | 0.26                    | 66±12            |                  |                          |                         | 24±4                        |                                |                                    |              |               |
| A 75          | 17.3 ±0.3              |            | AB,KO      | 29                | 1.0          | 1.89                    | 0.27                   | 0.29                    | 40±3             | 92±5             | 2.28±0.22                |                         | 70±3                        | 665±320                        | <0.10                              |              |               |
| A 78          | 13.04±0.01             | 13.25±0.01 | AB         | 54                | 1.0          | 1.74                    | 0.45                   | -0.45                   | 22±1             | 69±2             | 3.11±0.12                | H                       | 74±58                       | 1330±1090                      |                                    |              |               |
| A 79          | 18.1 ±0.3              |            | AB,KO      | 27                | 0.5          | 1.82                    | 0.24                   | -0.07                   | 47±11            |                  |                          |                         | 163±464                     |                                |                                    |              |               |
|               |                        |            |            | 48                | 0.5          | 1.29                    | 0.30                   | -0.05                   | 39±8             |                  |                          |                         | 82±233                      |                                |                                    |              |               |
|               |                        |            |            | 27                | 1.0          |                         |                        |                         |                  |                  |                          |                         | 101±301                     |                                |                                    |              |               |
|               |                        |            |            | 48                | 1.0          |                         |                        |                         |                  |                  |                          |                         | 51±151                      |                                |                                    |              |               |
| A 80          | 19.4 ±0.3 <sup>c</sup> |            | AB,KO      | 70                | 0.25         | 0.90                    | 0.31                   | -0.08                   | 214±42           | <233             | <1.35                    |                         | 225±148                     | <370                           |                                    |              |               |
|               |                        |            |            |                   | 1.0          |                         |                        |                         | 114±20           | <162             | <1.72                    |                         | 36±24                       | <140                           |                                    |              |               |
| A 82          | 13±1 <sup>c</sup>      |            | VV         | 47                | 0.75         | 1.43                    | 0.33                   | -0.12                   | 26±4             | 59±5             | 2.18±0.45                |                         | 145±186                     | 1190±1690                      | 0.53±0.36                          |              |               |
|               |                        |            |            |                   | 1.0          |                         |                        |                         | 25±4             | 57±5             | 2.33±0.44                |                         | 129±169                     | 1100±1610                      |                                    |              |               |
| A 84          | 18.67±0.01             | 18.49±0.01 | AB         | 66                | 0.8          | 1.12                    | 0.36                   | -0.20                   | 101±7            | 111±17           | 1.10±0.19                |                         | 27±8                        | 35±17                          | 0.30±0.10                          |              |               |
|               |                        |            |            |                   | 1.0          |                         |                        |                         | 92±7             | 107±16           | 1.16±0.19                |                         | 21±6                        | 32±15                          |                                    |              |               |
| Ba 1          | 17.1 ±0.4              |            | KO         | 20                | 1.0          | 2.72                    | 0.26                   | -1.19                   | 36±3             | 88±5             | 2.42±0.25                | H                       | 86±29                       | 937±374                        |                                    |              |               |
| BV 3          | 18±1                   |            | K83        | 15:               | 1.0          | 3.71                    | 0.27                   | -0.35                   | 47±13            | 84±15            | 1.80±0.58                |                         | 57±24                       | 281±223                        |                                    |              |               |
| Jn 1          | 15.72±0.01             | 16.13±0.01 | SL         | 166               | 0.10         | 0.70                    | 0.56                   | -0.34                   | 111±3            | 140±13           | 1.26±0.12                |                         | 59±3                        | 114±29                         | 0.67±0.27                          |              |               |
|               |                        |            |            |                   | 0.50         |                         |                        |                         | 61±1             | 104±7            | 1.72±0.13                |                         | 11±1                        | 49±10                          |                                    |              |               |
|               |                        |            |            |                   | 1.0          | 0.70                    | 0.56                   | -0.34                   | 49±1             | 94±6             | 1.91±0.13                |                         | 6±1                         | 36±6                           |                                    |              |               |
| K1 7          | 19.6 ±0.3              |            | AB,KO      | 17                | 1.0          | 3.25                    | 0.18                   | -0.80                   | 97±13            | 104±6            | 1.07±0.15                |                         | 51±9                        | 62±13                          |                                    |              |               |
| K1 14         |                        | 16.93±0.20 | KF         | 24                | 1.0          | 3.39                    | 0.40                   | 1.40                    | 35±2             | 91±5             | 2.64±0.23                | H                       | 28±4                        | 384±73                         |                                    |              |               |
| K1 16         | 14.74±0.01             | 15.09±0.01 | SL         | 58                | 1.0          | 1.66                    | 0.47                   | 0.78                    | 30±1             | 80±2             | 2.71±0.08                | H                       | 24±10                       | 337±151                        |                                    |              |               |
| K1 20         | 20.1 ±0.5              |            | KO         | 19                | 0.5          | 4.13                    | 0.37                   | -0.93                   | 73±14            | <97              | <1.64                    |                         | 36±7                        | <85                            |                                    |              |               |
|               |                        |            |            |                   | 1.0          |                         |                        |                         | 58±10            | <88              | <1.83                    |                         | 19±4                        | <65                            |                                    |              |               |
| K1 22         |                        | 17.89±0.20 | KF         | 91                | 1.0          | 0.85                    | 0.38                   | 0.36                    | 92±11            | <138             | <1.70                    |                         | 18±12                       | <76                            |                                    |              |               |
| K2 1          | 18.2 ±0.4              |            | KO         | 66                | 1.0          | 1.08                    | 0.35                   | -0.11                   | 76±10            | 138±14           | 1.83±0.31                | H                       | 22±5                        | 124±43                         | 0.11±0.05                          |              |               |
| K2 2          | 18.2 ±1.0 <sup>c</sup> |            | KO         | 207               | 1.0          | 0.52                    | 0.52                   | 0.04                    | 158±71           | 113±25           | 0.72±0.36                |                         | 9±4                         | 3±2                            | 0.34±0.10                          |              |               |
| K3 27         | 18.2 ±0.5              | 18.0 ±0.5  | K81        | 8:2               | 1.0          | 5.65                    | 0.23                   | 0.80                    | 58±10            | 114±11           | 1.95±0.39                | H                       | 85±11                       | 565±169                        |                                    |              |               |
| LT 5          |                        |            |            | 525               | 1.0          | 0.62                    | 0.78                   |                         |                  |                  |                          |                         |                             |                                |                                    |              |               |
| M2 51         | 16.3 ±0.5              |            | K83        | 21                | 0.75         | 1.59                    | 0.16                   | 0.02                    | 40±5             | 73±5             | 1.82±0.25                |                         | 418±139                     | 209±980                        | 0.37±0.09                          |              |               |
|               |                        |            |            | 35                | 0.75         | 1.17                    | 0.20                   | 0.01                    |                  |                  |                          |                         | 226±75                      | 1130±530                       |                                    |              |               |
|               |                        |            |            | 21                | 1.0          |                         |                        |                         | 38±4             | 71±5             | 1.89±0.25                |                         | 349±120                     | 1920±890                       |                                    |              |               |
|               |                        |            |            | 35                | 1.0          |                         |                        |                         |                  |                  |                          |                         | 189±65                      | 1040±480                       |                                    |              |               |
| M2 55         | 20±1                   |            | K83        | 25                | 0.75         | 1.64                    | 0.20                   | 0.24                    | 109±44           | 92±14            | 0.85±0.37                |                         | 174±67                      | 109±81                         | 0.65±0.43                          |              |               |
|               |                        |            |            |                   | 1.0          |                         |                        |                         | 97±38            | 89±13            | 0.92±0.38                |                         | 124±46                      | 97±8                           |                                    |              |               |

TABLE 5—Continued

| Nebul.a | B   | V                       | Ref | $\phi''$ | $\xi$ | $D_{kpc}$ | $R_{pc}$ | $Z_{kpc}$ | $T(H)K$ | $10^{-3}$ | $10^{-3}$ | $T(HeII)K$ | TR <sup>a</sup> | $L(H)/L_{\odot}$ | $L(HeII)/L_{\odot}$ | $N/O$    | He/H | Class |
|---------|-----|-------------------------|-----|----------|-------|-----------|----------|-----------|---------|-----------|-----------|------------|-----------------|------------------|---------------------|----------|------|-------|
| (1)     | (2) | (3)                     | (4) | (5)      | (6)   | (7)       | (8)      | (9)       | (10)    | (11)      | (12)      | (13)       | (14)            | (15)             | (16)                | (17)     | (18) | (19)  |
| M3      | 3   |                         |     | 6.4      |       | 5.85      | 0.18     | 0.54      |         |           |           |            |                 |                  |                     |          |      |       |
| PW      | 1   | 15.4 ±0.5               | PW  | 600      | 1.0   | 0.24      | 0.69     | 0.07      | 71±13   | 108±13    | 1.53±0.34 | 3±2        | 9±9             |                  |                     | 1.5 -0.8 |      |       |
| Sh2     | 71  | 14.59±0.20 <sup>d</sup> | K01 | 63       | 0.75  | 0.68      | 0.21     | -0.02     | >31     | >77       | 2.5       | <380       | <4200           |                  |                     | 6.8 -3.1 |      |       |
|         |     |                         |     | 112      | 0.75  | 0.48      | 0.26     | -0.01     | >29     | >74       | 2.6       | <190       | <2100           |                  |                     | +3.9     |      |       |
|         |     |                         |     | 63       | 1.0   |           |          |           |         |           |           | <330       | <3800           |                  |                     |          |      |       |
|         |     |                         |     | 112      | 1.0   |           |          |           |         |           |           | <170       | <1900           |                  |                     |          |      |       |
| Sp      | 1   | 14.31±0.10              | SL  | 40       | 1.0   | 1.33      | 0.25     | 0.05      | 32±1    |           |           | 119±22     |                 |                  |                     |          |      |       |
| Ym      | 29  | 15.67±0.01              | AB  | 319      | 1.0   | 0.29      | 0.44     | 0.07      | 115±23  | 126±13    | 1.09±0.25 | 12±5       | 16±4            |                  |                     | 1.1 ±0.5 |      |       |

<sup>a</sup> TR =  $T(He II)/T(H)$ ; the letter H following the value of TR indicates high excitation, ( $\lambda 4686$ ) He II > 90, for which L and T are considered to be lower limits. If TR < 1.2 the luminosity is an upper limit. See the text, and Tables 1 and 2.

<sup>b</sup> Magnitude may be in error; see text.

<sup>c</sup> Central star uncertain; a higher degree of uncertainty is indicated by a question mark. A82, K2-2, and A46 are not plotted in Fig. 6.

<sup>d</sup> Probably a companion to the true central star; see Kohoutek 1979. The assigned error reflects the variability. Temperatures and luminosities are lower and upper limits respectively; the values are not plotted in the figures.

REFERENCES AND NOTES.—AB: Abell 1966 (photoelectric magnitude have errors of  $\pm 0.20$ ). CU: Curtis 1918. EV: Evans 1950. HB21: Hubble 1921. HB22: Hubble 1922. KA3: Kaler 1978 (photoelectric magnitudes). K81: Kaler 1981a (photoelectric magnitudes). K83: This paper, estimated from POSS and King and Raff 1977. KO: Kohoutek, in Perik and Kohoutek 1967. K01: Kohoutek 1979 (not true central star; see text). KF: Kaler and Feibelman 1983. PW: Purgathofer and Weinberger 1980 (used for  $\phi$  also). SH: Sabbadin and Hamzaoglu 1981 (used for  $\phi$  also). SL: Shao and Liller 1973 (photoelectric magnitudes). VV: Vorontsov-Veljaminov 1961.

the errors are found, of course, from the spread of the individual values, but are not allowed to drop below  $\pm 0.3$  mag. The old photographic values (CU, HB21, HB22, EV) are given arbitrary errors of  $\pm 1.0$  mag: these desperately need remeasurement.

As a test of the data, extinction constants derived from the photoelectric colors are given in column (5) of Table 3. The unreddened color is assumed to be  $-0.38$  mag, and  $c = 1.41E_{B-V}$ . The agreement with the radio and/or nebular optical  $c$  is generally satisfactory, with some exceptions. The color of the A30 nucleus is anomalously red because of internal dust (Greenstein 1981). Perhaps a similar phenomenon affects A51. The radio and optical extinctions for NGC 6781 and NGC 6842 agree very well with one another, but not with the stellar  $c$ , implying that the SL magnitudes for these objects are questionable. The Abell 84 nucleus is in a fairly bright nebula, and the magnitudes are probably afflicted with larger errors than are assigned in Table 5.

The magnitude for A82 by VV results in very peculiar Zanstra temperatures, and the star is almost certainly a misidentification. That for K2-2 is noted as questionable by Kohoutek in Perek and Kohoutek (1967). Abell (1966) comments that the identifications of the nuclei for A5, 13, 71, and 80 are uncertain. Shao and Liller (1973) note that the NGC 2610 and NGC 6894 nuclei may be variable. They find the latter nearly 2 mag brighter than the KO measurement, which is the one used here. The central star of A46 is an eclipsing binary (Bond 1980) also called V477 Lyr, but the magnitude given is probably not significantly contaminated by the companion (Kurochkin 1980). The apparent nucleus of Sh 2-71 is variable and appears to be a B8 companion to the true central star (Kohoutek 1979).

#### b) Angular Radii and Geometric Filling Factors

The angular radii of the nebulae,  $\phi$ , in seconds of arc, are given in column (5). These are generally taken from Perek and Kohoutek (1967) and are preferentially the measurements by these authors (Pe or Ko in their notation); in the cases of the recently discovered nebulae, they are from the references in Table 1. The values given are the harmonic means of the major and minor axes, as expressed by Cahn and Kaler (1971). The nebulae are frequently considered as double shells, and the radii of both the inner and the outer are listed in the table. The latter are generally those given in parentheses by Perek and Kohoutek (1967). In some cases  $\phi$  was taken from the references in column (4), or was measured directly from the Palomar Sky Survey.

The next column (6), lists estimates of the geometric filling factor,  $\xi$ . This quantity expresses the fraction of the sky filled with nebula as seen at the central star,  $\Omega$  (nebula)/ $4\pi$ . It must not be confused here with the other use of the term "filling factor,"  $\epsilon$ , which denotes the volume of the equivalent spherical nebula actually filled with radiating matter. Its purpose is to account for ultraviolet radiation that escapes into space without ionizing any nebular material (see Harman and Seaton 1966). The underlying assumption, of necessity over-

simplified, is that the planetaries are either filled spheres (or closed shells), in which case  $\xi = 1$ , or that they are toroids that are seen in a variety of projections (see Khromov and Kohoutek 1968, and Greig 1971). In the latter case,  $\xi$  is of the order of one-half, depending on the dimensions, where radiation presumably escapes into space through the polar holes. The point is debatable. Atherton *et al.* (1978) show that the structure of NGC 6720, an archtypal "toroid," can be explained by a closed shell, so that  $\xi$  would be unity. For now, however, we will proceed under the assumption that nebulae can be toroidal, since the concept represents a limiting case, and discuss the matter further in § III f.

This filling factor is by far the most difficult of the listed parameters to estimate, as one must guess the three-dimensional structure from a two-dimensional, often badly exposed, image. Nevertheless an attempt was made, by examining photographs of all the listed objects from a variety of sources including Curtis (1918), Aller (1956, 1971), Minkowski (1964), G. H. Jacoby (1980, private communication), and the Palomar Sky Survey. In the case of double shell objects,  $\xi$  is derived from the inner shell or ring. If the nebula was judged to be toroidal,  $\xi$  was estimated by measuring the inner and outer diameter of the supposed ring. In two cases, A50 and K3-27, no structure could be discerned from the overexposed images, and  $\xi$  was set to unity because of the sharp edge and round appearance reminiscent of a circular shell. For K2-2,  $\xi$  was set to unity simply because the true structure could not be discerned. Since subjective judgement is required, errors in  $\xi$  will clearly be made, but we would hope that they are made at random.

#### c) Distances and Radii

Distances ( $D$ ) and physical radii ( $R$ ) of the nebulae have been calculated by the common method in which all planetaries are assumed to have the same ionized mass. The formulation is that used by Cahn and Kaler (1971) (which uses Seaton's 1968 scale factor) with the H $\beta$  fluxes and extinction constants taken from Tables 1 and 2, and the angular radii from Table 5. The results are presented in columns (7) and (8) of that table for both values of  $\phi$  when two are given.

This method has very obvious drawbacks. Certainly not all nebulae have the same total mass: we would expect that the mass might be related to the mass of the parent star, and indirectly be related to population type, and morphology. Systematic differences in mass will thus lead to systematic errors in the results of this and later sections (see Kaler 1980b). Some nebulae may be optically thick (Seaton 1966), in which case the ionized visible mass is less than the supposedly constant total mass, resulting in an overestimate of distance and radius. (The nebulae studied here all have radii above the minimum at which they become thin: see Cahn and Kaler 1971. Only a few with lower luminosity stars may be thick, as discussed below). Then in the case of double-shell objects there is the question of which of the angular radii to use. Finally, even assuming that the constant-

mass hypothesis is correct, there is the matter of the proper calibration and scale factor (see, for example, Cudworth 1974). Because of these fundamental difficulties, errors are not assigned to  $D$  and  $R$ .

However, it is the only method that we have that can be applied uniformly to all nebulae, and there is little choice but to use it. On the positive side, distance and radius are proportional only to the 0.4 power of the assumed mass, which considerably reduces the effect of mass variation. Systematic effects that may result from the use of this technique will be explored in a later section.

Finally, the distances from the galactic plane,  $Z$ , calculated from  $D$  in column (7), are given in column (9).

#### d) Distance and Observational Selection

Kaler (1980b) found that high velocity nebulae, presumably those of the galactic halo, tend to be of lower excitation. Weidemann (1981) and Schönberner (1981) criticize this result on the grounds of observational selection. They suggest that since the halo nebulae are more distant, the higher excitation planetaries, which are assumed to be of lower surface brightness due to a more advanced state of evolution, will not be as readily observed. The data of this paper cannot be used to verify Kaler's (1980b) results, since additional velocities are not available, and since the selection of nebulae with measured velocities is a separate matter, but these authors raise an interesting general question of selection that must be explored. Surface brightness is independent of distance as such, but it is critically dependent upon interstellar extinction. Consequently, we might expect that the low surface brightness nebulae in the halo

would be considerably more observable than those in the disk.

Examination of Table 5 shows that the smaller nebulae, with  $r < 0.4$  pc, are observed over a wide range of extinction, from  $c = 0$  to  $c > 2$ ; 36% have  $c > 0.5$ . For the nebulae larger than 0.4 pc, however, only one object, 5% of the set, has  $c > 0.5$ , and 85% have  $c < 0.1$  as opposed to only 25% for the set of smaller objects. Large objects are observed only when  $c$  is low. The effect is further illustrated by Figure 2, in which the nebular radii are plotted against distance from the galactic plane. The smaller nebulae are confined to the disk and are spread out into the halo in qualitative agreement with the space density of stars in general. But the larger objects are either nearby or are seen only at relatively large vertical distances from the plane. The large majority of these nebulae are optically thin (see below), especially those at higher  $|Z|$ , so that optical depth is not a consideration. The photometric observations have not yet been extended to the more heavily reddened and dimmer large objects in the disk that could be significant in the analyses later in this paper, since the disk contains the most massive stars.

Additional aspects of observational selection will be examined in sections that follow.

#### e) Zanstra Temperatures and Luminosities

Temperatures and luminosities of the central stars ( $T$  and  $L$ ) were calculated for nearly all the nebulae, based on the classic Zanstra method as formulated by Harman and Seaton (1966); see Kaler and Hartkopf (1981) or Kaler (1981a). The exceptions are LT-5 and M3-3, for which there are no stellar magnitudes, and NGC 1514 whose visible central star is a companion to the true

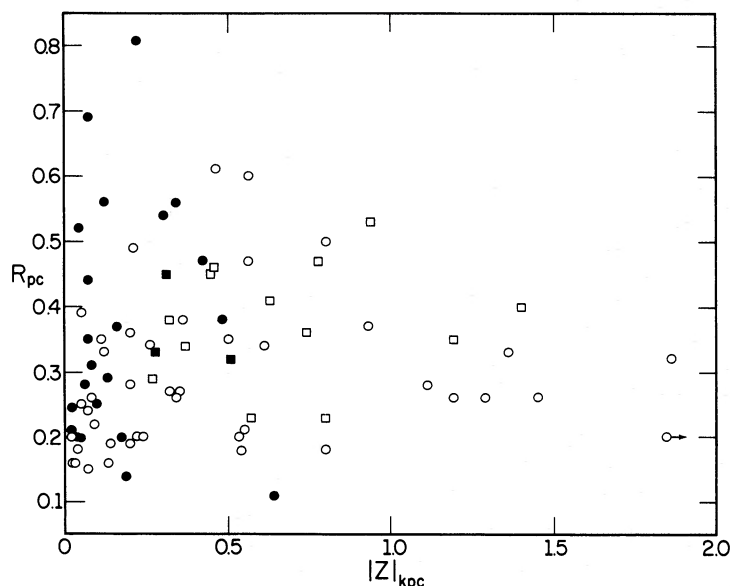


FIG. 2.—Radii of the planetaries,  $R$ , plotted against the absolute distance from the galactic plane, showing the effects of observational selection. Filled symbols: distance  $< 800$  pc; boxes: Kaler's 1981a high-excitation nebulae.

ionizing subdwarf (Kohoutek 1967). The nucleus of Sh 2-71 appears also to be binary (Kohoutek 1979; see § IIIa), and the observed magnitudes are used to place marginally significant limits on  $T$  and  $L$ . Two types of  $T$  and  $L$  were calculated, one based on the  $H\beta$  flux, which gives an effective blackbody temperature for the ionizing photons shortward of 912 Å, and the other on the He II  $\lambda 4686$  flux, which applies to the He II Lyman continuum shortward of 228 Å. The comparison of the two values provides information on optical depth.

The stars are all assumed to behave as blackbodies. The work of Pottasch *et al.* (1978) indicates that this assumption is not unreasonable for stars of the type considered here. Pilyugin, Sakhbullin, and Khromov (1978) show that the Zanstra temperature is not very sensitive to the model adopted, although Bohlin, Harrington, and Stecher (1982) do show a 30% model dependence in their study of NGC 7293. The major problem, however, is still model selection. The stars clearly have a wide range of abundances, varying from nearly pure helium for A30 and A78 (Hazard *et al.* 1980; Jacoby and Ford 1983) to relatively solar. Some have rapidly expanding thick outer atmospheres; others do not. For most nuclei, no suitable models exist, and the errors introduced by the uniform assumption of a blackbody are probably no greater than they would be under the assumption of any specific set of models, and the blackbody at least has the virtue of simplicity.

The problem of internal dust (Helfer *et al.* 1981) cannot be independently assessed and is tacitly subsumed in the general problem of optical depth. These points will be examined further in the discussion of comparative temperatures in the next subsection.

The derived H and He II Zanstra temperatures are presented in columns (10) and (11) of Table 5. Column (12) gives the ratio of  $T(\text{He II})/T(\text{H}) = \text{TR}$ , and columns (13) and (14) give the companion stellar luminosities based on the distances in column (7). Where both  $B$  and  $V$  are available,  $T$  and  $L$  are averages of individually derived values. Errors assigned to the observational parameters— $\log F(H\beta)$ ,  $c$ ,  $I(\lambda 4686 \text{ He II})$ ,  $B$ , and  $V$ —are propagated through the equations to determine errors on  $T$  and  $L$ . The final error also includes the difference between the individual values of  $T$  and  $L$  calculated from  $B$  and  $V$  and is the quadratic sum of all the individual errors. The errors on the luminosities do not include any dispersion in the mean nebular mass that is used for distance determination. A dispersion with a width a factor of 1.5 of the mean to either side will result in an additional error of  $\pm 38\%$  (74% if a factor of 2), which should be added quadratically to the luminosity errors in Table 5. See §§ IVc, IVe(iv), and V for further discussion of the problem.

If the estimated  $\xi$  is less than 1, temperatures and luminosities are calculated for the case of  $\xi = 1$  as well. When two values of angular radius are available, luminosities are calculated for both the resulting distances and both values of  $\xi$ , even if the lower value of  $\xi$ , derived from the inner shell, may not be appropriate

to the outer. Thus a nebula can have up to four line entries.

#### f) Choice of Temperature and Luminosity

Before we can embark on any discussion of the evolution of the central stars, we must be able to interpret the meaning of the variety of temperatures and luminosities given in Table 5. Two temperatures,  $T(\text{H})$  and  $T(\text{He II})$ , are provided for almost all of the nebulae. For nebulae with  $\xi < 1$ , there will be four calculations of temperature, and when two values of  $\phi$  are available, there can be as many as eight calculations of stellar luminosity. We must narrow the variety to the most likely values.

Consistent with our earlier assumption of a blackbody, and with the conclusions drawn by Harman and Seaton (1966), we may assume that  $T(\text{He II})$  more closely represents the true effective temperature of the star. The nebulae are generally optically thick to the ionizing photons of the He<sup>+</sup> Lyman continuum ( $\lambda < 228$  Å), or else the helium would all be doubly ionized. The  $T(\text{H})$  are frequently lower than the  $T(\text{He II})$  ( $\text{TR} > 1$ ) because the nebulae are optically *thin* to the hydrogen Lyman continuum (the basis for correct distance determination; see, e.g., Seaton 1966 and Cahn and Kaler 1971). In some instances, the nebulae are even optically thin in the He<sup>+</sup> continuum, so that  $T(\text{He II})$  will be a lower (but closer) limit. The  $T(\text{He II})$  and  $L(\text{He II})$  will thus be the values of choice; further interpretation in terms of optical depth will be deferred to the next subsection.

Next is the question of the preferred value of  $\phi$ . Only 20% of the tabulated nebulae have two values. The outer shell is always fainter; if it is always physically present (which it may not be), it will be detected only for the brighter objects. We should assume then that when only a single value is observed it corresponds in an evolutionary sense to the inner shell in the case where both are observed. Consequently, even though the total fluxes generally refer to the whole system, distances calculated on the smaller of the two would be at least relatively correct, and the errors would be absorbed by the error in the scale factor.

Finally, we again encounter the problem of the geometrical filling factor (see § IIIb). The nebulae with measured  $\xi < 1$  are akin to Greig's (1971) B nebulae (or classes 1 and 2 of Khromov and Kohoutek 1968), which both Greig, and Sabbadin and Minello (1977), show have stronger [N II] and [O II] lines than other types of planetaries. These results are confirmed by analysis of Tables 1, 2, and 5, which is summarized in Table 6, where the upper limits for  $\langle N/\alpha \rangle$  and  $\langle I(\lambda 3727) \rangle$  for  $\xi = 1$  are taken as true values. The mean intensities

TABLE 6  
MEAN  $\langle N/\alpha \rangle$  AND  $\langle I(\lambda 3727) \rangle$

| Parameter                               | $\xi < 1$ | $\xi = 1$ |
|---|-----------|-----------|
| $\langle N/\alpha \rangle$ .....        | 1.5       | <0.4      |
| $\langle I(\lambda 3727) \rangle$ ..... | 360       | <110      |

of the [N II] and [O II] lines are over 3 times greater in the nebulae with  $\xi < 1$  than they are in the others. The morphology as characterized by  $\xi < 1$  represents the nebula more as seen in the low excitation lines, or because of stratification, it represents the appearance of the outer parts of the nebula. The neutral hydrogen and ionized helium responsible for absorption of the stellar Lyman radiation may not be distributed in the same way, and thus the value of  $\xi$  estimated from broad-band photographs may not apply to the determination of Zanstra temperature.

This contention is supported by observational evidence. Young's (1982) long-slit spectrophotometry across the Helix (NGC 7293), a typical low- $\xi$  nebula, shows that the central hole is much less evident in H $\beta$  than in [O II] and [N II], and that it is absent in He II  $\lambda 4686$ . The effect can also be seen in Capriotti's (1978) H $\alpha$  and [N II] photographs of this object. Aller's (1956) and Atherton *et al.*'s (1978) isophotes of the Ring Nebula, NGC 6720, for which  $\xi$  is estimated to be 0.5, show a similar phenomenon. The gross distribution of radiation in H, and particularly He II, is smoother than it is in [O II] and [N II] in these objects, implying that for the purpose of Zanstra temperature determination  $\xi$  should be close to unity. Atherton *et al.* (1978) in fact demonstrate that NGC 6720 can be explained in terms of a closed shell, for which  $\xi = 1$ . A similar conclusion is reached by Phillips and Reay (1980) in their structural study of NGC 6720 and NGC 2474-5.

Still further evidence for  $\xi \approx 1$  comes from examination of the values of TR, the ratios of the He II and H Zanstra temperatures. These ratios should always be  $\geq 1$  (see above). As  $\xi$  is decreased,  $T_e(\text{H})$  increases faster than  $T_e(\text{He II})$ , and for NGC 7293, with  $\xi = 0.45$ ,  $\text{TR} = 0.78 \pm 0.08$ . If  $\xi = 1$ , however, TR is  $0.90 \pm 0.09$ , essentially within the error of unity. A similar but more marginal example is NGC 6853. Generally, the limit of  $\text{TR} = 1$  is fitted better with  $\xi = 1$  than with the measured values. This particular evidence is admittedly weak: the low TR might be an artifact of the model used (see Bohlin, Harrington, and Stecher 1982), and the total  $\lambda 4686$  flux integrated from Young's (1982) slit spectroscopy may not be accurate. The possibility that  $\xi$  may be 1 for He<sup>+</sup>, and under unity (but greater than the stated value) for H, does not invalidate the argument. We do not yet know whether we can generalize these arguments to include all nebulae, but for now the most consistent approach is to adopt a  $\xi$  of unity for the derivation of  $T$  and  $L$ . The measured values will play a further role in § IVe(ii). The problem should be studied further and fully resolved with monochromatic photographs of many more of the nominal low- $\xi$  nebulae, particularly of the more extreme cases such as A24 and Jn-1.

In summary, the most appropriate and self-consistent values of temperature and luminosity in Table 5 are  $T(\text{He II})$  and  $L(\text{He II})$  for the smaller  $\phi$  and for  $\xi = 1$ .

#### g) Optical Depths and Limiting Values

The determination of the temperature and luminosity is strongly affected by the optical depth of the nebula.

In accord with the original outline by Seaton (1966), three distinct cases can be recognized, assuming of course a blackbody, that there is no absorption by internal dust, and that our above assessment of  $\xi$  is correct:

1. The nebula is optically thick in both the hydrogen and He<sup>+</sup> Lyman continua,  $T(\text{H}) = T(\text{He II}) =$  effective temperature, and  $\text{TR} = 1$ . If the nebula is thick, however, the distance and the stellar luminosity will be overestimated (see § IIIc).

2. The nebula is optically thin in the hydrogen Lyman continuum, but is still thick in that of He<sup>+</sup>, that is, the He<sup>++</sup> zone is smaller than the H<sup>+</sup> or He<sup>+</sup> zone.  $T(\text{H})$  is then underestimated, but  $T(\text{He II})$  is correct and  $\text{TR} > 1$ . But now the optical depth condition for distance is satisfied, and the luminosity is also correct. This situation is obviously the ideal.

3. The nebula is optically thin in both Lyman continua, helium is fully doubly ionized, and both  $T(\text{H})$  and  $T(\text{He II})$  are lower limits. By a continuity argument,  $T(\text{He II})$  will be closer to the true temperature, and TR is larger yet. The distance is correct, and the  $L(\text{He II})$  is now also a lower limit.

The optical depth effects are independently confirmed by Figures 3 and 4, in which  $\log I(\lambda 3727)$  [O II] and  $\log (N/\alpha)$  are plotted against TR (for  $\xi = 1$ ), with which they correlate in the expected manner. At high optical depth, as evidenced by the similarity of the two

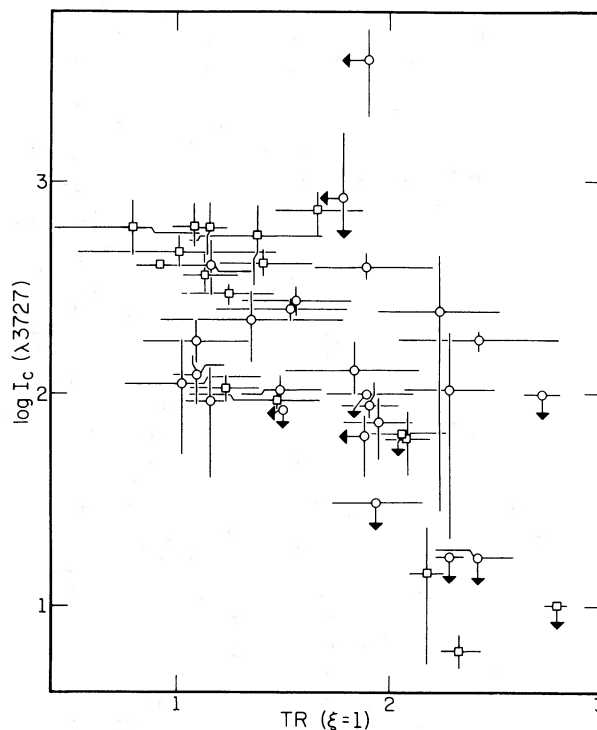


FIG. 3.— $\log I(\lambda 3727)$  [O II], corrected for interstellar extinction, plotted against TR, the ratio of the He II and hydrogen Zanstra temperatures, showing the effect of optical depth. The geometrical filling factor,  $\xi$ , is assumed to be unity. Circles: wide aperture data from Table 1; boxes: inhomogeneous data from Table 2.

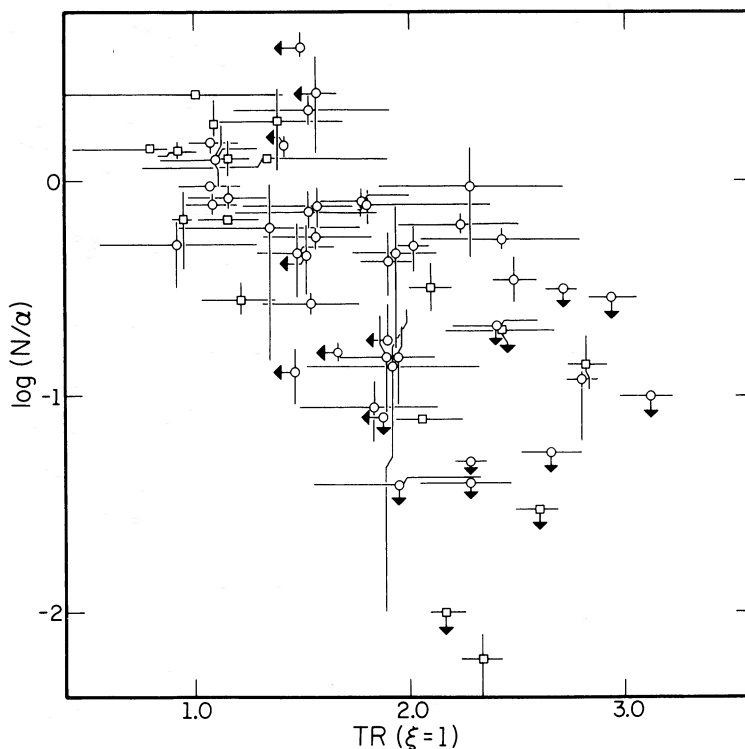


FIG. 4.— $\log I(\lambda 6584 [\text{N II}])/I(\text{H}\alpha) = \log(N/\alpha)$ , plotted against TR, showing optical depth effects. See the legend to Fig. 3.

Zanstra temperatures, we see clearly the expected development of extensive zones of low ionization.

Figure 5 shows the relation between  $I(\lambda 4686) \text{ He II}$  and TR. As optical depth decreases toward higher TR, we see also that the  $\text{He}^{++}$  shell grows until it occupies the entire nebula. At  $\text{He}/\text{H} = 0.10$  and  $T_e = 14,000 \text{ K}$ , this will occur at  $I(\lambda 4686) = 114$  (Brocklehurst 1971) and  $\text{TR} \approx 2.6$ .

Low nebular optical depth and high  $\lambda 4686$  occur in conjunction with high stellar luminosity. From Table 5,  $I(\lambda 4686) > 65$  and  $\text{TR} > 2$  occur generally only for  $\log L > 2$ , and  $\text{TR} > 2.5$  for  $\log L > 2.5$ . As expected, a high photon flux penetrates the nebula, expanding the  $\text{He}^{++}$  shell. Analogously, note that low TR occurs in conjunction with lower luminosity stars, also as expected.

These three figures also allow us to draw a conclusion regarding internal dust. Note that TR approaches unity as a limit, with no nebula significantly below unity. According to Helfer *et al.* (1981), internal dust acts to increase TR in the same manner as low optical depth. If dust were generally present, we would expect that TR would approach a limit somewhere above unity. We cannot ignore the likelihood, however, that dust may be selectively present for high  $\lambda 4686$  and high TR, as it appears to be for Abell 30 (Greenstein 1981). In that case it could not be distinguished from low gas optical depth. It is also possible, though unlikely, that low  $\xi$  (which lowers TR) and internal dust just compensate for one another.

Criteria for optical depth and for distinguishing among the three cases above must necessarily be rather arbitrary.  $\text{TR} = 1.2$  is generally within observational error of unity, and nebulae with TR below this value have a good chance of being optically thick. If  $I(\lambda 4686) \geq 90$ , the  $\text{He}^{++}$  shell approaches the outer boundary of the nebula, and there is a good chance of significant  $\text{He}^+$  Lyman leakage (the limit may well be lower depending on nebular morphology). In summary, the criteria adopted are as follows:

Case 1:  $\text{TR} \leq 1.2$ ,  $T(\text{He II})$  is correct,  $L(\text{He II})$  is an upper limit (Seaton 1966, class a i);

Case 2:  $\text{TR} > 1.2$ ,  $I(\lambda 4686) < 90$ ,  $T(\text{He II})$  and  $L(\text{He II})$  are correct (Seaton class a ii); and

Case 3:  $I(\lambda 4686) \geq 90$ ,  $T(\text{He II})$  and  $L(\text{He II})$  are lower limits (Seaton class a iii).

The case 3 optically thin nebulae are indicated by an "H" in column (12) of Table 5.

Two other instances involve limits. If only an upper limit is known for  $I(\lambda 4686)$ , as occurs for nine nebulae, the  $\text{He II}$  Zanstra temperature and luminosities will be upper limits as well. In the single case of Sh 2-71, where the observed magnitude sets a lower limit to the magnitude of the apparently unseen subdwarf,  $T$  is a lower limit, and  $L$  an upper limit.

#### h) Nitrogen-to-Oxygen Ratios

The intensities of the  $\lambda 3727 [\text{O II}]$  and the  $\lambda 6584 [\text{N II}]$  lines (or the  $\text{N}/\alpha$  ratios) are used to calculate

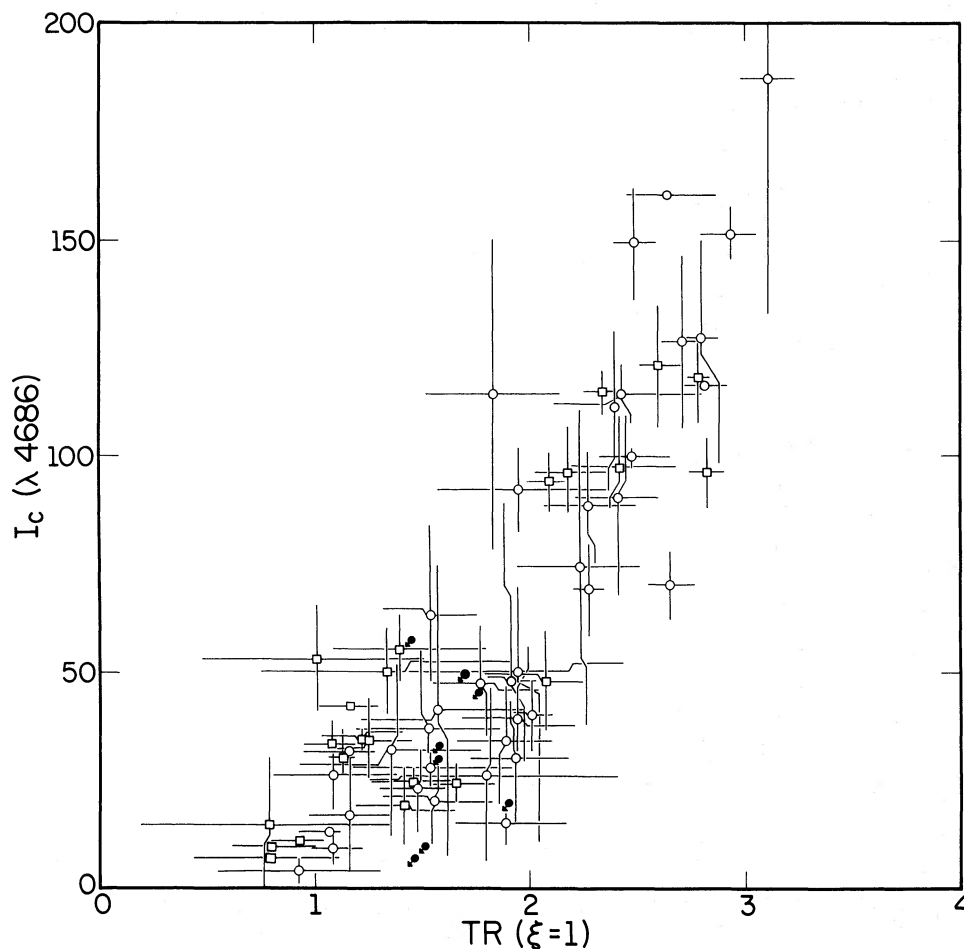


FIG. 5.— $I(\lambda 4686)$  He II plotted against TR, showing optical depth effects and the growth of the He<sup>++</sup> zone. See the legend to Fig. 3.

$N^+/O^+$  ratios, which are then by the usual practice considered equal to  $N/O$ ; see Kaler (1979) for details and for atomic parameters. The  $[N II]$  electron temperatures, those appropriate to the  $N^+$ - and  $O^+$ -emitting regions, are available from Kaler (1979) for only six of the planetaries considered here. Averages for these, and for all the higher excitation nebulae in that list, show  $\bar{T}_e \approx 10,000$  K, rather independent of nebular ionization, which is the value used in the calculations. Collisional de-excitation of the metastable states can be largely ignored because of the low electron densities (generally well under  $10^3 \text{ cm}^{-3}$ ) of these large nebulae. Given  $T_e = 10,000$  and  $N_e = 400 \text{ cm}^{-3}$ ,

$$N/O = 148(N/\alpha)/I(\lambda 3727), \quad (5)$$

after correction for interstellar extinction. The coefficient provides roughly the minimum probable values of  $N/O$ . A decrease in  $N_e$  to zero increases  $N/O$  by only 6%, and an increase in  $T_e$  to 14,000 K increases  $N/O$  by about 60%.

The  $N/O$  ratios computed with equation (5) are presented in column (15) of Table 5. For the nebulae of

Table 1 they are calculated directly from  $I(\lambda 3727)$  in columns (7) and (12) of that table. For the additional objects of Table 2, however, we must consider stratification and weighting effects. The  $\lambda 3727 [O II]$  intensities and the  $(N/\alpha)$  ratios in Table 2 are the means of all values given by the references in column (9), and since different authors often observe different parts of the spectrum in different locations in the planetary, the mean  $[O II]$  and  $[N II]$  intensities may not exactly relate to one another. For these objects,  $N/O$  is based on the mean  $(N/\alpha)/I(\lambda 3727)$  computed from those studies listed in column (9) in which both lines were observed. That mean ratio can be recovered by dividing the number in column (15) by 148. The assigned error includes errors in the line intensities and in  $c$ ; no error is assumed for  $T_e$ . The  $N/O$  ratios presented here are quite consistent with the values published by Kaler (1979) for objects in common.

#### i) Helium Abundances and a Note on Observational Selection

Helium-to-hydrogen ratios, taken from Kaler (1979) and Kaler and Hartkopf (1981), which will be used

below for comparison with the N/O ratios, are shown in column (16) of Table 5. Some further information on He/H ratios can be derived from the  $\lambda 4686$  He II intensities presented in Table 1. Nebulae with  $I(\lambda 4686) > 114$  must have He/H  $> 0.10$  (electron temperature has only a minor effect). Those with significantly high values are A20, A30, A78, and K1-14, for which  $\text{He}^{++}/\text{H}^+$  is in the neighborhood of 0.13 to 0.16. A30 and A78 are the two nebulae with internal zones of nearly pure helium (Hazard *et al.* 1980; Jacoby and Ford 1983), the line fluxes from which are averaged into the data presented here. Note that the southwest position of A78 (see Table 1), which apparently avoids the high helium zone, has a lower  $\lambda 4686$  intensity ( $\text{He}^{++}/\text{H}^+ \approx 0.13 \pm 0.03$ ). Nebulae with total  $I(4686)$  much above 125 ( $\text{He}^{++}/\text{H}^+ = 0.11$ ) are relatively rare.

Figure 5 exhibits a curious gap in the distribution of points, at  $I(\lambda 4686) \approx 65$ . The gap is present along the regression line but is not significant for the distribution along either  $I(4686)$  or TR. It may be an artifact of observational selection, since nebulae were usually chosen either on the basis of surface brightness, or on the brightness, or observability, of the central star. Or the effect may be real and reflect variation in evolutionary time scales. Only more data will resolve the issue.

#### IV. EVOLUTION

##### a) Distribution on the Log L-Log T Plane: Range of Core Masses

The planetary nuclei in Table 5 are displayed on the log L-log T plane in Figure 6, where nebular radii are given in units of 0.01 pc, and limits are indicated on  $L(=L/L_\odot)$  and  $T$  according to the precepts of § IIIg. Note the directions in which the points with limits may be moved, as described both there and in the figure legend. A82 and K2-2 are not plotted because of the uncertainty of their central stars, nor are the binaries A46 and Sh 2-71. Also displayed are the Paczyński (1971) evolutionary tracks for core masses of 0.6, 0.8, and  $1.2 M_\odot$ , Iben and Renzini's (1982) track for  $0.6 M_\odot$ , and the extrapolated track for  $0.55 M_\odot$  from Schönberner and Weidemann (1981b). The  $0.6 M_\odot$  track from the latter reference is quite similar to Iben and Renzini's.

Remember that the smaller nebulae are yet to be appended above  $\log L \approx 3$ ; this is done in preliminary form by Iben *et al.* (1983). Note principally the very large spread of points, from within the hook of the  $0.55 M_\odot$  track, down nearly to the  $1.2 M_\odot$  track. Almost all of the points within the hook are the large high-excitation nebulae of Kaler (1981a), for which  $L$  and  $T$  are lower limits. If these are moved up and to the left along loci parallel to the one displayed for A78, this area is effectively cleared of central stars. Iben *et al.* (1983) argue that at least some of these objects have suffered a thermal pulse on the declining portion of a track and are now retracing the horizontal portion, moving to the left. Of the few remaining within

the boundaries of this track, one (NGC 6720) is an upper limit, another (NGC 6781) apparently has poor central star magnitudes, and yet another (BV-3) has a poorly determined angular radius, and consequently an uncertain stellar luminosity. We then see, from this paper and from Iben *et al.* (1983), that the points are properly distributed around the diagram with a minimum core mass in the range  $\approx 0.55$ – $0.6 M_\odot$ .

The data further indicate that there may be a considerable range in final core mass from the minimum of  $\approx 0.55 M_\odot$ , up to as high as  $\approx 1 M_\odot$  (depending on the distance scale adopted; see below). This result agrees with that by Stecher *et al.* (1982), who find planetary nuclei in the Magellanic Clouds with masses  $\approx 1 M_\odot$ . This and the present study are complementary: Stecher *et al.* (1982) examined the luminous nuclei on the horizontal portion of the evolutionary track, here we look at nuclei on the cooling portion, and both studies agree quantitatively as to the existence of the higher mass cores.

##### b) Distribution of Core Masses

The distribution of core masses is shown in Figure 7, based on the location of the Paczyński tracks, and the interpolations between them. The selection of large nebulae in this paper requires that we be confined to discussing stars that are on the cooling tracks, for which the data are relatively complete. Thus for an initial analysis, the three stars to the upper right of Figure 6 that clearly appear to be on horizontal tracks (NGC 6058, NGC 6842, and M2-51) are excluded, plus those that are represented only by lower limits in  $L$  and  $T$  (the circled points). Most of these are probably on horizontal tracks, either as return visitors (see above), or as slowly-evolving low-mass cores (§ IVd below). Some may be on cooling tracks, but since their true locations are not known, it seems best to remove them as a set. For the remainder, upper limits (either in  $T$  or both  $T$  and  $L$ ) are taken as true values, and any star on a mass-division line is assigned to the lower mass group. Those for which  $T$  and  $L$  are both upper limits [for which only an upper limit in  $F(\lambda 4686)$  is known] move diagonally to the lower right as  $F(\lambda 4686)$  is decreased, roughly parallel to the Iben-Renzini  $0.6 M_\odot$  cooling track, so that the stellar mass is still reasonably reliable. The resulting percentage distribution is shown as the solid line Figure 7.

For comparison, and to provide a limiting case, the distribution of all the points in Figure 6 is shown by the dashed line in Figure 7, which is probably overweighted to masses under  $0.6 M_\odot$  because of improper placement of the circled points. However, observational selection may overweight the restricted distribution, the solid line, toward higher masses (see the discussion below), so that the true distribution may be between the two. The distributions derived from  $T$  and  $L$  by consideration of the measured filling factors,  $\xi$ , are similar.

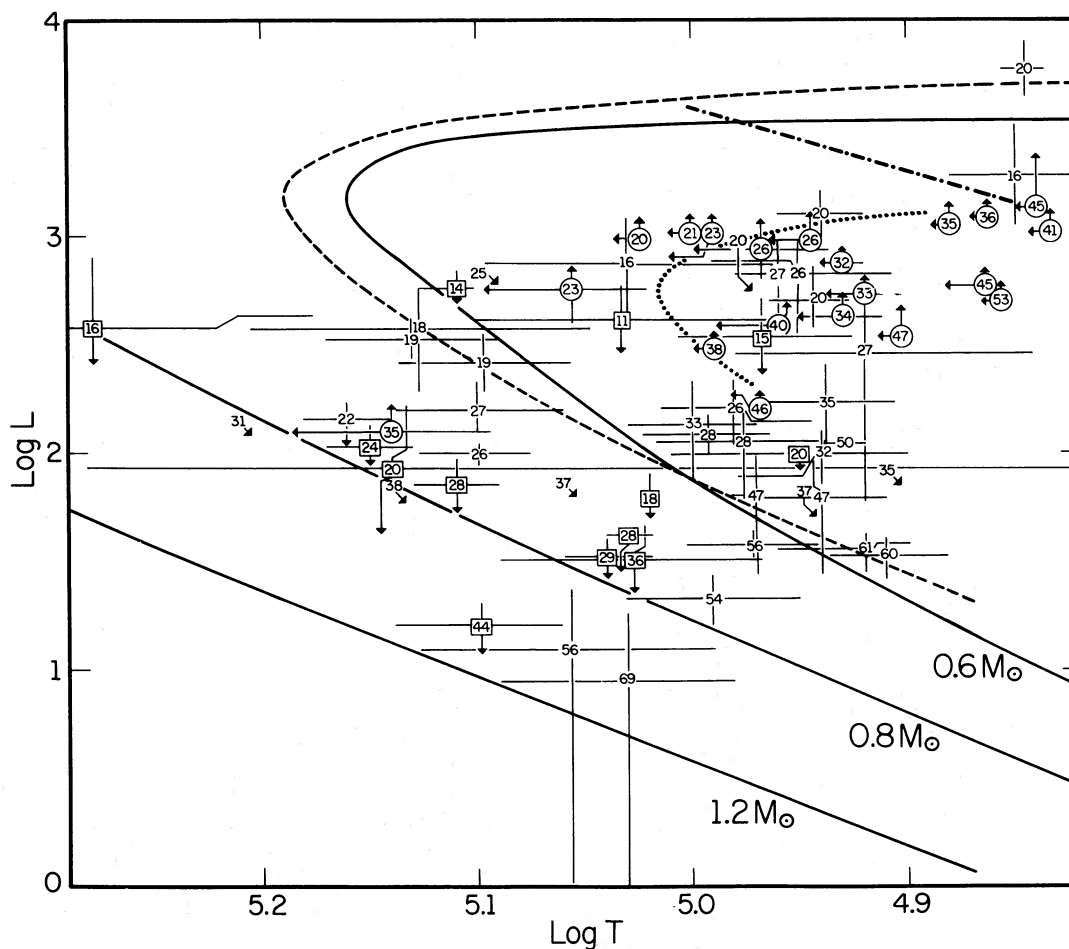


FIG. 6.—The planetary nuclei on the log  $L$ -log  $T$  plane, indicated by numbers that express the nebular radii in units of 0.01 pc. The solid curves are the Paczyński 1971 tracks for 0.6, 0.8 and  $1.2 M_{\odot}$ . The dashed curve is Iben and Renzini's 1982 track for a  $0.6 M_{\odot}$  core, and the dotted curve is Schönberner and Weidemann's 1981*b* extrapolated track for  $0.55 M_{\odot}$ . The horizontal and vertical arrows indicate optically thick and thin nebulae, and the consequent upper and lower limits on  $T$  and  $L$ , as discussed in the text (§§ IIIg and IVb). Boxes around the numbers denote nebulae that are optically thick in the hydrogen Lyman ultraviolet, for which  $L$  is an upper limit. Circles indicate nebulae that are thin in the  $\text{He}^+$  Lyman continuum, for which  $T$  and  $L$  are lower limits. The dot-dashed line, which originates at the Abell 78 point, is the locus along which the star moves as optical depth is taken into account and the temperature is increased from the lower limit; all circled points may be moved parallel to this line. The arrows pointing downward at  $45^\circ$  indicate nebulae for which only upper limits on  $F(\lambda 4686) \text{ He II}$ , and  $T_r(\text{He II})$  are available. These points may be moved down and to the right roughly parallel to the Iben-Renzini  $0.6 M_{\odot}$  cooling track.

Schönberner (1981) has examined the core mass distribution of planetary nuclei through a comparison of nebular radii (or ages) and absolute visual magnitudes to those predicted from theory. He finds a sharp peaking to low mass cores, with 85% of the cores under  $0.61 M_{\odot}$ , and also states that 80% (decreased by Schönberner 1983 to 75%) of the faint nuclei ( $M_v > 5$ ) have cores under  $0.65 M_{\odot}$ . For comparison, Schönberner's distribution is replotted from his Figure 10*a* (the corrected total ensemble) onto Figure 7. (Note that his mass intervals are different, so that for comparison with the new distribution, his two points below  $0.6 M_{\odot}$  must be added.) Like his, the new distribution climbs toward lower mass cores, but not as steeply, with between 52% (solid line) and 65% (dashed line) of the cores under  $0.6 M_{\odot}$ . This difference is reflected by a general

broadening of the mass distribution that is particularly noticeable for masses above  $0.7 M_{\odot}$ .

For further comparison, the DA white dwarf distribution from Koester, Schulz, and Weidemann (1979), as taken from Schönberner's Figure 10, is shown as the dot-dash line in Figure 7, where all the percentages for  $M < 0.6 M_{\odot}$  are added and displayed as the horizontal bar from 0.5 to  $0.6 M_{\odot}$ . Note that the average of the distribution derived here and that found by Schönberner broadly fits that of the white dwarfs up to  $0.8 M_{\odot}$ , the maximum. Note also that some of the other mass distributions presented by Koester, Schultz, and Weidemann (1979) indicate masses up to  $1 M_{\odot}$ , consistent with Figure 7.

If we now restrict the selection of stars to those with  $M_v > 5$  (represented by a line running from  $\log T = 4.8$ ,

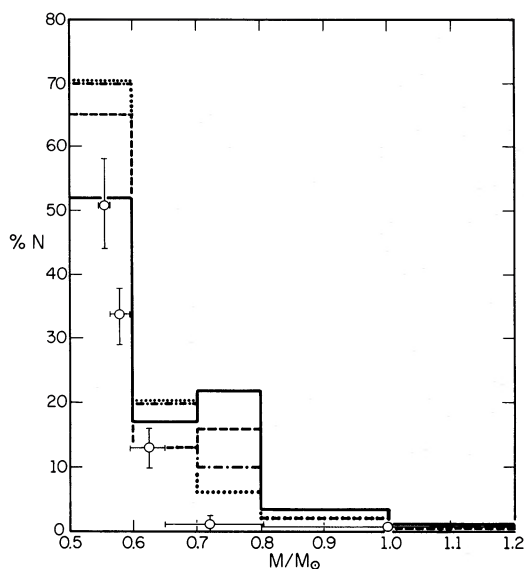


FIG. 7.—The mass distribution of planetary nuclei. *Solid line*: this paper, from Cahn-Kaler distances and Paczyński's tracks, excluding stars represented by lower limits in Fig. 6 and the three other stars clearly on the horizontal tracks; *dashed line*: the same, except for all the stars on Fig. 6, accepting the lower limits as placed; *dotted line*: this paper with Schönberner's 1979 tracks, extrapolated to higher mass, and with the distances increased by 20% to match Schönberner's 1981 analysis, again including all the stars of Fig. 6; *dot-dash line*: white dwarf distribution from Koester, Schulz, and Weidemann 1979, as taken from Schönberner 1981, with all masses below  $0.6 M_{\odot}$  indicated by the line between  $0.5$  and  $0.6 M_{\odot}$ ; *points*: Schönberner's 1981 mass distribution for his corrected total ensemble (for comparison, note the mass range for each point indicated by the horizontal line).

$\log L = 2$  to  $\log T = 5.2$ ,  $\log L = 3.2$ , placed by using the same bolometric corrections used by Schönberner), we find that 45%, about twice Schönberner's numbers, have core masses  $> 0.65 M_{\odot}$  (irrespective of whether the circled points in Fig. 6 are used). From the present work, it thus seems evident that the stars in the mass range that produce planetaries result in a significant range in post-AGB remnant mass. Further discussion of the relation between initial and final mass will be discussed in § IVe below.

The Schönberner distribution and those derived here are not based upon identical assumptions, which in part accounts for the difference between them: he uses his own tracks (Schönberner 1979, which are more like the dashed line in Fig. 6) instead of the Paczyński tracks, and he uses a distance scale 20% larger (see § IVc). Application of the Schönberner tracks to Figure 6 (where it is assumed that the relative relation between the Schönberner and Paczyński tracks at  $0.6 M_{\odot}$  is the same for the other masses) will narrow the mass distribution somewhat, increasing the numbers under  $0.6 M_{\odot}$  and between  $0.6$  and  $0.7 M_{\odot}$  by about 4%, and similarly decreasing the percentage between  $0.7$  and  $0.8 M_{\odot}$ .

A 20% increase in the distances (44% in luminosity) produces a somewhat similar effect. The combination of these two changes, coupled with the full data set (i.e.,

including the circled points in Fig. 6) yields the narrowest possible distribution from the data points in Figure 6, given by the dotted line in Figure 7. Although closer to Schönberner's, it is still wider, with 70% less than  $0.6 M_{\odot}$ , and is quite close to the white dwarf distribution. (If we again restrict the data to stars with  $M_{\odot} > 5$ , the percentage of stars with  $M > 0.65 M_{\odot}$  drops somewhat, to 40%.) These narrowing effects are offset by the conservative procedures used to assign stellar masses: some stars that are on the mass division lines and some that are given by upper limits in  $L$  may belong to a higher mass group, thus widening the distribution, but in an unknown way. The deletion of central stars of questionable identification and magnitude (§ IIIa) has little effect since they are well distributed.

Part of the difference between Schönberner's distribution and the new wider one could also be ascribed to observational selection, which is difficult to evaluate. The acquisition of data for this study was biased toward the largest objects, for which  $L$  is often very low, which tends to broaden the mass distribution. But these objects are observed only locally in the disk, which limits the number that can be seen because of interstellar extinction (§ III d), and that should tend to narrow the distribution. In contrast, Schönberner's distribution is biased in the other direction, because he did not have these data on large objects available to him. The truth probably lies somewhere in between. Recent work by D. Schönberner (1982, private communication) on a local sample using these new data and the lower distance scale in fact shows better agreement between the two techniques. The only real solution is to increase considerably the amount of data in order to produce more reliable statistics.

### c) Critique

Here, we will look in more detail at some of the problems other than observational selection that afflict the core mass distributions as derived here, and as derived by Schönberner (1981). In drawing any conclusion regarding stellar mass, we must be very aware of some large error bars (note NGC 6445 and NGC 6563) and of possible systematic effects in the distances. If the objects near the  $0.8$  and  $1.2 M_{\odot}$  tracks have systematically high nebular masses, we would be underestimating their distances and stellar luminosities (see Cahn and Kaler 1971). To bring the three lowest planetaries up to the  $0.6 M_{\odot}$  curve, however, would require a factor of 3 increase in distance, and a factor of 16 increase in the assumed nebular mass of  $0.18 M_{\odot}$ , which seems unlikely.

Evidence supporting the relative placement in Figure 6 can be found by comparing the measured extinctions with those predicted for the distances in Table 5 from Cahn's (see Cahn 1976) galactic interstellar extinction model. We must restrict the comparison to planetaries that have substantial extinction, those within  $10^{\circ}$  of the galactic plane. The plot of  $c(\text{model})$  versus  $c(\text{observed})$  is shown in Figure 8, where the more reliable  $B-V$

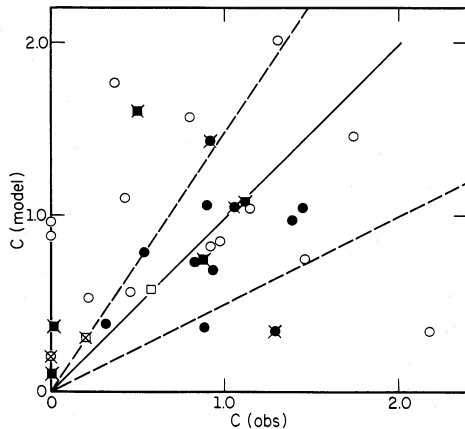


FIG. 8.—Extinction constants from Cahn's dust model for the calculated distances of Table 5, plotted against the observed extinction constants for nebulae with galactic latitude  $< 10^\circ$ . The boxes represent the nebulae below or near the  $0.8 M_\odot$  track. The filled symbols are nebulae with  $\xi < 1$ . Optically thick nebulae, with  $TR < 1.2$  (see text, § IVb) are indicated by an "X" through the symbol.

extinction is used for A13. Two-thirds of the nebulae are within about  $\pm 50\%$  of the  $45^\circ$  slope. However, Cahn constructed the model in order to fit a large set of planetaries, some of which are included here, and a correlation is naturally expected. Figure 8 cannot therefore be used to test the calibration of the distance scale, but it *can* be used to examine systematic differences among different types of nebulae. The seven nebulae with cores near the  $0.8 M_\odot$  track that satisfy the latitude criterion (NGC 2438, NGC 6445, NGC 6563, NGC 6853, A71, A80, and K2-1) are shown as boxes in the figure. Elevating these to the  $0.6 M_\odot$  track requires an approximate doubling of distance, and we would then expect these nebulae to have observed extinctions roughly twice those calculated from the model. That trend is not seen in Figure 8; if anything, these nebulae tend to lie above the  $45^\circ$  slope rather than below. There is also no significant difference in Figure 8 between these seven nebulae near the  $0.8 M_\odot$  cooling track and those isolated specifically near the  $0.6 M_\odot$  cooling track that might indicate that the apparently higher mass cores have underestimated luminosities. Unfortunately, the argument is weakened by the large errors on the placement in Figure 6 and on the extinctions for three of the objects. In addition, six of the above set of seven may be optically thick, with the distance and  $c(\text{model})$  overestimated, but that is not likely to cause an effect as large as a factor of 2. Note that the thick and thin nebulae have no general systematic variation in placement in Figure 8. Further support against systematic relative distance effects is provided by Cudworth's (1974) statistical parallaxes; the matter is discussed further in § IVe(iv).

Finally, even if we can be convinced that the relative distances are correct, the distance scale factor, or the assumed nebular mass, may be in error. Cudworth (1974), for example, derived a scale factor 1.45 times greater than that used by Cahn and Kaler (1971), in

agreement with the older Seaton (1966) scale. The effect would be to increase all the luminosities by about 0.3 in the log. The upper core mass limit would be the more affected of the two, resulting in a range of from perhaps just under  $0.55 M_\odot$  to just over  $0.8 M_\odot$ , thus narrowing the mass distribution, as discussed in the last section. To resolve the issue, we must make use of the distribution of luminous planetary nuclei on the horizontal tracks, for which an increase in the distance will *broaden* the mass dispersion. In fact, with a complete sample of stars, and proper allowance for optically thick nebulae, the match between mass dispersions from the horizontal and the cooling tracks can be used to test and determine the distance scale factor.

The placement in Figure 6 can be further tested by referring only to measured temperatures, which are much more reliable than the luminosities. Note from the figure that the maximum observed temperatures are about the same as that of the  $0.6 M_\odot$  evolutionary track. The situation does not change if the compact planetaries are included; see Iben *et al.* (1983). If some stars truly have core masses of 0.8 to  $1 M_\odot$ , where are those with high temperatures? From Paczyński (1971), we would expect temperatures up to 270,000 K ( $\log T = 5.43$ ) for  $0.8 M_\odot$ , and perhaps 400,000 K for  $1.0 M_\odot$ . If we use the measured  $\xi$ , and exclude NGC 6445 (the left-most point), the maximum moves out to about  $\log T = 5.22$ , somewhat over the  $0.6 M_\odot$  maximum, but still far short of that for  $0.8 M_\odot$ .

The temperature data alone tend to support Schönberner's (1981) contention of a narrow range of core mass. There are, however, two likely explanations, both of which involve some form of observational selection. As pointed out by Renzini (1979), the time scales of evolution work against detection of the high temperature nuclei. Those of higher core mass move around the bend very quickly, and we see them only when the course of evolution has slowed down at lower temperatures. In this case, our sample is simply too small to have picked up any of the rarer high-temperature stars.

The second likely explanation is simply the matter of observability. If high temperature stars are intrinsically rare, they tend to be distant, and consequently faint and undetected. In addition, it is frequently difficult, if not impossible, to detect a star against a bright nebular background. If we move the star to the left in Figure 6 at constant luminosity, the nebula stays near constant luminosity, and the visual magnitude of the star drops. Several planetaries of this sort are known, the classic case being NGC 7027 for which a nucleus has not been unambiguously found. Shaw and Kaler (1982) suggest a minimum  $\log T$  of 5.27, well above the  $0.6 M_\odot$  maximum, by finding the point at which  $T(\text{H}) = T(\text{He II})$  for hypothetical stars of different magnitude.

The Schönberner (1981) technique is not without its problems, either. Both methods share the uncertainty in the distances, which here affect only luminosities but in the Schönberner approach affect both absolute magni-

tudes and nebular radii. The latter also includes additional sources of systematic error by assuming: (1) a constant expansion velocity of  $20 \text{ km s}^{-1}$ , when Sabbadin and Hamzaoglu (1981) and Robinson, Reay, and Atherton (1982) show large variation and a possible age-related gradient, and (2) that we theoretically know the moment of ejection of the planetary, that is, that the theoretical ages actually refer to the time interval from the liftoff of the nebular shell (see § IVd).

A noticeable problem with Schönberner's (1981) study is seen by examining the relation between central star temperature and nebular radius illustrated in his Figure 7. Over one-third of his points are above the curve for  $\log T = 4.8$ , or are cooler than  $T = 63,000 \text{ K}$ . From both Harman and Seaton (1966) and Kaler (1976c), the associated nebulae should have weak or absent  $\lambda 4686$ , or rather they should have little or no  $\text{He}^{++}$ . The radii of nebulae with no  $\lambda 4686$  are almost all small: 70% of those with measured central star magnitudes have  $r < 0.10 \text{ pc}$ , from recalculation of the Cahn and Kaler (1971) distances, or  $r < 0.12$  on the scale used by Schönberner. But in his Figure 7, there are a considerable number (60%) with radii greater than 0.12, which should have central star temperatures greater than indicated, that is, the placement of stars on this graph by absolute magnitude and radius greatly underestimates the actual central star temperatures of some nebulae as determined from the Zanstra and Stoy (Kaler 1976c) methods. The problem is in part relieved by reverting to the Cahn and Kaler (1971) distances (D. Schönberner 1982, private communication).

In summary, the data presented here support the concept of a range of core masses and a mass distribution wider than indicated by Schönberner (1981), although the truth may be somewhere in between. The agreement with Stecher *et al.* (1982) on the subject of high core masses is encouraging, but real proof will require a larger sample of data. For further progress we must examine many of the more heavily reddened large objects of the galactic plane in order to test distances for various types of nebulae on the basis of extinction and to examine more fully the set of massive stars that occupy the plane. Then we must examine the heretofore unobserved nebulae with the faintest central stars, search for and measure the magnitudes of stars where they are now unidentified (which includes 25% of the Abell 1966 list), and improve the techniques for the measurement of stellar magnitudes against a bright nebular background.

#### d) Time Scales

A critical test of evolutionary theory, the approach by Schönberner (1981), is the comparison of the predicted ages against those determined by nebular radius and expansion velocity. There is general qualitative agreement in Figure 6: along an evolutionary track, the nebulae increase in size from the lower limit of this study,  $\approx 0.2 \text{ pc}$ , up to the current detectability limit of  $\approx 0.6 \text{ pc}$ . And the envelope enclosing the limit of the largest nebulae below  $\log L \approx 2$  curves down and to

the left as predicted by Schönberner and Weidemann (1981).

An accurate quantitative comparison is difficult because of the small number of expansion velocities for nebulae of this type—only 12 and 17 of the nebulae studied here are represented in the lists of Sabbadin and Hamzaoglu (1982) and Robinson, Reay, and Atherton (1982), respectively—and because of the uncertainty of the interval between the ejection of the nebula and the time at which it first becomes visible (see Iben and Renzini 1982). At the point where the  $0.6 M_{\odot}$  cooling track crosses  $\log T = 5.0$ , both Schönberner (1981) and Iben and Renzini (1982) calculate an age of  $\approx 20,000$  years. For an average current expansion velocity of  $30 \text{ km s}^{-1}$  for these large nebulae from Sabbadin and Hamzaoglu (1982), they should grow to a radius of  $\approx 0.6 \text{ pc}$ , substantially larger than observed; this large radius does not occur until farther along the track. V. Weidemann (1982, private communication) points out that the location of stars beyond the point at which the nebulae are theoretically expected to fade to invisibility suggests that either  $T$  or  $L$  may be in error. Alternatively, the mean expansion averaged over the lifetime of the nebula may be closer to the canonical value of  $20 \text{ km s}^{-1}$ , in which case the agreement is better with an expected radius at this point of  $0.4 \text{ pc}$ , or possibly, the fading times for planetary nuclei may be shorter than currently expected.

One last point involves the large high-excitation planetaries, those for which lower limits are given in Figure 6, which were involved in the discussion of the mass distribution in § IVb above. Note from Schönberner (1981) or from Schönberner and Weidemann (1981b), that the  $0.55 M_{\odot}$  track evolves very slowly, and that those low-mass cores would have very large nebular radii in the region of the turnaround, and even on the horizontal part of the track. Schönberner (1983) invokes this explanation to interpret the differences between A43 and A50 observed by Kaler and Hartkopf (1981). We must thus consider the possibility that some of these objects have low-mass cores and are not in the same category as A30 and A78, which from the arguments of Iben *et al.* (1983) are stars that are evolving to the left for the second time following a last thermal pulse. Accurate temperatures derived from ultraviolet observations are needed to decide the issue, so that these stars can be properly included in the mass distribution.

#### e) Evolution and Stellar Mass

Renzini (1979) and Iben and Renzini (1982) predict variations in nebular composition across the  $\log L$ - $\log T$  plane as a result of the evolution of stars of different initial mass, and the presumed positive correlation between initial mass, final mass, and the efficiency of convective dredge-up: see § I of this paper. The N/O ratios calculated for the nebulae presented here can be used to test this thesis.

##### i) Extreme N/O Ratios

Peimbert (1978) defined a set of planetaries that he called "Type I," which are highly enriched in nitrogen

and helium. (We ignore here the highly enriched zones inside A30 and A78, and consider only the nebulae proper.) They include such objects as NGC 6302, NGC 6445, Hu 1-2, and NGC 2440, and they can be found at the limits of the N/O–He/H correlations shown by Kaler (1979). One of these, NGC 6445, is included in this study. Table 5 shows several other nebulae with extreme N/O ratios ( $> 1$ ): NGC 2474–5, A24, A71, PW-1, Sh-71, and Ym 29. Sh 2-71 is particularly interesting, since it is more compact than the others and bears some similarity to NGC 6445. Several more nebulae have N/O in the range 0.5–1.0. The fact that the calculations incorporate a uniform electron temperature of  $10^4$  K (see § III*f*) is of little consequence; see the next subsection. From Becker and Iben (1980), these objects should be produced by the most massive stars that produce planetaries. They should all be examined in more detail, particularly for measurement of He/H.

A62 shows an extremely low value of N/O. I( $\lambda 3727$ ), which is very high, is probably in error.

#### ii) Composition and Morphology

Of the new type I nebulae, two (NGC 2474–5 and A24) exhibit a very distinct bi-lobed structure. From inspection of Table 5 we see that higher N/O generally correlates with nonspherical symmetry as expressed by the measured geometrical filling factor  $\xi$  (see § III*b*). In this paper,  $\xi$  is uniformly set to unity for the purpose of temperature determination, i.e., hydrogen and helium are assumed to form a generally closed shell around the star (§ III*f*). Nevertheless, the measured  $\xi$  is still some determinant of distinctive morphology, even if it is appropriate only to mass distribution within a closed shell or pertains only to the outer parts of a nebula where we find the lower ionization zones.

The correlation is shown in Figure 9, where A3, A13, and A35 are ignored because of high errors in N/O, K 2-2 is dropped because of uncertain morphology, and the special zones in A30 and A78 are also excluded. The correlation now becomes quite clear. Eighty percent of the nebulae with  $\xi \leq 0.5$  have N/O  $> 0.4$ , whereas the figure is only 25% for those with  $\xi = 1$ . The different distributions of N/O for  $\xi \leq 0.5$ ,  $\xi < 1$ , and  $\xi = 1$  are shown in a normalized plot in Figure 10. Morphology is an extremely difficult concept to quantify, as it involves considerable subjective judgement. It is thus very important to state that nearly all the values of  $\xi$  were determined at the beginning of this program, before most of the observations were made, and before there could be any preconceived notions about the correlation. For the few exceptions, which include Sh 2-71 and two or three others, the rules developed earlier were applied as rigorously as possible. Therefore  $\xi$  and N/O are objectively and independently determined. This quantitative morphology is supported by the independently determined Greig (1971) class, given in column (17) of Table 5. Nebulae with  $\xi < 1$  are generally Greig class B, those with bi-lobed structures, and those with  $\xi = 1$  are non-B (or C); of the 26 nebulae so classified, there

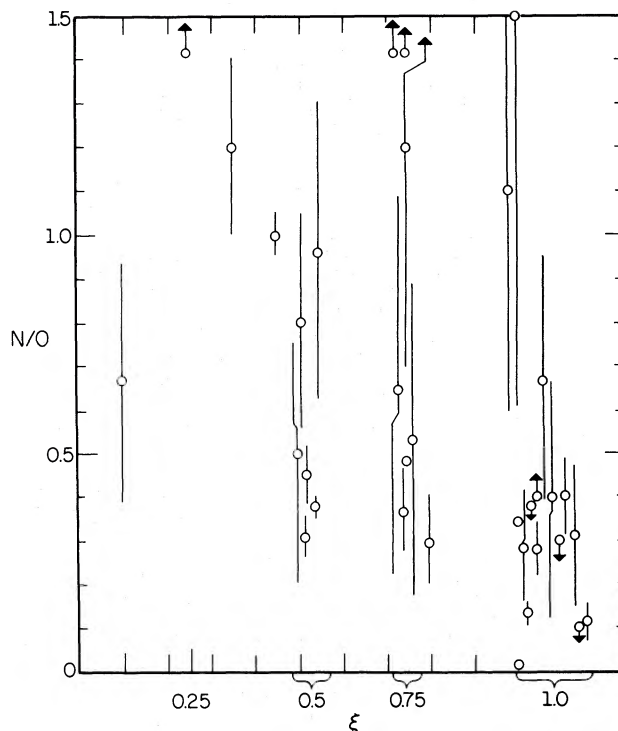


FIG. 9.—N/O for  $T_e = 10,000$  K, plotted against the geometrical filling factor,  $\xi$ .

are only four exceptions. If A50, with uncertain morphology (see § III*b*) is moved to the set with  $\xi < 1$ , the correlation of Figure 9 would be slightly weakened. Reconsideration of two of the high N/O nebulae with  $\xi = 1$ , however, strengthens the correlation. Ym 29 is a peculiar object that appears as a single large arc around the central star, and it may well be a B-type nebula. IRS data of A4 show that N/O is actually at the lower end of the error bar, under 0.4.

Although there are fewer nebulae to work with, the relationship is strengthened by examining the He/H ratios in column (16) of Table 5. These correlate with N/O as they do in Kaler, Iben, and Becker (1979) (note

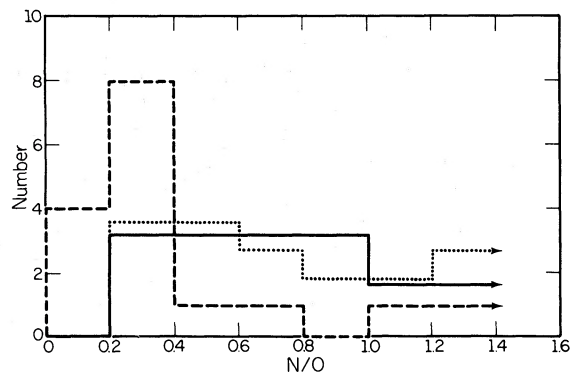


FIG. 10.—Histograms of the numerical distribution of N/O for nebulae with  $\xi = 1$  (dashed line),  $\xi < 1$  (dotted line), and  $\xi \leq 0.5$  (solid line). The latter two are normalized to the first.

particularly NGC 6445 and NGC 7293), and also with  $\xi$ . All the nebulae with  $\xi < 1$  have  $\text{He}/\text{H} > 0.11$ , whereas the figure is only 20% for those with  $\xi = 1$ .

The exact relation between element abundance enrichment and stellar mass (see Becker and Iben 1980; Renzini and Voli 1981) is not yet clear. The observed relation between C/O and He/H does not conform to that expected (Kaler 1981*b*), which implies that we are not yet certain theoretically as to how N/O should vary with initial mass. In addition,  $\text{N}/\text{O} > 1$  cannot be obtained theoretically unless we invoke Renzini and Voli's (1981) envelope burning, but the general correlation between observed N/O and He/H does not follow any specific correlation predicted by this mechanism (see Kaler 1983*c*). Finally, the highest observed He/H ( $\geq 0.17$ ), which correlate with the highest N/O, cannot be predicted by either of those pairs of authors under any of their circumstances. Nevertheless, from the theoretical work available, and the limited conformance with the observations, it is hard to avoid at least the qualitative conclusion that high N/O and He/H are the products of stars of higher mass. The obvious interpretation of Figure 9, then, is that nebular morphology is tied to stellar mass, with Greig's (1971) B-type nebulae the product of higher mass progenitors. This result is much the same as that found by Acker (1980) from a different and generally smaller set of nebulae (there is about 10% overlap); apparently it is true for planetaries in general. Both studies confirm Greig's (1972) analysis, in which he showed that the B-nebulae are confined to the galactic plane and thus should be related to a younger population, and by inference, to stars of generally higher mass.

Heap (1982) shows that the WC planetary nuclei correlate with the class B nebulae and presumably are also generated by the more massive set of stars. By inference, then, the nitrogen-rich planetaries correlate with the carbon-rich nuclei. We may tentatively speculate that the hydrogen envelopes of the more massive stars, which are nitrogen-rich due to dredge-up processes, were ejected to form the planetaries, leaving a bare core that is rich in carbon as a result of helium burning. Caution is advised here, however, as Heap's WC stars belong to the more compact set of planetaries, and there is little direct overlap with the nebulae studied in this paper: the compact B-nebulae may not be directly related to the large B-nebulae.

### iii) Caveats

The concept that stars of different initial mass produce nebulae with different apparent structure is so significant to present and future theories of the origin and development of planetaries that we must look very carefully at inconsistencies, alternate interpretations, and selection effects. The last of these is perhaps the most important. The [N II] and especially the [O II] lines will not be measured by the filter photometry if they are weak, and consequently we tend to determine N/O ratios for nebulae with the stronger lines. Nebulae are included in this part of the study primarily by the detectability of

[O II], however, and so they are not preselected on the basis of the overabundance of nitrogen. But the effect does result in a significant deficiency of data for high excitation planetaries, especially those for which  $\xi = 1$ .

At least some of these nebulae have abundance anomalies that are not considered in the correlations of the last subsection. A30 and A78 have the by now well-known internal zones of very high He/H, but the abundances within the main bodies of the planetaries are unknown. From § IIIi, two others, A20 and K1-14, may have He/H of 0.13 or greater. If these two are included, the He/H- $\xi$  correlation described above is weakened, although the  $\xi = 1$  set still contains all four nebulae with  $\text{He}/\text{H} \leq 0.11$ . The higher He/H for A20 and K1-14 implies the likelihood of a high N/O, which would also weaken that correlation. However, it may be reasonable to exclude these, and perhaps the whole set of large high-excitation nebulae, those that bear outward similarity to A30 and A78 (Kaler 1981*a*), since their overabundances may be produced by a mechanism other than convective dredge-up. Some of these stars may have been stripped of their hydrogen shells, and they may be now ejecting the exposed surfaces of their helium-rich cores. Iben *et al.* (1983) suggest that this effect may occur after a final thermal pulse: see the discussions in §§ I and IVa. If that is the case, the relation of the phenomenon to initial and final core mass is not known, and the high-excitation objects should not be included with those nebulae that were used to establish the correlation of Figure 9. These latter then stand by themselves as a self-consistent set of nebulae whose overabundances are caused by physical phenomena that take place during the normal giant stages of stellar evolution. Nevertheless, it is imperative that accurate abundances be derived for the high excitation nebulae, particularly for those that may have undergone a final thermal pulse.

The discussions above are predicated on the belief in the reliability of the listed N/O ratios. Can the assumption of uniform  $T_e = 10,000$  K produce a false correlation? Considering the large range of N/O, temperature effects are not very significant. Analysis of Kaler's (1979) listed [N II] temperatures shows that the mean is near 10,000 K, but that there is small systematic effect in that nebulae with  $\text{He}^{++}/\text{He} > 0.5$  are about 15% hotter than the others. Adjustment for a systematic temperature effect of this sort would only act to increase the strength of the correlation. More importantly, does  $\text{N}^+/\text{O}^+$ , the derived parameter, really reflect N/O? Kaler (1979) suggested that  $\text{N}^+/\text{O}^+$  may not be a good indication of N/O for high excitation nebulae ( $\text{He}^{++}/\text{He} > 0.5$ ), where the ionization correction factors would be quite large. A plot of N/O from Table 5 against  $I(\lambda 4686)$  shows no significant correlation, however. If the nebulae with  $I(\lambda 4686) > 60$  are removed from Figure 9, the correlation weakens, but the fraction with  $\text{N}/\text{O} > 0.4$  for the  $\xi < 1$  set is still over twice as large as it is for the  $\xi = 1$  group.

Kaler (1979) also showed that  $\text{N}^+/\text{O}^+$  becomes very large, perhaps an order of magnitude larger than N/O,

for nebulae with the coolest central stars. Although the stars considered here are much hotter, the nebulae with  $\xi < 1$  often have extensive  $O^+$  and  $N^+$  zones, with powerful  $[O\ II]$  and  $[N\ II]$  lines, and in that sense are akin to the very low-excitation nebulae. Could the two disparate sets of nebulae share a similar kind of ionization imbalance? It seems unlikely. Several objects with very strong  $[O\ II]$  and  $[N\ II]$  lines (e.g., NGC 6853, NGC 6720) have low  $N^+/O^+$ ; among the nebulae with  $\xi < 1$  there is no correlation between  $N^+/O^+$  and the intensity of  $\lambda 3727\ [O\ II]$ . In addition Hawley and Miller (1977, 1978) show that for the above two nebulae,  $N^+/O^+$  usually stays well within 50% of the mean even while  $I(\lambda 3727)$  varies through a factor of 10 or more. NGC 6853 shows a correlation between the two, but NGC 6720, with the larger  $I(3727)$  variation, does not. Aller (1976) showed a similar constancy in  $N/O$  for NGC 6720, with only about a 60% difference between the center and the ring. And in one of the high-nitrogen nebulae, NGC 7293, Hawley (1978) demonstrates a maximum 25% variation while  $I(3727)$  wanders with no correlation over a factor of 2.5. Finally, the reality of the  $N/O$  ratios are supported by the theoretically expected correlation with  $He/H$ ; see the previous subsection. While systematic errors in  $N/O$  are probably present to some degree, they do not seem large enough to affect the correlation between  $N/O$  and  $\xi$ .

iv) *Discrimination of Evolutionary Tracks, and Stellar Mass*

If we accept the above correlations and interpretations, then we should be able to use nebular  $N/O$  and morphology, through  $\xi$ , to trace the evolutionary paths of stars with different initial mass through the planetary regime of the  $\log L$ - $\log T$  plane. Figure 11 shows a plot of those stars from Table 5 for which the nebular  $N/O$  is known (less those two with the largest errors). Open

symbols represent  $N/O \leq 0.40$ , consistent with the division in § IVe(ii), half-filled symbols,  $0.4 < N/O < 1.0$ ; and filled symbols,  $N/O \geq 1$ . There is a distinct tendency for the higher  $N/O$  values to fall to the lower left of the diagram into the region of the higher mass cores. If we first divide the nebulae at  $N/O = 0.4$ , as was done for the correlation with  $\xi$ , and look at all the points irrespective of whether or not they are limits, the correlation is marginal: of the objects positioned outside the  $0.6 M_{\odot}$  Paczyński track (toward higher mass), 56% have  $N/O > 0.4$  compared to 47% for those inside that track (where M2-51, which appears to be on a horizontal track at high luminosity, is included). However if we drop from the latter set the stars represented by limits, for which the core mass is ambiguous, the difference becomes more significant as the latter quantity drops to only 33%. (There are no similar ambiguities for stars already outside the  $0.6 M_{\odot}$  track, but the percentages could be changed by stars moved into that region from inside the track. Some are upper limits, and some are lower limits; in the extreme case, if the two low  $N/O$  points inside the  $0.6 M_{\odot}$  track are moved upward to outside of it, and the others keep their places, the percentages for both regions above  $N/O = 0.4$  would be much closer.)

The correlation becomes much stronger if we divide the nebulae at  $N/O = 1$ . There are no nebulae with  $N/O \geq 1$  for stars inside the  $0.6 M_{\odot}$  track, compared to 44% for those outside it. These in fact, with one exception, are outside the  $0.7 M_{\odot}$  track.

Since  $\xi$  correlates with  $N/O$ , we both expect and find similar behavior on the  $\log L$ - $\log T$  plane. In Figure 12, the nebulae are discriminated according to  $\xi$ : filled circles represent  $\xi \leq 0.5$ ; half-filled,  $0.5 < \xi < 1.0$ ; and the rest,  $\xi = 1$ . Outside the  $0.6 M_{\odot}$  Paczyński curve, 58% of the nebulae have  $\xi < 1$ . Inside the track, considering all the nebulae without regard to whether or not the stars are

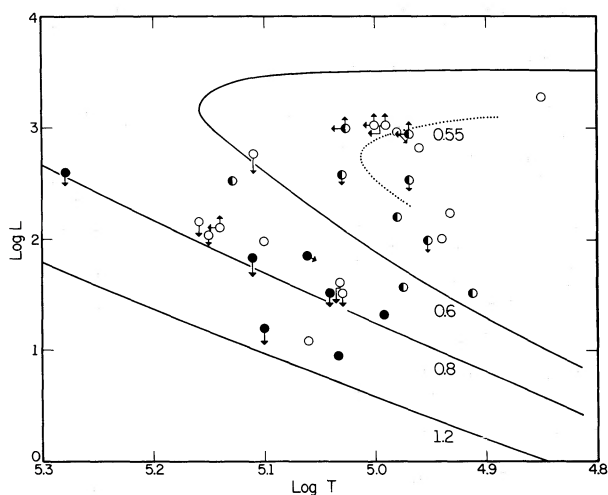


FIG. 11.—The distribution of nebular  $N/O$  on the  $\log L$ - $\log T$  plane. Error bars are removed; arrows indicate optical depth and limiting values as in Fig. 6. Filled symbols:  $N/O \geq 1.0$ ; half-filled symbols:  $0.4 < N/O < 1.0$ ; open symbols:  $N/O \leq 0.4$ . The evolutionary tracks are the same as those in Fig. 6.

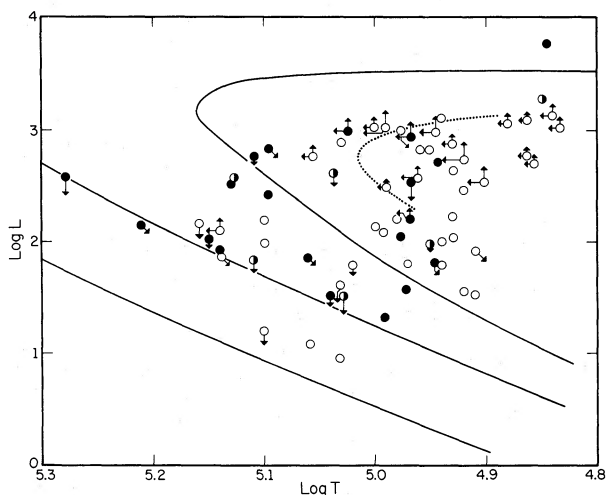


FIG. 12.—The distribution of nebular morphology, as expressed by the geometrical filling factor  $\xi$ , on the  $\log L$ - $\log T$  plane. Arrows indicate optical depth and limits as in Fig. 11. Filled symbols:  $\xi \leq 0.5$ ; half-filled symbols:  $0.5 < \xi < 1$ ; open symbols:  $\xi = 1$ . The evolutionary tracks are the same as those in Fig. 6.

represented by limits, the figure is 26%. If we again eliminate inside the track those whose masses are made ambiguous because of limits, the latter figure changes to 32%. These numbers are essentially unchanged if we remove the nebulae with uncertain central stars or questionable stellar magnitudes (§ IIIa) and morphology (§ IIIb).

At this point the results are largely qualitative, and there are still serious difficulties. First, we encounter the problem of possible systematic errors in the distances that may produce a false correlation (see § IVa), and again we can appeal, even if marginally, to the interstellar extinction data plotted in Figure 8. The nebulae with  $\xi < 1$  and with  $\xi = 1$  show no significant systematic differences. More important is Cudworth's (1974) result that Greig's (1971) B and C nebulae yield the same distance scale factors, implying that the masses of the planetaries are indeed similar and that the precepts of the distance method are largely correct.

Second, there is a fair degree of scatter in the relations among N/O,  $\xi$ , and position on the  $\log L$ - $\log T$  plane. Some nebulae with higher mass cores seem really to have  $\xi = 1$ , and low N/O and He/H. This inconsistency strengthens the case [see § IVe(ii)] that the relation between N/O and initial stellar mass is not yet well known; for example, it may well be that not all higher mass stars dredge up material as currently predicted. The problem is compounded by the distance scale problem, the frequently large errors in the N/O measurement, and by the determination of  $\xi$ , which is notoriously difficult to establish with real precision. There is also an uncomfortably small number of measurements of N/O. We very much need high-quality data for all the nebulae on the diagram to confirm the trend now seen on the  $\log L$ - $\log T$  plane.

Nevertheless, we now seem for the first time to be able to discriminate the evolutionary tracks of planetary nuclei as a function of initial stellar mass. Since in spite of the above uncertainties there is still strong evidence that nebulae with high N/O, and by correlation low  $\xi$ , result from high mass progenitors, Figures 11 and 12 show that the higher mass stars develop higher mass final cores, as expected. The very existence of the correlation supports the contention of a range of core masses. The results seem clearly to support the qualitative aspect of the theory laid out by Renzini (1979) and Iben and Renzini (1982).

Quantitatively, however, we encounter inconsistencies. We have already examined the problems involving the enrichment of carbon, nitrogen and helium in § IVe(ii). From Figure 11, we see that  $N/O \geq 1$  for, very roughly,  $M_{\text{core}} > 0.7 M_{\odot}$ . From Iben and Truran (1978), as well as from Renzini and Voli (1981), a  $0.7 M_{\odot}$  core is generated by a star with an initial mass of  $1.5 M_{\odot}$ . But Becker and Iben (1980) require a  $5 M_{\odot}$  initial mass even to get N/O up to 0.8; at  $1.5 M_{\odot}$ , N/O should not exceed 0.45, even under favorable carbon burning conditions. Even with the extreme envelope-burning conditions envisioned by Renzini and Voli (1981) ( $\alpha = 2$ ),  $N/O > 1$  does not occur until  $M(\text{initial}) \gtrsim 3.4 M_{\odot}$ . From

Iben and Truran (1978), a star of  $3.5 M_{\odot}$  generates a core of  $1.1 M_{\odot}$ , and we should not see  $N/O \geq 1$  in Figure 6 above (toward higher  $L$ ) that cooling curve.

Admittedly, the number of nebulae is small, and the errors could be large, causing the filled ( $N/O \geq 1$ ) points to scatter upward to the  $0.7 M_{\odot}$  track, but taken at face value, the data indicate that either (1) significant amounts of enriched matter is dredged up at initial masses which are lower than expected, or (2) a given initial mass produces a remnant core less massive than presently calculated, or some combination of both. Given our poor knowledge of winds and mass loss, which influence the ultimate size of the core, the second possibility seems the more likely and supports a similar conclusion drawn by Iben and Frogel (1983) from the luminosities of carbon stars. These possibilities are in the same direction as the conclusions derived by Schönberner (1981), but not as extreme, as he found a significantly narrower mass range, and no relation between overabundances and core mass at all.

Because of the relation between N/O and  $\xi$ , we might now conclude that stars over about  $3.5 M_{\odot}$ , those that rotate most rapidly on the main sequence, produce the bi-nebulous planetaries, those with  $\xi < 1$ , Greig's (1971) class B. Several authors (Louise 1973; Terzian 1975; Heap 1982) have noted the role that stellar rotation may play in determining the structure of the nebulae, and the data are supportive of such a notion.

The numbers and discussions in the preceding paragraphs cannot be accepted uncritically at the present time. They mostly demonstrate what can be achieved with data of this sort, and the directions we must go for improvement. This work shows at least the general consistency of several theories that predict phenomena in the domain of the planetaries. With better N/O ratios, a full set of He/H ratios, improved distances, and continued improvement of the theory relating nebular abundances to stellar mass, much finer discrimination of the above parameters should be possible, which will ultimately lead toward accurate values for total mass loss and the lower mass limit for carbon-core supernova production.

#### V. SUMMARY

As a result of the new data and analyses of large planetary nebulae presented in this paper, we begin to see detailed agreement between the theory of evolution of planetary nebulae and the observations. The observed temperatures and luminosities of the central stars follow the theoretical tracks for remnant cores over a range from about  $0.55 M_{\odot}$  to about  $1 M_{\odot}$ . The upper limit is in agreement with the stars studied in the Magellanic Clouds by Stecher *et al.* (1982). The core mass distribution found from this study, which shows that between about one-third and one-half of the stars have masses greater than  $0.6 M_{\odot}$ , is wider than that given by Schönberner (1981). Part of the difference in the two studies is due to slightly different distance scales and evolutionary tracks, and another part to observational selection, whose exact effects are presently unknown,

and the final portion to problems intrinsic to each of the methods used. The true mass distribution probably lies somewhere between the two.

Stars of higher initial mass, identified here by high nebular N/O, develop the higher mass cores. In spite of uncertainties laid out in earlier sections, the observations are in substantial agreement with the concepts outlined by Renzini (1979) and Iben and Renzini (1982), who predicted the variation of nebular abundances as a function of stellar position on the  $\log L$ - $\log T$  plane. Taken as a whole, the new work demonstrates general qualitative consistency of theories of evolution (Paczynski 1971; Schönberner 1979, 1981; Iben and Renzini 1982), mass loss (Iben and Truran 1978; Reimers 1975), and convective dredge-up (Becker and Iben 1979, 1980; Renzini and Voli 1981). Quantitatively, however, the observations imply that the final core masses are smaller than expected for a given initial mass, implying more rapid and extensive mass loss than currently accepted.

The N/O ratios, as well as the few He/H ratios available, correlate with nebular structure. By using dredge-up theory as our link to stellar mass, we see that the non-spherically symmetric nebulae, typified by Greig's (1971) bi-nebular (or B) nebulae, are produced by systematically higher mass progenitors (with higher initial rotation speeds, which may be significant), consistent with Greig's (1972) relation between morphology and galactic kinematics.

The placement of the nuclei of the large high-excitation nebulae allows us to surmise that some may have undergone a thermal pulse that ejects their outer hydrogen envelopes and forces them to repeat a portion of the evolutionary tracks; see Iben *et al.* (1983) for the full argument, as derived from the data herein presented.

Numerous other results are listed below, in no particular order:

1. New total fluxes were measured for a large set of nebulae (57) with large diameters.
2. New coordinates were determined for 61 objects, mostly drawn from the above set.
3. Three sets of photographic total fluxes (two in H $\alpha$  plus [N II] and one in H $\beta$ ) are calibrated with the new photoelectric data.
4. The high hydrogen Zanstra temperatures derived for several stars by Abell (1966) result from the inclusion of very strong [N II] in the H $\alpha$  flux.
5. High electron temperatures ( $\approx 20,000$  K) are inferred for several nebulae by comparing the radio flux density with the H $\beta$  flux corrected for extinction.
6. N/O ratios are derived for nearly 40 nebulae, and several new extreme objects (Peimbert's type I) are identified.
7. Selection effects are more important for large nebulae in the galactic disk than in the halo.
8. Hydrogen and He II Zanstra temperatures and luminosities are calculated for the central stars of almost all of the new nebulae plus 25 others that fit into the category of large objects. These include several with only limiting values. Errors assigned to the input data are

propagated through the equations to produce realistic errors in the final temperatures and luminosities.

9. In spite of the fact that the geometrical filling factor,  $\xi$ , is used to describe a morphological type for a nebula, the available monochromatic surface photometry, plus results presented in this paper, show that hydrogen and doubly ionized helium are more uniformly distributed, and that we derive the proper Zanstra temperatures by setting  $\xi$  uniformly to unity.

10. We can use the comparison of the hydrogen and He II temperatures to establish the average Lyman optical depths of the nebulae, in concert with the original discussion by Seaton (1966). If  $T_z(\text{H}) = T_z(\text{He II})$  the nebula is optically thick, and distance and luminosity are overestimated. If  $T_z(\text{He II}) > T_z(\text{H})$ , and the  $\lambda 4686$  He II flux is not too strong, the nebula is thin in the H-Lyman continuum, but thick in He II, as outlined earlier by Harman and Seaton (1966). If  $T_z(\text{He II}) > T_z(\text{H})$ , and the  $\lambda 4686$  He II flux is comparable to the H $\beta$  flux, the He<sup>++</sup> zone has expanded to encompass the whole nebula, which is then thin in the entire Lyman continuum. Any estimate of Zanstra temperature or luminosity is then a lower limit. The ratio of the He II to the H-Zanstra temperature correlates as expected with  $I(3727)$  and  $I(\lambda 6584)$ , which will become very strong for optically thick nebulae.

11. The observations argue against the general inclusion of internal dust (Helfer *et al.* 1981) since the ratio of  $T_z(\text{He II})/T_z(\text{H})$  approaches unity as a limit. Dust can clearly be a problem in specific cases, however.

There is a rich and open field for pursuing future research. The body of data presented here must be joined to the set of compact objects. A major problem with this work is the lack of very hot stars that are predicted to lie on the evolutionary tracks of the more massive cores. Do these stars not exist, or are selection effects related to the evolutionary time scales and the detectability of the central stars at work? We need to gather fundamental data on many more central stars and work on the detection of stars in nebulae in which they are now unidentified. We also need to probe into the galactic plane, in order better to sample the set of massive stars, and to try to improve the statistics of the stars near the higher mass tracks, so as to identify and reduce effects of observational selection. The error bars on some of the data points in the figures are uncomfortably large. Some of the observational data, particularly stellar magnitudes and  $\lambda 4686$  He II line fluxes, need to be significantly improved. The Zanstra temperatures need to be examined by an extensive body of ultraviolet data from satellites. Directly determined ultraviolet temperatures can be used to test the statements about optical depth made above, the placement on the  $\log L$ - $\log T$  plane of the stars that we contend are repeating their evolutionary loops, and the existence of internal dust. We also need re-examination of the theory, particularly dredge-up theory, in order that we may better relate nebular abundances to initial stellar masses, and those to final core masses.

As in all papers of this kind, we can state that the

distances need improving. We cannot be certain of the vertical placement of the stars with respect to the evolutionary tracks with the present distance method based upon uniform nebular mass. It is not consistent to state that core mass correlates with initial mass and at same time assume that the nebular masses do not change as well. However, it may not be unreasonable to surmise that nebular masses are proportional not to the initial masses, but to core masses, which vary only by a factor of 2 or so. It would take an order of magnitude or more variation in nebular mass to destroy the correlations apparent on the log  $L$ -log  $T$  plane. Support for the general validity of the relative distances is seen in comparisons between the observed interstellar extinction and those calculated on the basis of a galactic dust model, and in Cudworth's (1974) analysis of the kinematical properties of the two types of nebulae that are here related to different mass cores. Still, the problem of distance cannot be overemphasized. Even if the relative distances are largely correct, the proper scale factor to use is still open to question.

All of these improvements are needed to establish the true core mass distribution of planetary nuclei for comparison with that of their progeny, the white dwarfs. It is important for future work with improved data sets that the technique used here be combined with that used by Schönberner (1981), as each will illuminate problems inherent in the other, leading toward improved solutions.

Finally, much more work needs to be done on the nebular abundances, particularly He/H for which the

data are more scarce, in order to improve the detail of the correlations. The high-excitation planetaries are a priority set because selection works against them and because the processes for enrichment may be other than simple convective dredging. We also need to see whether there really is a substantial mix in nitrogen and helium overabundances for stars of a given range of core mass as implied by the data, or whether this is just an artifact of distance determination, or methodology.

The pieces of this puzzle seems slowly to be falling into place. But much more extensive work, both observational and theoretical, is needed before we can truly see the stars properly in transit from the asymptotic giant branch into the realm of the white dwarfs.

I would like to thank the National Science Foundation for its support of this work through NSF grant AST 80-23233 to the University of Illinois. I would also like to thank R. Shaw, who assisted in observing; I. Iben, J. Truran, A. Renzini, S. Maran, J. Lutz, A. Tutukov, D. Schönberner, and V. Weidemann for very valuable discussion; the latter two individuals, G. Jacoby and J. Young, for sending data and manuscripts in advance of publication; J. Cahn for help with the extinction model; E. C. Olson for providing a well-maintained photometer system; G. Whitaker for extraordinary service in keeping the 1 m telescope properly functioning; and D. Griffin and R. MacFarlane for the many hours at the word processor and drafting table through the numerous drafts of the manuscript.

## REFERENCES

- Abell, G. O. 1966, *Ap. J.*, **144**, 259.  
 Abell, G. O., and Goldreich, P. 1966, *Pub. A.S.P.*, **78**, 232.  
 Acker, A. 1980, *Astr. Ap.*, **89**, 33.  
 Aller, L. H. 1951, *Ap. J.*, **113**, 125.  
 ———. 1956, *Gaseous Nebulae* (New York: Wiley).  
 ———. 1971, *The Planetary Nebulae* (Cambridge: Sky Publishing Corp.)  
 ———. 1976, *Pub. A.S.P.*, **88**, 574.  
 Aller, L. H., and Czyzak, S. J. 1979, *Ap. Space Sci.*, **62**, 397.  
 Aller, L. H., Czyzak, S. J., Craine, E., and Kaler, J. B. 1973, *Ap. J.*, **182**, 509.  
 Aller, L. H., and Faulkner, D. J. 1964, in *IAU Symposium 20, The Galaxy and the Magellanic Clouds*, ed. F. J. Kerr and A. W. Rodgers (Canberra: Australian Academy of Science), p. 45.  
 Aller, L. H., Ross, J. E., Keyes, C. D., and Czyzak, S. J. 1979, *Ap. Space Sci.*, **64**, 347.  
 Aller, L. H., and Walker, M. F. 1965, *Ap. J.*, **141**, 1318.  
 Atherton, P. D., Hicks, T. R., Reay, N. K., Worswick, S. P., and Smith, W. H. 1978, *Astr. Ap.*, **66**, 297.  
 Barker, T. 1978, *Ap. J.*, **219**, 914.  
 Becker, S. A., and Iben, I., Jr. 1979, *Ap. J.*, **232**, 831.  
 ———. 1980, *Ap. J.*, **237**, 111.  
 Bohlin, R. C., Harrington, J. P., and Stecher, T. P. 1982, *Ap. J.*, **252**, 635.  
 Bond, H. 1980, *IAU Circ.* 3480.  
 Brocklehurst, M. 1971, *M.N.R.A.S.*, **153**, 471.  
 Cahn, J. C. 1976, *A.J.*, **81**, 407.  
 ———. 1983, in preparation.  
 Cahn, J. C., and Kaler, J. B. 1971, *Ap. J. Suppl.*, **22**, 319.  
 Campbell, W. A. 1968, *Pub. A.S.P.*, **80**, 689.  
 Capriotti, E. R. 1978, in *IAU Symposium 76, Planetary Nebulae*, ed. Y. Terzian (Dordrecht: Reidel), p. 263.  
 Chopinet, M. 1963, *J. des Obs.*, **46**, 27.  
 Chopinet, M., and Lortet-Zuckerman, M. C. 1976, *Astr. Ap. Suppl.*, **25**, 179.  
 Collins, G. W., II, Daub, C. T., and O'Dell, C. R. 1961, *Ap. J.*, **133**, 471.  
 Cudworth, K. M. 1974, *A.J.*, **79**, 1384.  
 Curtis, H. D. 1918, *Lick Obs. Pub.*, **13**, 57.  
 D'Odorico, S., Rubin, V. C., and Ford, W. C. 1973, *Astr. Ap.*, **22**, 469.  
 Doroshenko, V. T., and Kolotilov, E. A. 1973, *Astr. Zh.*, **50**, 1186.  
 Evans, D. S. 1950, *M.N.R.A.S.*, **110**, 37.  
 Greenstein, J. 1981, *Ap. J.*, **245**, 124.  
 Greig, W. E. 1971, *Astr. Ap.*, **10**, 161.  
 ———. 1972, *Astr. Ap.*, **18**, 70.  
 Harman, R. J., and Seaton, M. J. 1966, *M.N.R.A.S.*, **132**, 15.  
 Hawley, S. A. 1978, *Pub. A.S.P.*, **90**, 370.  
 Hawley, S. A., and Miller, J. S. 1977, *Ap. J.*, **212**, 94.  
 ———. 1978, *Pub. A.S.P.*, **90**, 39.  
 Hayes, D. S. 1970, *Ap. J.*, **159**, 165.  
 Hayman, P. G., Hazard, C., and Sanitt, N. 1979, *M.N.R.A.S.*, **189**, 853.  
 Hazard, C., Terlevich, R., Morton, D. C., Sargent, W. L. W., and Ferland, G. 1980, *Nature*, **285**, 463.  
 Heap, S. 1982, in *IAU Symposium 99, Wolf-Rayet Stars: Observations, Physics, and Evolution*, ed. C. de Loore and A. Willis (Dordrecht: Reidel), in press.  
 Heap, S., Aller, L. H., and Czyzak, S. A. 1969, *Ap. J.*, **157**, 607.  
 Helfer, H. L., Herter, T., Lacasse, M. G., Savedoff, M. P., and van Horn, H. M. 1981, *Astr. Ap.*, **94**, 109.  
 Higgs, L. A. 1971, *M.N.R.A.S.*, **153**, 315.

- Hubble, E. P. 1921, *Pub. A.S.P.*, **33**, 174.  
 ———. 1922, *Ap. J.*, **56**, 400.
- Iben, I., Jr., and Frogel, J. A. 1983, in preparation.
- Iben, I., Jr., Kaler, J. B., Truran, J. W., and Renzini, A. 1983, *Ap. J.*, **264**, 605.
- Iben, I., Jr., and Renzini, A. 1982, Illinois Astrophysical Preprint, IAP 82-2.
- Iben, I., Jr., and Truran, J. W. 1978, *Ap. J.*, **220**, 980.
- Jacoby, G. H. 1981, *Ap. J.*, **244**, 903.
- Jacoby, G. H., and Ford, H. A. 1983, *Ap. J.*, **266**, 298.
- Kaftan-Kassim, M. A. 1969, *Ap. J.*, **155**, 469.
- Kaler, J. B. 1976a, *Ap. J.*, **210**, 113.  
 ———. 1976b, *Ap. J. Suppl.*, **31**, 517.  
 ———. 1976c, *Ap. J.*, **210**, 843.  
 ———. 1978, *Ap. J.*, **226**, 947.  
 ———. 1979, *Ap. J.*, **228**, 163.  
 ———. 1980a, *Ap. J.*, **239**, 78.  
 ———. 1980b, *Ap. J.*, **237**, 491.  
 ———. 1981a, *Ap. J. Letters*, **250**, L31.  
 ———. 1981b, *Ap. J.*, **249**, 201.  
 ———. 1983a, in preparation.  
 ———. 1983b, *Ap. J.*, **264**, 594.  
 ———. 1983c, in *IAU Symposium 103, Planetary Nebulae*, ed. D. Flower (Dordrecht: Reidel), in press.
- Kaler, J. B., Aller, L. H., and Czyzak, S. J. 1976, *Ap. J.*, **203**, 636.
- Kaler, J. B., and Feibelman, W. A. 1983, *Ap. J.*, in preparation.
- Kaler, J. B., Gallagher, J. S., and Hunter, D. A. 1983, in preparation.
- Kaler, J. B., and Harkopf, W. I. 1981, *Ap. J.*, **249**, 602.
- Kaler, J. B., Iben, I., Jr., and Becker, S. A. 1978, *Ap. J. (Letters)*, **244**, L63.
- Khromov, G. S., and Kohoutek, L. 1968, *Bull. Astr. Inst. Czechoslovakia*, **19**, 1.
- King, I. R., and Raff, M. I. 1977, *Pub. A.S.P.*, **89**, 120.
- Ko, H. C., 1967, *Ap. J.*, **148**, 927.
- Koester, D., Schulz, H., and Weidemann, V. 1979, *Astr. Ap.*, **76**, 262.
- Kohoutek, L. 1967, *Bull. Astr. Inst. Czechoslovakia*, **18**, 103.  
 ———. 1971, *Astr. Ap.*, **13**, 493.  
 ———. 1979, *Inf. Bull. Var. Stars*, No. 1672.
- Kondratyeva, L. N. 1979, *Trudy Ap. Inst. Kazahkstan*, **34**, 53.
- Kurochkin, N. E. 1980, *Astr. Tsirk.*, No. 1143.
- Liller, W., and Aller, L. H. 1963, *Proc. Nat. Acad. Sci.*, **49**, 675.
- Longmore, A. J., and Tritton, S. B. 1980, *M.N.R.A.S.*, **193**, 521.
- Louise, R. 1969, *Astr. Ap.*, **3**, 29.  
 ———. 1973, *Mem. Soc. Roy. Sci. Liège*, 6e Sér., **5**, 465.
- Miller, J. S. 1973, *Mèm. Soc. Roy. Sci. Liège*, 6e Sér., **5**, 57.
- Milne, D. K. 1979, *Astr. Ap. Suppl.*, **36**, 227.
- Milne, D. K., and Aller, L. H. 1975, *Astr. Ap.*, **38**, 183.
- Minkowski, R. 1942, *Ap. J.*, **95**, 243.  
 ———. 1964, *Pub. A.S.P.*, **76**, 197.
- Minkowski, R., and Aller, L. H. 1956, *Ap. J.*, **124**, 93.
- O'Dell, C. R. 1962, *Ap. J.*, **135**, 371.  
 ———. 1963a, *Ap. J.*, **138**, 67.  
 ———. 1963b, *Ap. J.*, **138**, 1018.  
 ———. 1963c, *Ap. J.*, **138**, 293.
- O'Dell, C. R. 1968, in *IAU Symposium 34, Planetary Nebulae*, ed. D. E. Osterbrock and C. R. O'Dell (Dordrecht: Reidel), p. 361.
- Oke, J. B., and Schild, R. E. 1970, *Ap. J.*, **161**, 1015.
- Osterbrock, D. E., and Stockhausen, R. E. 1961, *Ap. J.*, **133**, 2.
- Paczyński, B. 1971, *Acta Astr.*, **21**, 417.
- Peimbert, M. 1978, in *IAU Symposium 76, Planetary Nebulae Observations and Theory*, ed. Y. Terzin (Dordrecht: Reidel), p. 215.
- Peimbert, M., and Torres-Peimbert, S. 1971, *Bol. Obs. Tonantzintla y Tacubaya*, **6**, 21.
- Perek, L. 1971, *Bull. Astr. Inst. Czechoslovakia*, **22**, 103.
- Perek, L., and Kohoutek, L. 1967, *Catalogue of Galactic Planetary Nebulae*, (Prague: Czechoslovakia Acad. of Sci.).
- Phillips, J. P., and Reay, N. K. 1980, *Ap. Letters*, **21**, 47.
- Pilyugin, L. S., Sakhbullin, N. A., and Khromov, G. S. 1978, *Astrofizika*, **14**, 665.
- Pottasch, S. R., Wesselius, P. R., Wu, C.-C., Fieten, H., and van Duinen, R. J. 1978, *Astr. Ap.*, **62**, 95.
- Purgathofer, A., and Weinberger, R. 1980, *Astr. Ap.*, **87**, L5.
- Reimers, D. 1975, in *Proc. 19th Liege International Astrophysical Colloquium*, p. 369.
- Renzini, A. 1979, in *IAU 4th European Regional Meeting in Astronomy, Stars and Star Systems*, ed. B. E. Westerlund (Dordrecht: Reidel), p. 155.
- Renzini, A., and Voli, M. 1981, *Astr. Ap.*, **94**, 175.
- Robinson, G. J., Reay, N. K., and Atherton, P. D. 1982, *M.N.R.A.S.*, **199**, 649.
- Sabbadin, F. 1977, *Astr. Ap.*, **57**, 307.
- Sabbadin, F., and Hamzaoglu, E. 1981, *Astr. Ap.*, **94**, 25.  
 ———. 1982, *Astr. Ap.*, **110**, 105.
- Sabbadin, F., and Minello, S. 1978, *Astr. Ap. Suppl.*, **33**, 233.
- Schönberner, D. 1979, *Astr. Ap.*, **79**, 108.  
 ———. 1981, *Astr. Ap.*, **103**, 119.  
 ———. 1983, in *IAU Symposium 103, Planetary Nebulae*, ed. D. Flower (Dordrecht: Reidel), in press.
- Schönberner, D., and Weidemann, V. 1981a, *Physical Processes in Red Giants*, ed. I. Iben, Jr. and A. Renzini (Dordrecht: Reidel), p. 463.  
 ———. 1981b, private communication.
- Seaton, M. J. 1966, *M.N.R.A.S.*, **132**, 113.  
 ———. 1968, *Ap. Letters*, **2**, 55.
- Shao, C.-Y., and Liller, W. 1973, private communication.
- Shaw, R. A., and Kaler, J. B. 1982, *Ap. J.*, **261**, 510.
- Stecher, T. P., Maran, S. P., Gull, T. R., Aller, L. H., and Savedoff, A. J. (Letters), **262**, L41.
- Terzian, Y. 1975, *Bull. AAS*, **7**, 244.
- Torres-Peimbert, S., and Peimbert, M. 1978, *Rev. Mexicana Astr. Ap.*, **2**, 181.
- Vorontsov-Velyaminov, B. A. 1961, *Astr. Zh.*, **38**, 75.
- Warner, J. W., and Rubin, V. C. 1975, *Ap. J.*, **198**, 593.
- Webster, B. L. 1969, *M.N.R.A.S.*, **143**, 79.
- Weidemann, V. 1981, *Mitt. Astr. Ges.*, No. 52, p. 159.  
 ———. 1982, private communication.
- White, M. L. 1952, *Ap. J.*, **115**, 71.
- Whitford, A. E. 1958, *A.J.*, **63**, 201.
- Young, J. A. 1982, private communication.

JAMES B. KALER: 341 Astronomy Building, University of Illinois, 1011 West Springfield, Urbana, IL 61801